University of Alberta

The Analysis of Inter-joint Coupling with Applications in the Rehabilitation of Arm Function

by

Andrew John Ganton 

A thesis submitted to the Faculty of Graduate Studies and Research
in partial fulfillment of the requirements for the degree of

Master of Science

Department of Biomedical Engineering

Edmonton, Alberta
Fall 2007

Your file Votre référence
ISBN: 978-0-494-33244-3
Our file Notre référence
ISBN: 978-0-494-33244-3

Abstract

The overall goal of this study was to investigate how the nervous system co-ordinates the action of multiple muscles in preparation for voluntary arm movements. The organization and consistency of synergism between arm and forearm muscles during simple voluntary elbow movements was examined, and the coupling between these muscles was also assessed using coherence analysis. The temporal and spectral techniques employed were capable of revealing the characteristics of muscular synergism and, potentially, the neural mechanisms responsible for it. The results of this study suggest the existence of stored motor programs that contain specific commands encoding inter-joint coupling. Further investigation of the modulation of synergism and coupling in able-bodied individuals, as well as those affected by injury or disease of the nervous system may yield important insights into the neural control of movements. It may also aid in the development of novel rehabilitative interventions for spinal cord injury or stroke.

Acknowledgements

First and foremost, I would like to thank those closest to me for their love and support through the last two years. Candice, Mom and Dad, Michael, David and Janina, thank you so much for your love, motivation, encouragement, inspiration and welcome distractions. I honestly couldn't have done this without you all and I thank you so much.

There are many people in Edmonton who have made my time here memorable besides, of course, Candice. So, I would like to acknowledge some of the wonderful people here that made this experience enjoyable: Jason Pearman, Jason Dyck, Pam Dyck, Emily Krauss, Sherif ElBasiouny, Dan Miller, Clark Schommer and Jeff Douziech. Thank you all for so many great times, so much support and, on occasion, so much ridiculousness. There are many other people who have been such great friends as well and to all of you, I honestly hope to stay in touch and maintain our friendship.

To my advisor, Vivian Mushahwar, I would like to thank you for your motivation and support. And to Rob Burrell and Maisie Goh for your tireless help – thank you.

Table of Contents

List of Tables

List of Figures

List of Symbols, Nomenclature and Abbreviations

AD: Anterior deltoid muscle

ANOVA: Analysis Of Variance

BB(long) and BB(short): Lateral and short heads of biceps brachii muscle

BRD: Brachioradialis muscle

CNS: Central Nervous System

ECRL: Extensor carpi radialis longus muscle

ECU: Extensor carpi ulnaris muscle

EEG: Electroencephalography

EMG: Electromyography

FCR: Flexor carpi radialis muscle

FCU: Flexor carpi ulnaris muscle

FFT: Fast Fourier Transform

MEG: Magnetoencephalography

SSR: Spinal Stretch Reflex

TB(lat) and TB(long): Lateral and long heads of triceps brachii muscle

TFO: Time of First Onset (of EMG activity)

THSD: Tukey's Honestly Significant Difference

1 Introduction

1.1 Overview

In preparation for fast reaching movements, the central nervous system (CNS) utilizes feed-forward control to drive the arm in an appropriate direction to reach its goal before sensory information can evoke compensatory feedback mechanisms. As a result of the latency between feed-forward and feedback mechanisms, fast reaching movements may be achieved through pre-programmed patterns within the spinal cord (i.e. Fetz et al. 2000; Fetz et al. 2002). In order to help understand the changes that take place following damage to the CNS which may affect reaching movements, it is important to be able to understand the characteristics of synergistic muscle activation in able-bodied individuals. As such, the goal of this study was to examine the characteristics of synergistic muscle activation in the upper arm and forearm in preparation for multi-joint reaching movements and to measure reliably the degree to which synergistic muscles receive common neural input.

Targeted volitional movements involve extensive integration between descending neural inputs and segmental neural circuits at the level of the spinal cord (McCrea 1992). The descending drive from supraspinal centres formulating

the strategy for executing the movement may be delivered to select populations of interneurons (Burke 1992). Networks of interneurons at the spinal cord level are capable of coordinating the activity of multiple muscle groups to produce desired movement trajectories (McCrea 1992). The interconnection of motoneuronal pools through interneurons produces functional co-activation of muscle groups in what is commonly known as a muscle synergy. It has been proposed that muscle synergies simplify the task of controlling complex multi-joint movements by reducing the degrees of freedom of the nervous system (Bernshtein 1967). The use of muscle synergies may be particularly important in rapid movements where coordinated muscle activation must occur in a pre-programmed fashion due to the inability for state feedback to influence the ongoing execution of a motor program. Furthermore, synergies may be an effective strategy that the nervous system employs to coordinate or "couple" the action of multiple muscles that span different joints such as uniarticular muscles crossing the shoulder, elbow or more distal joints in reaching movements.

It is important to understand the characteristics of synergistic muscle activation so that we may better understand how to modify neural activity following damage or disease. Operant conditioning of the spinal stretch reflex has been demonstrated (Wolpaw et al. 1983; Segal and Wolf 1994; Wolpaw 1997; Wolpaw and Tennissen 2001) and holds promise as a potential method of inducing targeted plasticity in the CNS following injury or disease. It is expected that conditioning of stretch reflexes will induce changes in not only the targeted motor pools, but also in motor pools of other muscles that are connected through interneuronal networks. There is currently no appropriate method to measure the reorganization that takes place in the interneuronal networks.

In this study, synergistic activation of muscle pairs was assessed by

quantifying statistically the variability in the onset of electromyographic (EMG) activity and the degree of coupling between muscles of the elbow and wrist during single joint movements of the elbow using coherence analysis. Coherence is a measure of signal similarity in the frequency domain and its presence in EMG activity before the kinematic onset of a movement may indicate that a pair of motoneuron pools is receiving common input from spinal interneurons or cortical centres (Baker et al. 1997; Kilner et al. 1999). This thesis examines the degree of coherent motor activation between muscles of the elbow and wrist, the role it may play in the control of volitional movements, and its modulation with movement parameters (movement direction and movement speed) during constrained elbow movements. This knowledge will aid in the understanding of the neural processes responsible for the coordinated control of multi-joint movements in healthy subjects and how this control is altered following CNS injury or disease.

1.2 Layout of Thesis

The ensuing chapters are organized as follows. Chapter 2 discusses the relevant background on inter-joint coupling, interneuronal networks and coherence analysis. Chapter 3 describes the apparatus and data collection methods used in these experiments. It also discusses the mathematical approaches that were used to assess the prevalence of coupling between muscles throughout the arm. Chapter 4 reports the results of these analyses and Chapter 5 discusses the relevance of these results in the context of motor systems and clinical application. Finally, Chapter 6 discusses ways in which this line of research may continue.

2 Background and Motivation

"...to move things is all that mankind can do; for such the sole executant is muscle, whether in whispering a syllable or in felling a forest"

Charles Sherrington, 1924

The ultimate goal of this body of research is to better understand how neural circuits within the CNS contribute to the production of volitional arm movements and how these circuits change with injury and subsequent rehabilitation. Thus, the most relevant background information relates to the production of motor output, neural plasticity and current techniques that have been employed in order to charaterize these proceses. This chapter discusses each of these topics in some detail.

2.1 The Production of Movement

2.1.1 - Muscles and Motor Units

Skeletal muscle is comprised of thousands of parallel contractile elements called muscle fibres. Many muscle fibres (a muscle unit) are simultaneously innervated by a single motoneuron. This entire complex is referred to as a motor

unit. The number of muscle fibres contained within a motor unit can vary widely throughout the body, depending on the precision required of a muscle. For example, a motoneuron controlling eye muscles would innervate far fewer muscle fibres than would a motoneuron associated with the knee extensor quadriceps muscle group, due to the finer control we exert over eye position.

Motoneurons are arranged into groups of similar function called motor pools. Motor pools contain all the cell bodies of motoneurons innervating a single given muscle. In this arrangement, all of the cell bodies of a given muscle are in close proximity within the spinal grey matter. However, pools may extend longitudinally beyond one spinal segment, depending on the muscle they innervate.

Motoneurons synapse on muscle fibres at end-plates. Post synaptic depolarization of muscle fibres via acetylcholine and repolarization due to the hydrolyzation of acetylcholine occurs rapidly such that muscle fibres respond synchronously to each action potential. Each action potential produces a muscle twitch. Higher frequency action potentials reaching the muscle fibres produce the summation of successive twitches and higher overall force output. At a maximal activation frequency, individual twitches fuse together to produce the maximal force output. This is known as fused tetanus (Loeb and Ghez 2000).

There are three broad definitions of motor units, related to their speed of contraction, peak force and fatigability. These are 'slow' (I), 'fast fatigue resistant' (IIa) and 'fast fatigable' (IIb). Type I fibres produce relatively low forces quite slowly, but can sustain their maximal force output for long periods of time because they derive their energy (adenosine triphosphate - ATP) directly from glucose and oxygen in the bloodstream. Type IIb fibres rely on energy

retrieved from glycogen for their needed ATP. They can produce their maximal force output quickly and powerfully, but rapidly deplete their glycogen stores and, so, their force output declines rapidly (within minutes). A continuum of the contribution of glycogen and aerobic reliance produces a wide range of varying muscle properties between I and IIb fibres (Loeb and Ghez 2000).

The force output of a motor unit depends on the fibre type characteristics of its constituent muscle fibres and the number of fibres within the unit. For example the motoneurons innervating fast twitch type IIb fibres have fast conduction velocities and tend to innervate a large number of muscle fibres (Henneman et al. 1965). Thus the entire motor unit is capable of producing large force rapidly. The motoneuron cell bodies for these units, on the other hand, are large, resulting in relatively low input impedance. The converse properties are true for type I fibres (Henneman et al. 1965). Therefore, these cell bodies will depolarize differently to the same stimulus current. Thus, motor units are recruited (activated) according to the Henneman size principle with slower type I fibres activated first and faster type IIb fibres activated as more force output is required (Loeb and Ghez 2000).

With a multitude of muscles and their varying properties present throughout the human body, the nervous system has a considerable job to do in deciding how to control each of them. It must take into account the mechanical action of each muscle and the efficient combinatory action of multiple muscles required to perform a given task. Further, it must be able to compensate quickly for external influences, such as loading. While muscles themselves are capable of a certain degree of adaptation, much of the responsibility for this activity lies within the CNS.

2.1.2 - Reflexes

In 1906, Charles Sherrington proposed that simple reflexes within the spinal cord are the basic units for movements and that complex movements are "chains of reflex responses linked together" (Sherrington 1906). Further, the combination of these reflexes with descending motor commands could produce ever more complex movements.

Following from the early ideas of Sherrington, it is now clear that the availability of reflex activity can greatly simplify cortical signals. For example, with the timing and coupling of agonist and antagonist muscles left to the spinal cord, higher centres need only decide on what needs to be done and selectively excite or inhibit specific circuits within the spinal cord. The famous Canadian neuroscientist, Donald Hebb, long ago postulated his theory of motor equivalence that suggests that some form of motor programming exists within the CNS (Hebb 1949). These programs would specify the spatial features of movement and joint angles required to accomplish them (i.e. the kinematics) as well as the forces required to produce the desired joint angle changes (i.e. the dynamics). Thus, any movement could be based on the combination of stereotyped muscle activation patterns to produce any desired output (Pearson and Gordon 2000). These basic stereotyped patterns are now often referred to as motor *primitives* due to their elemental nature.

The mass of excitatory and inhibitory interneurons within the spinal cord all receive afferent input from proprioceptors (muscle spindles, joint capsules and Golgi tendon organs) and descending input (from supraspinal centres). For a review see (Jankowska 1992). Further, they may project to close adjacent segments (these are referred to as 'segmental interneurons'), separated spinal

segments (these are 'propriospinal interneurons'), or ascend to the cortex ('ascending tract neurons'). Thus, the vastly inter-connected network within the spinal cord is well situated to be highly involved in the preparation for and control of complex voluntary movements.

The structure of a reflex is relatively simple. Muscle spindles - which are wound around intrafusal muscle fibres - are sensitive to muscle stretch (length and velocity). Hence, spindles are the driving factor behind spinal stretch reflexes. The spinal stretch reflex is a well characterized reflex pathway. In this monosynaptic pathway, Ia afferent fibres synapse directly on homonymous motoneurons (Hultborn et al. 1986) as well as heteronymous motoneurons (Edgley et al. 1986) innervating other synergistic muscles. These synergistic muscles may have a similar activity about one joint, or may participate in coordinated multi-joint synergies, as well. Ia fibres from muscle spindles may also synapse on Ia inhibitory interneurons. These neurons reciprocally innervate antagonistic motoneurons (Simoyama and Tanaka 1974) so that when the original muscle is stretched, the antagonist muscle may relax so as not to impede an intended movement. These reflex pathways form the simplest basis of organization within the spinal cord necessary to simplify the commands required from higher centres when performing voluntary movements. Importantly, these same networks can also facilitate co-contraction – contracting opposing muscles to stiffen a joint. Thus, Ia interneurons provide a high degree of connectivity so various agonist and antagonist muscles may act cooperatively to provide the basis for simple motor 'programs' within the spinal cord (Loeb 1985) .

Ib interneurons provide afferent input to the spinal cord from Golgi tendon organs – tension sensors. By sensing small changes in muscle tension (force), these pathways can facilitate precision control through inhibitory networks. Ib

fibres are heavily involved in networks with motoneurons innervating muscles acting at different joints (Pierrot-Deseilligny et al. 1982). Therefore, Ib fibres are likely highly important in precision grip tasks (when delicate modulation of force output is required) and, also, in whole limb movements in general, such as those that are investigated in this thesis.

Activity in the spinal cord is also mediated by Renshaw interneurons. These interneurons are excited by motoneuron collaterals and they serve to control the strength of excitation and inhibition in both the same motoneuron, as well as related (antagonist, agonist) neurons with activity at the same joint (Jankowska 1992). Thus, Renshaw cells are important in recruiting motoneurons of a similar function.

2.1.3 - Spinal Motor Systems

Control of voluntary movement is largely under the influence of descending control to spinal interneurons. In fact, there are considerably denser descending projections to intermediate spinal laminae than to motoneurons (Dum and Strick 1996). Since afferent feedback from the periphery also synapses in intermediate spinal laminae, these neurons seem an appropriate region to integrate various inputs and distribute appropriate activation patterns to motor pools.

Long thought to be subordinate in the control of movement, the spinal cord has been shown to have activity prior to movement execution that is consistent with motor planning (Bizzi et al. 2000), similar to the preparatory activity that has been observed in supraspinal centres such as motor cortex, premotor cortex, supplementary motor area and basal ganglia. During an instructed delay task (a task in which an animal has been trained to plan for a movement while waiting for a 'go' cue), evidence seems to suggest that the spinal motor network is

'primed' with rate changes in the same direction as the subsequent movement while 'global' inhibition prevents that movement from being conducted (Prut and Fetz 1999).

Fetz's group recorded from spinal interneurons while a monkey performed multidirectional wrist movements (Perlmutter et al. 1998). They found significant modulation of spinal activity during instructed delay periods, consistent with that of cortical premotor activity. Interestingly, these 'premotor' interneurons had varying activity that appeared to facilitate or suppress synergistic/antagonistic muscle groups (Fetz et al. 2002). Thus, these networks were able to activate multiple co-operative muscle groups simultaneously, such as those that would be necessary to guide the arm during voluntary movements. A defining feature of these interneurons was that they were active in multiple movement directions, unlike cortical neurons that classically exhibit activity that is highly 'tuned' to a particular movement direction (Fetz et al. 2002).

Cortical projections and spinal interneurons involved in voluntary movements exhibit very different properties. For example, Fetz's group found that the 'muscle fields' associated with a corticomotor cell (the number of muscles associated with the spiking of a cortical cell) were much larger (Fetz and Cheney 1980) than the muscle fields associated with spinal premotor interneurons (Perlmutter et al. 1998). That is, interneurons tended to facilitate or suppress small sets of synergistic muscles. Interestingly, however, interneurons were 'bidirectionally' active during wrist movements such that they were active to some degree in both flexion and extension of a target muscle (Perlmutter et al. 1998). Corticomotor cells, on the other hand were selective: they fired, for example, in flexion or extension, but not both (Fetz and Cheney 1980).

This group took the question one step further, by examining the diverging roles of muscle connectivity based on the task. For example, in one movement, two muscles may be synergistic and in another they may be antagonistic to each other. To investigate this, monkeys were trained to perform a multidirectional wrist tracking task. Analysis of the preferred direction of spinal interneurons showed that about half of the neurons were 'cosine tuned' for the movement direction (their firing rate was related to the direction of movement) and another quarter of them were broadly active (Perlmutter et al. 1998). This is an interesting result based on the cosine tuning that has long been known to exist in some populations of cortical neurons (Georgopoulos et al. 1982). Further, preferred directions of spinal interneurons were biased towards radial, as opposed to ulnar components (Perlmutter et al. 1998). Premotor interneurons also had post-spike effects on flexor muscles almost twice as often as on extensor muscles. These results appear to suggest that the spinal cord is organized to influence flexor motoneurons preferentially. The reason for these biases is not entirely clear but one possible explanation may be the expected anti-gravity role of these muscles in primates and lesser mammals.

The final interesting aspect of the results of Perlmutter et al. (1998) is the evidence for synchronous activity in populations of spinal interneurons. Synchronous discharge of cells has been reported in many neural areas and is considered to represent a way in which the nervous system may temporally 'bind' activity in disparate cortical areas. This synchrony gives rise to the phenomenon of coherence, indicating that neurons receiving common inputs fire in a rhythmic fashion (i.e. Farmer et al. 1993). For the current thesis, it is important to note that synchrony effects in EMG activity are likely produced by the collective activity of premotor circuits that receive common supraspinal and

feedback signals (Perlmutter et al. 1998). Thus, synchrony effects as recorded at the muscle may be caused by any of those systems but the relative contribution of each system is largely indeterminate.

2.1.4 - Descending Pathways and Voluntary Movement

The control of voluntary movement originates in higher centres such as the parietal and motor cortices, but takes advantage of the interconnected networks in the spinal cord for simplification and control. Corticospinal neurons synapse in various regions of the spinal cord and, so, modulate the background activity of reflex pathways (Krakauer and Ghez 2000). Modulation of reflex gain and sensitivity is a highly dynamic process and is constantly adjusted during various tasks. Furthermore, activity in spinal circuits may be facilitated by descending fibres during voluntary movements. By connecting to populations of interneurons, cortical signals can excite or inhibit a great many more neurons than would be possible with direct connections, developing the organization of complex multi-joint synergies such as reaching.

Planning and initiation of voluntary movements is largely attributed to cortical centres including the parietal cortex, premotor cortex and primary motor cortex. Further, the basal ganglia have been shown to be of great importance in the initiation of movement (the degradation of which leads to the cardinal symptoms of Parkinson and Huntington disease) and the cerebellum is highly important for the active control of movement. The activity of these areas in relation to voluntary movements is largely beyond the scope of this current discussion. A good review can be found in Shadmehr's book. (Shadmehr and Wise 2005) For the current purposes, the assumption will be made that the activation of appropriate spinal interneurons and/or motoneurons is initiated by

premotor and motor cortices.

Descending activity from higher centres is transmitted via pathways: connections between supraspinal centres and the spinal cord. Pathways from the brainstem include vestibulospinal, reticulospinal, tectospinal and rubrospinal pathways (Krakauer and Ghez 2000). The first three pathways, which all lie medially within the spinal cord, terminate on interneurons and propriospinal projections within the spinal grey matter. They are largely responsible for basic postural control, such as anticipatory postural adjustments performed in preparation for voluntary movements. The rubrospinal pathway, on the other hand, is the only lateral brainstem pathway. It connects the red nucleus to populations of interneurons in the dorsolateral grey matter. The red nucleus is highly active during goal-directed movements in cats and monkeys but, because the cerebral cortex is largely responsible for these movements in higher mammals such as humans, the rubrospinal pathway is largely vestigial in humans (Krakauer and Ghez 2000). Voluntary movement in humans is largely facilitated via the corticospinal tract. The ventral corticospinal tract originates primarily from premotor and primary motor cortices related to trunk areas and terminates on interneuronal populations in the spinal grey matter. The lateral tract is derived from premotor and motor cortex and is related more to distal muscles, such as those in the arms (Krakauer and Ghez 2000). All of these pathways synapse on motoneurons and interneurons at the spinal segmental level and are important in initiating the selected movement.

2.1.5 - Muscle Synergies and Inter-joint Coupling

Inter-joint coupling is a strategy employed by the nervous system to reduce a limb's 'degrees of freedom', the complexity inherent in a limb's design. It is a

strategy whereby activity of a muscle at one joint is linked to that of another joint to produce some useful effect (Almeida et al. 1995). For example, in a rapid elbow movement, a certain degree of unwanted movement of the shoulder would be expected due to inertia and mechanical coupling. The nervous system has learned this from experience and, hence, will simultaneously activate the deltoid during an elbow movement to minimize shoulder movement. If a joint is mechanically fixed, however, muscle activity at 'non-focal' joints should no longer be needed. Interestingly, the activation of the shoulder muscles has been shown to persist even though no movement has occurred (Debicki and Gribble 2005). Therefore, it must be concluded that the activation of the shoulder muscles was not due to peripheral feedback but was, in fact, coupled to the activation of the elbow muscles in a feed-forward manner. This must be accomplished at the neural level and may be highly dependent on spinal cord processes (Debicki and Gribble 2004).

Work from Fetz's lab has highlighted the capabilities of spinal networks to activate multiple synergistic and antagonistic muscles simultaneously during motor tasks. Therefore, adaptable spinal networks may underlie the phenomenon of inter-joint coupling. In this scheme, a small number of specific muscle groupings linked via interneuronal circuits is present at the spinal segmental level (Bizzi et al. 2000). These groupings facilitate muscle synergies, the "coherent" activation in space and time of a group of muscles (d'Avella and Bizzi 2005). Their activation would create specific force fields that could be summed with other force fields to create any desired motor output (Mussa-Ivaldi et al. 1994). This has led to the general hypothesis that during ballistic movements the nervous system can recruit appropriate muscle synergies by relying on modular 'internal' or 'pre-programmed' movements.

Intraspinal microstimulation is a technique that has been employed to investigate connectivity at the spinal segmental level as well as advance potential neuroprosthetic applications. The results of these experiments, therefore, provide important information regarding the organization of motor pool connectivity, muscle synergies and the hypothesis of modularity.

Initial microstimulation experiments in the frog lumbar spinal cord demonstrated that focal stimulation could activate multiple leg muscles in a stereotypical fashion (Giszter et al. 1993) and that stimulation of multiple sites simultaneously would result in a vectorial sum of the independent action of each site (Mussa-Ivaldi et al. 1994). Similarly, microstimulation in the cat spinal cord was demonstrated to produce muscle synergies required for specific functional tasks, such as limb extension (Mushahwar et al. 2000; Mushahwar et al. 2002; Saigal et al. 2004) and standing (Lau et al. 2007). These experiments demonstrated that the interconnectivity of the spinal cord is capable of activating multiple synergistic muscles simultaneously in order to produce a specific motor output. Such responses are likely possible because spinal stimulation can activate interneurons and fibres in passage (axons, descending tracts, etc.) and exploit the natural connectivity of the spinal cord (Gaunt et al. 2006).

Because many of these previous studies have focused on the lumbar spinal cord, it is unclear if the cervical cord is arranged in a similar fashion in order to facilitate functional arm movements. Recent experiments in monkeys sought to investigate this question. Moritz et al. (2007) electrically stimulated sites in the cervical enlargement (C7-C8). Consistent with experiments involving frogs, rats and cats, these experiments found that spinal stimulation evoked muscle synergies unrelated to the spatial proximity of motor pools (Moritz et al. 2007). This is important because it implied that multiple muscles were not simply being

activated because they were near the stimulation site but, rather, that they were activated because of their functional interconnectivity to the stimulated site. A statistical cluster analysis revealed that specific groups of muscles co-activated by spinal stimulation fell into distinct functional groups (i.e. finger flexors, finger extensors, elbow muscles, etc.) (Moritz et al. 2007). Interestingly, these researchers also noticed that flexor muscle synergies were activated almost two times more commonly than extensor synergies. This is consistent with reports by the same group that spinal interneurons exhibit responses in flexor muscles of the arm twice as often as in extensor muscles (Perlmutter et al. 1998).

While experiments involving intraspinal microstimulation allude to the interconnectivity of the spinal cord, they also suggest an interesting simplifying feature of the nervous system in terms of the modularity of synergies. That is, a small set of muscle synergies, or modules, may be scaled and combined to form the activity associated with volitional and automatic actions (Flash and Hochner 2005). Support has been found for such an organization in a wide range of mammals, ranging from frogs to humans. Using principal components analysis, for example, human gait (i.e. Ivanenko et al. 2004) and human reaching movements (i.e. d'Avella et al. 2006) have been largely described by only a few muscle activation patterns that have been scaled and temporally aligned. The activation of muscular synergies through spinal cord stimulation from works cited above supports this modular view.

A recent study of fast reaching movements by d'Avella et al (2006) provides some of the most compelling evidence for a modular organization of muscle synergies in humans. In this study, the researchers extracted four or five synergies for each of nine subjects performing fast point to point reaching movements. Generally, they found that these synergies - with scaling in

amplitude and shifting in time - could account for the muscle activity across a wide range of tasks, including different arm postures, different arm loads and different movement directions (d'Avella et al. 2006). That is, scaling of individual muscle synergies, which presumably could be based on feed-forward or feedback mechanisms, could produce the wide range of output necessary for sinuous and robust arm control. Interestingly, these muscle activation patterns exhibited a rough cosine tuning function depending on the direction of movement (d'Avella et al. 2006). Importantly, each synergy was composed of activation and deactivation of specific muscles, something the interneuronal networks within the spinal cord have been shown to be able to accomplish (Perlmutter et al. 1998).

Although vectorial summation of synergies was observed in frogs (i.e. Mussa-Ivaldi et al. 1994) and rats (i.e. Tresch and Bizzi 1999), it was observed to a lesser degree in cats (Aoyagi et al. 2004; Lemay and Grill 2004; Mushahwar et al. 2004). However, it is likely that higher mammals rely more on cortical centres as opposed to the relative automaticity of the spinal cord (Nakajima et al. 2000). Certainly, in mammals, the control of movement involves the cerebral cortex, basal ganglia and cerebellum, as well. This is not contradictory to the motor primitive hypothesis since higher centres may still flexibly recruit and modulate specific modular networks within the spinal cord (Todorov 2000). In fact, given the parallel preparatory activity in primate spinal interneurons (Fetz et al. 2002), it is likely that the cortex and the spinal cord act in concert to produce flexible motor output with but a few specific synergies.

Based on contemporary knowledge of various motor systems, a unified view emerges. Take, for example, the cosine tuning function for muscle activation patterns described by d'Avella et al (2006). Some cortical single units

(particularly in more rostral pre-central motor areas) are cosine tuned to the direction of an upcoming movement (Georgopoulos et al. 1982). Perhaps, then, these units recruit appropriate synergy modules depending on the direction of the movement. Now, many cortical units are not modulated for a preferred movement direction, but for the amplitude of an ensuing movement (Kakei et al. 1999). These units could appropriately scale particular muscle synergies. However, a problem occurs in this interpretation given the consideration that many cortical cells exhibit a modulation with arm posture or load (Kakei et al. 1999). While it is not clear, one theory may be that these cells calculate an inverse model of expected muscle activations for use in a feedback control scheme (d'Avella et al. 2006).

A growing body of evidence suggests that humans, like lesser mammals, use pre-programmed synergies to simplify the co-ordination of complex tasks such as that of controlling the arm. These synergies are likely manifested as densely inter-connected networks of interneurons at the spinal level. Supraspinal centres may, then, be able to select and inhibit various networks appropriately to produce any desired motor output.

2.2 Motivation and Application

2.2.1 - Ramifications of Spinal Cord Injury

Spinal cord injury results in the disruption or complete cessation of supraspinal influence over spinal pathways and may therefore affect motor, sensory, autonomic and reflex functions. The initial mechanical injury can completely sever ascending and descending pathways, or may impair transmission. That is, some residual function across the site of injury may be

possible. The injury tends to damage primarily the grey matter (segmental cell bodies), with relative sparing of white matter (descending and ascending tracts) (Dumont et al. 2001). Generally, grey matter is irreversibly damaged within the first hour post injury, whereas white matter is irreversibly damaged within 72 hours post injury (Dumont et al. 2001). A range of biochemical modifications, generally referred to as secondary injury, begins to take place soon afterwards. Subsequent morphological changes in neuron properties, local sprouting of afferents and the lack of descending influence over spinal cord circuitry can lead to the characteristic changes that take place caudal to an injury site, such as reflex hyper-reflexia (Pierrot-Deseilligny and Burke 2005).

Destruction of spinal cord pathways initiates a sequence of changes in spinal cord function below the lesion that develops over short and long periods of time. Spinal shock abates over several weeks in humans. Over time, reflexes become abnormally strong and easily elicited due to their hyper-activity (Pierrot-Deseilligny and Burke 2005). These changes reflect the destruction of supraspinal connections as well as plastic changes at the spinal cord level. Spinal interneuronal pathways change after spinal cord injury Recurrent inhibition (mediated by Renshaw cells) and reciprocal inhibition (mediated by Ia inhibitory interneurons) are increased (Boorman et al. 1991). .

One common result of spinal cord injury is spasticity. Spasticity can result following many different insults to the nervous system, including spinal cord injury, traumatic brain injury, stroke, cerebral palsy and Parkinson disease. Classically, it has been defined as "a motor disorder characterized by a velocity-dependent increase in tonic stretch reflexes, resulting from hyper-excitability of the stretch reflex as a component of the upper motoneuron syndrome" (Lance 1980). Essentially, residual voluntary movement is disrupted because reflex

circuitry within the spinal cord exhibits larger-than-normal activity (Pierrot-Deseilligny and Burke 2005). Current treatments for spasticity include systemic medication (i.e. baclofen) administration, physical therapy and, less commonly, peripheral nerve block via phenol or botulinum toxin (botox) (Satkunam 2003).

While it is clear that exaggerated stretch reflexes are a culprit in the clinical features of spasticity, it is less clear what the causal factors of reflex hyper-excitability are. Certainly, a lack of descending influence over segmental spinal regions produces a lack of pre-synaptic inhibition on both α-motoneurons and Ia interneurons, but these immediate factors do not account for the dynamic changes that take place over the time following injury. Changes in the connectivity between neuronal elements, such as alterations in reciprocal and non-reciprocal group I inhibition and excitation, alterations in recurrent (Renshaw) inhibition, and increases in gamma (γ) activity (Pierrot-Deseilligny and Burke 2005), as well as changes in intrinsic motoneuron properties (Bennett et al. 2001) and local collateral sprouting have all been implicated in reflex hyper-excitability following injury. While it is not clear which or to what extent each of these factors contributes to the overt clinical manifestation of spasticity, it is clear that dynamic changes do occur following injury and that some or all of these changes cause an increase in the 'gain' of spinal reflex arcs.

It should be noted that reflex hyper-excitability as the cause of spasticity is equivocal. Some researchers have argued that spasticity may, in fact, be caused by changes in intrinsic properties of muscle fibres and that the contribution of reflex hyper-activity is minimal (Dietz 1992). While this is largely seen as a relatively isolated view (Pierrot-Deseilligny and Burke 2005), it is still important that there remains controversy over the exact cause of spasticity.

The clinical measurement of spasticity normally relies on qualitative tests administered by a physiotherapist. This has long relied on the 5-point Ashworth scale (Ashworth 1964) or, more recently, the modified Ashworth scale (Bohannon and Smith 1987). While these tests are still common-place, their use is subjective and, importantly, do not identify the cause of spasticity, only its relative severity (Johnson 2002). The less used Tardieu scale relies on moving the limb at different velocities so as to modulate the effects of reflex activity throughout many different movements and, as such, has been proposed to be more effective at identifying the neural (as opposed to mechanical) influences on spasticity (Pierrot-Deseilligny and Burke 2005). Measurement devices have been proposed to offer a quantitative means of measuring spasticity (Johnson 2002), but their clinical usage has yet to be demonstrated.

Various clinical measures also exist for measuring arm function in general. The Fugl-Meyer test is the most commonly used to assess motor function. Other tests include the Motor Assessment Score, Functional Independence Measure and Van Lieshout Test (Spooren et al. 2006) . All tests rely on the visual scoring of performed motor tasks by trained physiotherapists.

2.2.2 - Neural Plasticity and Rehabilitation

Long or short term modifications within the nervous system are termed 'plastic' changes due to their dynamic nature. The controlled induction of long-lasting plasticity in spinal networks has been repeatedly demonstrated (Wolpaw and Tennissen 2001). Therefore, it seems likely that the selective modification of spinal circuits may have important benefits for rehabilitation following damage to the nervous system.

Reflexes in the isolated spinal cord can show habituation and sensitization

(Mendell 1984). Spinal cord plasticity that underlies training-induced functional improvement depends on the pattern of afferent, efferent and interneuronal activity (Wolpaw and Tennissen 2001). In incomplete spinal cord injury, CNS reorganization might occur at two levels: in pre-existing circuits by modifications of synaptic strength or through sprouting. Furthermore, interconnections between motor systems indicates that plasticity that occurs at one level can result from and/or influence changes occurring at other levels. Sites of plasticity include synaptic connections made by incoming fibres, interneuronal populations interposed between these inputs and motoneurons, synaptic connections on motoneurons and the motoneurons themselves (Wolpaw and Tennissen 2001).

Numerous methods for inducing targeted plasticity within the nervous system are currently being explored. The efficacy of robotic training (i.e. Reinkensmeyer et al. 2004) and functional electrical stimulation (i.e. Sheffler and Chae 2007) have been demonstrated clinically. These training methods, as well as other training paradigms based on operant conditioning continue to be explored both academically and clinically.

2.2.3 - Operant conditioning

Conditioning of spinal stretch reflexes or Hoffman (H)-reflexes via operant training has been demonstrated in humans. Individuals receiving a reward for either "up" or "down" training their stretch reflex amplitudes have shown persistent and significant amplitude modifications in these reflexes.

The potential for operant conditioning to possess clinical application has been noted for some time, but has not been put into use. As Wolf and Segal noted "spinal stretch reflex (SSR) conditioning could have consequences for the

rehabilitation of patients with hyper-reflexia, especially if it would affect synergist muscles" (Wolf and Segal 1996). To examine this effect, this group operantly conditioned stretch reflex activity associated with biceps brachii. Following twenty-four training sessions, subjects reduced their biceps SSR magnitude by 24%. More interesting, however, is that SSR activity associated with agonist and antagonist muscles displayed a similar down-regulation. Brachioradialis, and triceps brachii exhibited 18% and 25% reduction, respectively.

It is the ability of operant conditioning to affect multiple synergistic muscles that makes it a fascinating clinical tool to investigate. Unfortunately, it is not known to what extent different muscles are functionally coupled and it is not clearly understood if, how and to what extent training modifies existing neural connections. It is with this issue in mind that I am interested in quantifying the degree to which the activation of muscles of the arm are coupled.

2.3 Coherence

2.3.1 - What is coherence?

Even relatively simple movements require the synergistic activation of multiple muscles (Gibbs et al. 1995). A common excitatory drive to motor pools of co-contracting muscles is one such strategy that the nervous system may employ in order to accomplish these synergies. This may allow the nervous system to activate populations of motor units in a manner flexible enough to generate the complex repertoire of movements exhibited by humans (Conway et al. 1995).

Coherence analysis can be used to measure this common excitatory input.

Coherence can be thought of as the similarity of two signals in the frequency domain. Therefore, it offers the ability to assess common inputs to two muscles by assessing components in the two signals that are driven at a common frequency. These common inputs may be common cortical areas or may be facilitated by interneuronal connections.

Accepting that synergistic and antagonistic muscles receive common input from some source (be it interneuronal connections or common descending input), the relevance of consistent frequency components to motor units remains unclear. One hypothesis suggests that the 10Hz range is a fundamental frequency used by the motor system to synchronize activity (Gross et al. 2002). In this sense, the nervous system handles information somewhat like the discrete components of a computer would - requiring a 'clock' to provide a common timing to input and output elements. In this sense, coherent activation of multiple cortical and subcortical motor areas may be seen as a 'binding' mechanism in the motor system (Conway et al. 1995).

Synchronized firing of homonymous motor units may exhibit coherence (Farmer et al. 1993). This could be due to common descending input or is a consequence of the action of interneuronal circuitry within the spinal cord. Interestingly, heteronymous motor units of muscles acting on a common joint have also been shown to exhibit coherence (Farmer et al. 1993), suggesting that they may be linked at the neural level by similar mechanisms.

One major question with surface EMG-EMG coherence is the source of activity. The simple answer is that it is largely indeterminate. A few studies have suggested that, generally, lower frequency (<15Hz) activity is driven from the spinal cord while higher components are driven from supraspinal areas

(Grosse et al. 2002). However, little direct evidence exists for this distinction, as a wide range of studies have detected synchrony in broad frequency bands in multiple neural areas.

While a reasonable degree of consistency in the frequency content may be seen between subjects, it is important to note that a variety in the frequency bands (Baker et al. 1997) and strength of coupling (Bremner et al. 1991) might be expected. This may either reflect real differences in motor cortical signals generated for a given task, or may represent differences in muscle activation patterns elicited by a person in a given task (Baker et al. 1997). Therefore, coherence spectra averaged across subjects (Evans and Baker 2003) must be interpreted carefully.

Coherence has been reported not just in EMG signals, but also in electroencephalography (EEG) and magnetoencephalography (MEG), as well. While much of this discussion compares the current results to studies involving EEG-EEG, EEG-EMG or MEG-EMG coherence, it should be noted that the same activity that leads to coherence between cortex and muscle also leads to coherence between EMG signals of muscles activated in the same task (Kilner et al. 1999). Also, EMG-EMG coherence shows the same task dependence as cortical signals (Baker et al. 1997). Therefore, EMG-EMG coherence offers a convenient method to gain insights into the modulation and binding of neural activity in the preparation and execution of voluntary movements.

2.3.2 - Coherence in relation to sustained motor output

Coherence has been reasonably well characterized in simple force related tasks. For example, it has been repeatedly shown that 15-30Hz coherence is predominantly present during maintained voluntary contractions such as

precision grip tasks (Farmer et al. 1993; Conway et al. 1995; Kilner et al. 1999). Furthermore, this 15-30Hz coherence is modulated with the performance of a movement. That is, it is abolished during active contractions and greatest during steady hold just after the initiation of movements (Kilner et al. 2000). Similarly, Evans and Baker noted that synchrony was especially strong at the onset and offset of movements when, they postulated, coupling needs to be established and broken (Evans and Baker 2003). These realizations are consistent with the observations of Jasper and Penfield, who recorded 15-30Hz oscillations over the cortex during a 'steady state' that disappeared during movements (Jasper and Penfield 1949).

2.3.3 - Coherence in relation to phasic voluntary movement

Because of the experimental paradigms used by earlier researchers examining the role of synchrony in controlling movements, frequency components other than the beta range (15-30Hz) have largely been ignored. However, more recent experiments, particularly those examining the dynamic modulation of synchrony, have identified other important frequency components, as well.

The first insights into the frequency components of spinal circuits during voluntary movements came from experiments by Vallbo and Wessberg (1993). In these experiments, subjects performed slow tracking movements of the wrist. A distinct 8-12Hz bursting pattern was observed between agonist and antagonist muscles (Vallbo and Wessberg 1993). The researchers postulated that this represented a pulsatile flow of central information. Later research showed that seemingly smooth movements are, in fact, discontinuous with peak velocities in the 8-10Hz range (Wessberg and Kakuda 1999). Thus, it seems reasonable to

hypothesize that movement discontinuities are not caused by motor units firing at 8-10Hz, but rather that the on-going movement is being actively modulated in the frequency domain. This hypothesis is lent more credence with the consideration that coherence peaks between 8-12Hz are conspicuously absent during sustained contractions (Farmer et al. 1993).

In an EEG-EMG study investigating the dynamics of coherence, it was noted that motor cortical areas and EMG activity exhibited synchronized activity in a systematic relationship with phasic voluntary movement (Feige et al. 2000). Phasic voluntary movements were preceded by desynchronization in the 10-13Hz range (Feige et al. 2000).

2.3.4 - The modulation of coherence with motor parameters

If coherence is truly related to the modulation of motor output, it would be expected that it would be heavily modulated with the demands of an on-going dynamic movement. Numerous studies have shown this to be the case, albeit in isolated conditions. For example, Wessberg and Kakuda noted larger coherence values between single motor units when voluntary movements became faster (Wessberg and Kakuda 1999). Supraspinal areas have also been shown to be coupled in a similar fashion, with motor cortex activation and coupling greater for faster movements (Toma et al. 2002). However, the effect of movement rate on the activation of motor cortical areas was not linear but, rather, significant differences were only observed between broad groupings of 'slow' and 'fast' movements (Toma et al. 2002). This would seem to suggest that different mechanisms govern slow and fast movements.

When Kilner et al. had subjects perform simple precision grip tasks, the level of coherence co-varied with the degree of compliance (the amount of force

required to maintain the same grip on an object) (Kilner et al. 2000). They suggested that coherent activity scales in relation to the force and displacement required to maintain grip (Kilner et al. 2000).

2.3.5 - Coherence in relation to fast and multi-joint movements

The discussion thus far has focused on sustained contractions and on slow voluntary movements. If rhythmic components play a role in generating motor commands, it might be expected that rapid movements may exhibit a unique modulation of coherence, as well. Further, the experimentation described thus far has been limited to muscles about simple joints such as the knee and finger (with the notable exception of wrist tracking movements). How, then, is coherence modulated about complex joints with many degrees of freedom or between muscles operating different joints entirely?

A cross-correlation motor unit study noted distinct evidence for a common drive between pairs of muscles that share a common joint, though no evidence for common drive to muscles between joints (Gibbs et al. 1995). However, in their interpretation, these researchers noted that common drive was found to be present between the same and different digits of the hand during finger movements. Their argument that the metacarpophalangeal joints are not independent is questionable and, hence, it seems that these researchers did, in fact, note common drive to muscles between joints. Furthermore, caution should be taken in conclusively interpreting a lack of a cross-correlation peak as a lack of common drive (Gibbs et al. 1995) as it has been shown that common excitatory potentials can occur without a peak in the cross-correlation (Kirkwood and Sears 1978). This is not to say that the cross-correlation is a useless tool in the interpretation of neural activity but, rather, that it should be used in conjunction

with other tools to best elucidate neural mechanisms. Also, it suggests that further investigation into the possibility of inter-joint coupling is warranted.

A recent study has taken the first step at addressing the question of common drive in rapid movements by analyzing quick voluntary movements of the wrist. These researchers noted the distinct presence of low (5-12Hz) EEG-EMG coherence (Conway et al. 2004) before and during the movements. This is consistent with the low frequency activation of motor cortex noted during rapid voluntary movements (Hoffman and Strick 1995).

While recent studies have suggested that common input may play an important role in the generation of fast feed-forward movements, few studies have investigated coherence in relation to these movements. It will therefore be important to characterize the degree to which muscles involved in these movements receive common input and, further, the modulation in this common input in relation to movement parameters.

2.4 Goals and Hypotheses

The goals of this study are to develop appropriate methodology to characterize common input to synergistic muscles, and to employ this methodology in the investigation of pre-programmed muscle synergies. Hence, an objective is to develop temporal and spectral analyses that are capable of revealing the characteristics of inter-joint coupling.

Following the development of appropriate analysis techniques, the specific hypotheses are:

1. Multi-joint coupling exists even during single-joint movements
2. Coupling (coherence) is modulated with the parameters of a movement.

These hypotheses will be tested during the performance of simple elbow movements. It is expected that similar muscle activation patterns will be observed in wrist flexors and extensors as will be observed in elbow flexors and extensors. Such a result would indicate that the wrist muscle activity is dependent on the elbow muscle activity. Previous research has indicated that the wrist muscles will produce a similar triphasic (agonist-antagonist-agonist bursting) activation pattern to those muscles of the elbow joint (Latash et al. 1995). This triphasic pattern will only be evident in those movements that are too fast to rely upon feedback to control them and, hence, are entirely reliant on feed-forward commands. Following mechanical fixation of the wrist joint, no change in the timing or patterns of EMG in any of the wrist or elbow muscles is expected compared the non-fixed wrist condition.

It is expected that coherence analysis will be capable of revealing common input to muscles. This is important because it provides evidence for 'pre-programmed' synergies based on the fact that the activation of these muscles is synchronized by the nervous system. If coherence is systematically modulated with the performance of various movements, it may be expected that neural synchronization has an important role to play in motor behaviours. Further, the measurement of neural coupling may provide a greater understanding of the changes that take place following injury and subsequent rehabilitation and may therefore aid in improving future rehabilitation interventions.

3 Methodology

3.1 Overview of Experimental Procedures

Able-bodied subjects were instructed to perform many trials of constrained voluntary arm movements in order to characterize the muscle activation patterns associated with the movements. The trials consisted of simple elbow flexion or extension movements about a motor shaft fitted with a potentiometer to measure elbow angle. Electromyographic (EMG) signals were collected from numerous muscles of the arm and forearm to allow for the investigation of coupling between 'elbow' muscles and 'wrist' muscles. In half of the trials, the wrist was mechanically constrained with a strap in order to evaluate the prevalence of feed-forward muscle activation. If the 'neural controller' is, indeed, operating in a feed-forward fashion, then mechanical fixation of the wrist should not change the characteristics of wrist muscle activity. The EMG signals were processed in a temporal fashion in order to understand the characteristics of inter-joint muscle activation patterns and their consistency of activation, as well as in a spectral manner in order to investigate the mechanisms that may give rise to synergistic muscle activation.

3.2 Subjects and Experimental Protocol

Six able-bodied volunteers, 2 females and 4 males, ages 21 – 44 (mean ± SD: 29.3 ± 11.1 years), participated in the study. The subjects manifested neither neurological deficits nor history of upper extremity disease. After signing consent forms approved by Emory University's Human Investigation Committee explaining the experimental protocol and possible risks, subjects were seated in front of a computer monitor with their right forearm resting on a manipulandum secured to a torque motor shaft located coaxially to the elbow joint (PMI Motion Technologies, Commack, New York). The manipulandum allowed elbow flexion and extension movements in the horizontal plane. For all subjects, the shoulder was abducted to 70° and the forearm was pronated with the palm of the hand parallel to the ground (**Figure 1A**). In half of the trials the wrist was immobilized and in the other half it was allowed to move freely. Volitional elbow flexion and extension movements were performed at different amplitudes and velocities starting from a common elbow position (70° of flexion) and against a constant opposing torque equal to 5% maximum voluntary contraction (MVC) of the flexor and extensor muscles depending on direction of movement. Three movement amplitudes (10, 25 and 40°) and five velocities (50, 150, 250, 350 and 450°/s) were used resulting in movement times ranging from 22 ms for the fastest, smallest movements to 800 ms for the slowest, largest movements. Movement amplitude and velocity were controlled by varying the amplitude and slope of a trajectory trace presented to the subjects on the monitor (**Figure 1B**). The vertical spacing of the target trace (the displacement between the upper and lower red boundary traces) was held constant at 5°. Subjects were instructed to maintain the position of the cursor indicating the elbow joint angle within the target trace as closely as possible. The thick blue trace in **Figure 3A** is an

example of a subject's actual elbow trajectory. The various combinations of movement amplitudes and velocities were presented in pseudo-random order and for each movement combination, subjects performed blocks of 12 to 16 trials. Additional trials per movement combination (up to 25) were occasionally obtained if the subject had difficulty concentrating or performing the movement.

3.3 Experimental Setup and Data Acquisition

3.3.1 - Kinematic Measurements

Elbow joint angle was monitored through a potentiometer on the motor shaft. The output of the potentiometer was digitized at a rate of 1000 samples per second, digitally low-pass filtered at 20 Hz and was continuously displayed on the monitor to provide subjects with feedback regarding their elbow position and movement performance. Elbow joint angular velocity was obtained from the first derivative of the angular position trace.

3.3.2 - Electromyographic Activity

Bipolar electromyographic (EMG) activity was recorded from 10 arm and forearm muscles through miniature (4 mm diameter) Ag-AgCl surface electrodes (In Vivo Metric, Healdsburg, California) placed over the belly of each of the muscles of interest. The inter-electrode spacing was 15 mm, and a reference electrode (8 mm diameter) was placed over the subjects' acromion process. Electrode-skin interfacial resistance was 5 kΩ or less. The sampled muscles were the long and short heads of biceps brachii [BB(long) and BB(short)], lateral and long heads of triceps brachii [TB(lat) and TB(long)], brachioradialis (BRD), extensor carpi radialis longus (ECRL), extensor carpi ulnaris (ECU), flexor carpi radialis (FCR), flexor carpi ulnaris (FCU), and anterior deltoid (AD) (**Figure 2**

and 3B). The AD showed virtually no activity for all subjects and, therefore, data from AD were not considered further. Electrode selectivity was determined by supporting the subjects' arm and asking the subject to perform: 1) resisted elbow flexion and extension movements while noting the presence of activity only in BB(long), BB(short), BRD and TB(lat), TB(long), respectively; 2) unresisted forearm supination while noting the presence of activity in the BB(long) and BB(short) electrodes only; and 3) resisted wrist radial and ulnar deviation movements while noting activity only in ECRL, FCR and ECU, FCU, respectively. No attempts were made to ensure selectivity of recordings between BB(long) and BB(short) nor between TB(lat) and TB(long). However, cross-correlation analyses in the time domain, phase estimates in the frequency domain and inspection of the coherence estimates allowed for post-hoc assessment of any potential cross-talk between these muscles.

Prior to the beginning of a movement trial, subjects were presented with the target trajectory trace on the monitor (**Figure 1B**). Subjects were instructed to begin all movements from a common position and to maintain the background EMG activity of the primary agonist (i.e. BB(long) & BB(short for elbow flexion and TB(lat) & TB(long) for elbow extension) muscles at about 5% of the maximum recorded activity from that muscle. In order to ensure the baseline consistency between trials, the data acquisition program was designed such that a trial could not be initiated unless these conditions were met. The EMG signals were bandpass filtered (3 to 300 Hz) and amplified 1000 times.

Subjects began the movements upon receiving an auditory cue presented at a random time between 0.5 and 2 s after the subjects met and maintained the initial conditions criteria described above. The generated EMG activity was digitized at a rate of 1000 samples per second for 2 seconds and saved for later

analysis. The EMG signals were further digitally low-pass filtered at 200 Hz by an 8-pole zero-phase digital Bessel filter and full-wave rectified.

3.4 Data Analysis

All data analyses were performed in Matlab (The MathWorks, Natick, MA) using custom written programs.

3.4.1 - Onset of EMG Activity

The time of first onset (TFO) of EMG activity for each muscle was determined relative to the kinematic onset of elbow movement. **Figure 3A** shows a typical trial of a 40° elbow extension movement performed at 250°/s and **Figure 3B** shows the EMG activity associated with this movement. The solid vertical line in **Figure 3A** and the line at 0ms in **Figure 3B** marks the kinematic onset of elbow movement. Baseline EMG activity was defined as the mean rectified EMG activity within a 100 ms window during the steady hold period before movement onset. The onset of EMG activity in a given muscle was determined by comparing the mean rectified EMG activity within a 15 ms-moving window to the baseline activity. EMG activity was considered to exceed baseline if the activity within the moving window was larger than baseline activity + 2 standard deviations (SD).

3.4.2 - Pre-movement Coherence

In order to assess the degree of coupling that occurs between two muscles before the kinematic onset of a movement, coherence spectrograms (maps of frequency and time) were constructed by performing coherence analysis. In the present study, coherence spectrograms depict the frequency components of

common inputs to pairs of muscles, the change in inputs over the course of a movement, and the modulation of inputs in response to the kinematic demands of the movement.

In order to produce time-coherence spectrograms using Fourier techniques, coherence was computed multiple times across the full range of data using a sliding window. In the present analysis, all trials of each movement combination were temporally aligned to the kinematic onset of the movement and 1.024 seconds (1024 points) of EMG data centred on the kinematic onset were extracted. 1024 points were necessary due to the use of Fast Fourier Transforms (FFT). The sliding window used here consisted of subsets of 256 points (256 ms) overlapped by 224 points (224 ms). Because the first window starts at 1ms (or -512ms relative to the kinematic onset) and ends at 256ms (or -256ms relative to the kinematic onset), the first window is centred on 128ms (or -384ms relative to kinematic onset). The time axis on all of the coherence spectrograms, therefore, represents the centre of the window in which coherence was calculated. A schematic representation of the sliding window methodology is given in **Figure 4**. These same subsets were also extracted from all trials of the same movement and subsequently concatenated together to produce a record with a length equal to 256 times the number of trials. Multiple 256 point FFTs were calculated within each time interval, permitting a frequency resolution of about 3.9 Hz. Each 256 point section was linearly de-trended to ameliorate possible non-stationarities and fit with a Hanning window to improve the spectral estimate by reducing spectral "leakage" prior to the calculation of the FFT (Farmer et al. 1993). Auto- and cross-spectra were obtained (Halliday et al. 1995) from the FFTs and coherence was then calculated between pairs of muscles as:

$$\left|R_{yx}(\lambda)\right|^2 = \frac{\left|f_{yx}(\lambda)\right|^2}{f_{xx}(\lambda)\cdot f_{yy}(\lambda)}$$

where f_{yx} is the cross-spectrum between two muscles while f_{xx} and f_{yy} are the autospectra of each individual muscle (Halliday et al. 1995). Statistical confidence limits of 95% (α=0.05) were constructed for the coherence estimate according to:

$$S = 1 - \alpha^{1/(L-1)}$$

where L represents the number of sections (FFTs) used to calculate coherence and S represents the computed confidence interval (Rosenberg et al. 1989). For clarity of representation in the spectrogram, coherence values below the statistical confidence limits were suppressed (Baker et al. 1997). Coherence was computed for each window of time across the extracted 1024 points of data, producing 25 overlapped time intervals aligned as per **Figure 5**. Data were plotted as a two dimensional map with frequency on the ordinate axis and time on the abscissa (Baker et al. 1997; Kilner et al. 1999). Rather than utilizing a surface plot, contour lines depicting the slope of adjacent coherence windows were generated for visual representation. **Figure 6** shows the generation of these contour lines and their relationship to the discrete windowed coherence estimates. Finally, **Figure 7** shows the same coherence spectrogram in its final form aligned to the mean EMG of all trials used to compute it. Qualitatively, it can be seen that the largest peaks in coherence in that example bear a strong relationship to the mean TFO of the EMG.

Cross-correlation and phase plots were calculated as diagnostic tests of the

validity of the coherence estimates (Rosenberg et al. 1989). Cross-correlations were calculated with an inverse FFT of the cross-spectrum between two muscles. Phase represented the argument (angle) of the cross-spectrum. Voltage conduction across electrodes (electrode cross-talk) would be seen as a narrow spike in the cross-correlation at time zero or a nearly flat phase estimate (Halliday et al. 1995). Muscle pairs that may be expected to contain cross-talk (i.e. BB(short) and BB(long)) were excluded from further analysis.

3.4.3 - Validation of Coherence

In the above analysis, 95% confidence limits were applied to all of the coherence estimates based on published methodology (Rosenberg et al. 1989). However, in order to rule out the potential for coincidental coherence as opposed to true inter-muscular coherence due to neural mechanisms, two checks were conducted. Firstly, data were qualitatively assessed to determine if the simple coincidence of EMG activity produced coherence. If that were the case, it would not be possible to determine what amount of coherence is due to physiological mechanisms and what is not. **Figure 8** shows an example of this qualitative assessment. More rigourously, a second test of the null hypothesis was constructed. For each muscle pair and movement condition, data were "shuffled" by performing coherence analysis on the same sections of data, but from mismatching trials. This technique is analogous to the 'shift predictor' that is commonly performed for cross correlations. The cross-correlation technique is commonly used to determine synchrony between the firing patterns of two single cells. For that technique, one firing record is compared against another record of a cell from a different trial. Essentially, this removes any 'real' physical relationship between the two records, and leaves only the cross correlation caused by the co-variation of the two cells' firing rates. Thus, the subtraction of

the predictor from the proper cross correlation (computed between the same two cells, but from the same trial), produces the relationship between the two cells that can be attributed to synaptic connectivity or common input.

In the frequency domain, there have been no reports of a similar technique to the shift predictor. In this study, however, the 'shuffled' coherence is seen as an important step in validating and confirming the prevalence of 'real' coherence due to neuronal interconnectivity. For a particular movement consisting of multiple trials, coherence was computed on each of the corresponding sections of data from another trial (**Figure 9A**). The null hypothesis was computed in four different frequency bands on a mis-matched trial (**Figure 9B/C**). The mean and standard deviation from each frequency band was calculated. A coherence estimate was deemed significant if its value exceeded the mean plus 2 standard deviations of the coherence calculated from shuffled data in the same frequency band. Fifty-four percent (5609/10198) of the muscle pair/condition combinations were deemed significant and used for further analysis. All of the coherence spectrograms shown in the results have been subjected to new confidence limits based on their own shuffled coherences. A significant ($p<0.01$; t-test) difference was seen between the properly aligned and the shuffled data in each frequency band (**Figure 9C**), indicating that the coherence reported herein is due to neural mechanisms and are not methodological artifacts. This result is a confirmation of this technique and, further, suggests that caution must be exercised when computing coherence between records from different trials.

A final diagnostic test of the shuffling technique was performed whereby all of the trials were aligned to the same TFO, as opposed to the kinematic onset. This test thus ensured that all of the EMG activity was, in fact, perfectly temporally aligned. **Figure 9** shows the results of this test. Even though all

trials' EMG was aligned to the same onset, the shuffled coherence was greatly reduced from the properly aligned coherence estimate.

3.4.4 - Statistical Analysis

The effect of movement amplitude and velocity (movement time) on the time of first onset (TFO) of muscle activity was statistically assessed using Maximum Likelihood Repeated Measures analysis of variance (ANOVA) and Tukey Honestly Significant Difference (THSD) post-hoc analysis. These analyses were used to determine the between-muscle TFO differences per movement combination and the within-muscle TFO differences across movement combinations.

To compare coherence between conditions, all significantly coherent muscle pairs were divided into one of two groups based on the condition to be tested (i.e. wrist mobility and movement direction) and the groups were compared with a t-test ($p<0.05$). To quantify the degree of coherence, the average coherence from 200ms before the movement onset to movement onset was computed for each movement. In order to assess whether coherence is related to the speed of the upcoming movement, simple linear correlation was performed for average coherence versus actual movement time. A power (exponential decay) fit was computed. Pearson r of each correlation was calculated and assessed for significance.

3.4.5 – Comparison Across All Conditions

In order to compare the prevalence of coherence obtained across various movement parameters, analysis was conducted in which unshuffled coherence was compared to shuffled coherence for all combinations of muscle pairs and

movement conditions in each of the four frequency bands. Each band was determined to contain significant coherence if its unshuffled value exceeded the shuffled value plus two standard deviations. If any of the bands passed this test, that particular combination was given a value of 1. Otherwise, it received a value of 0. The prevalence of coherence (as shown in **Figures 19-21**) is therefore expressed as a percentage of how frequently that muscle combination contained significant coherence.

3.4.6 – Data Sufficiency

In the FFT-based spectral analysis approach, there is a systematic trade-off between frequency resolution and confidence limits. This is because frequency resolution is determined by the FFT section length over the sampling rate and the confidence limits are proportional to the number of FFT sections used. In the present analysis ~4Hz frequency resolution was deemed acceptable, which means that 256ms FFT sections were employed. Smaller sections would produce coarser frequency resolution but permit more sections (and, hence, lower confidence limits) and vice versa. The analysis performed in this study used the combined data from multiple trials, so a simulation was constructed to determine how many trials would be necessary to detect coherence confidently. **Figure 11** depicts this simulation for a subset of data from the present study. Coherence and confidence limits were calculated for all numbers of trials available (up to 15). The amount of coherence over the confidence limits was calculated for each number of trials. No coherence could be detected with a few trials, but, as more trials were employed, the amount of coherence detected increased until it began to plateau. The sigmoidal shape of the resulting average detected coherence would suggest that adding more trials would have little effect on the estimate of coherence for this study.

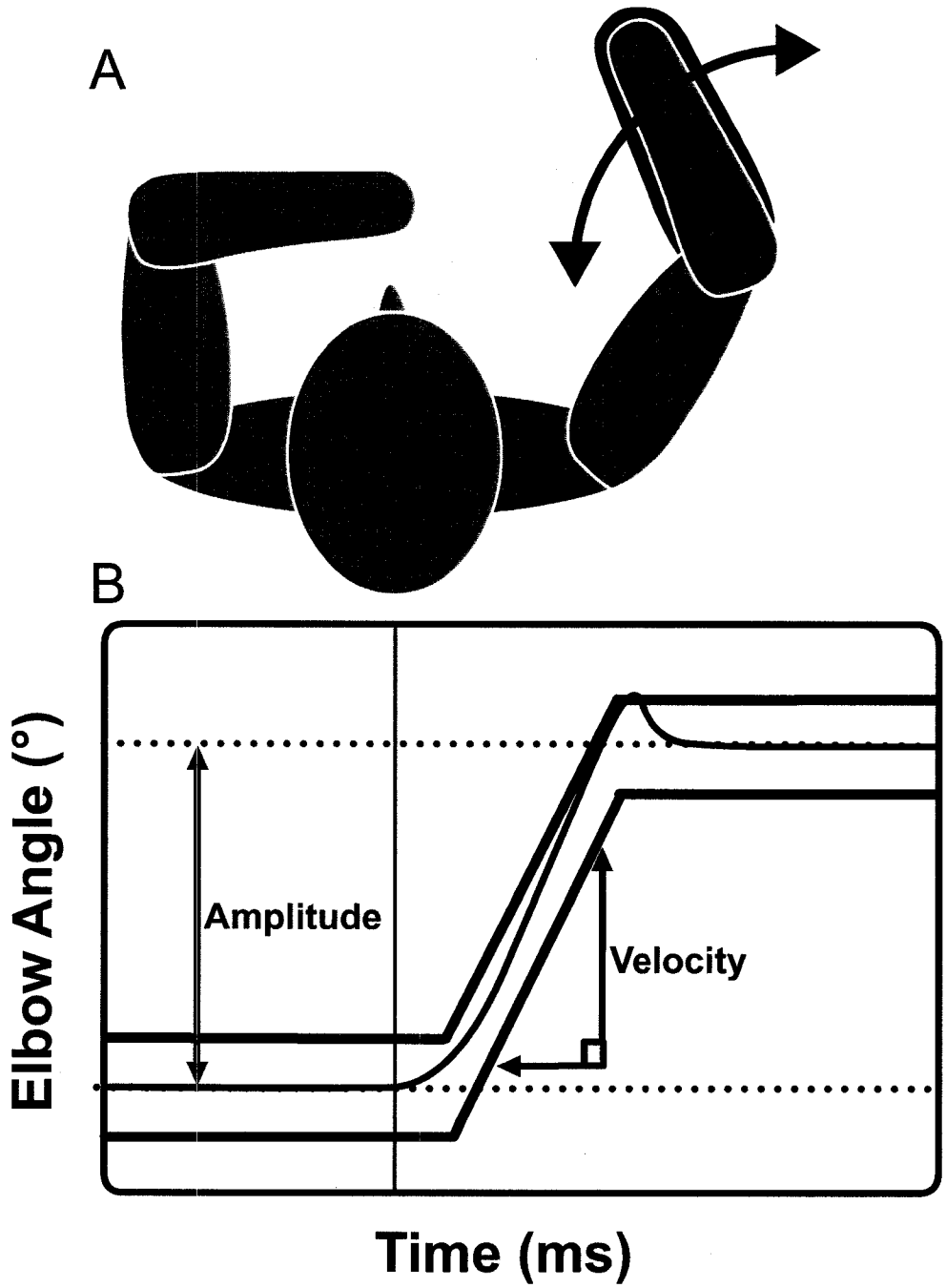

Figure 1: Schematic of the procedural setup. (A) A view of a subject with his/her right arm constrained at the elbow. The mechanical setup allowed elbow flexion or extension with an abducted arm. **(B)** An example view of the trace that the subjects were presented with. The red lines represent the desired combination of excursion (amplitude) and velocity. The blue line represents the real-time trace of the subjects' elbow position while the movement was performed. By varying the slope and distance between the two red lines, all combinations of velocity and amplitude could be performed.

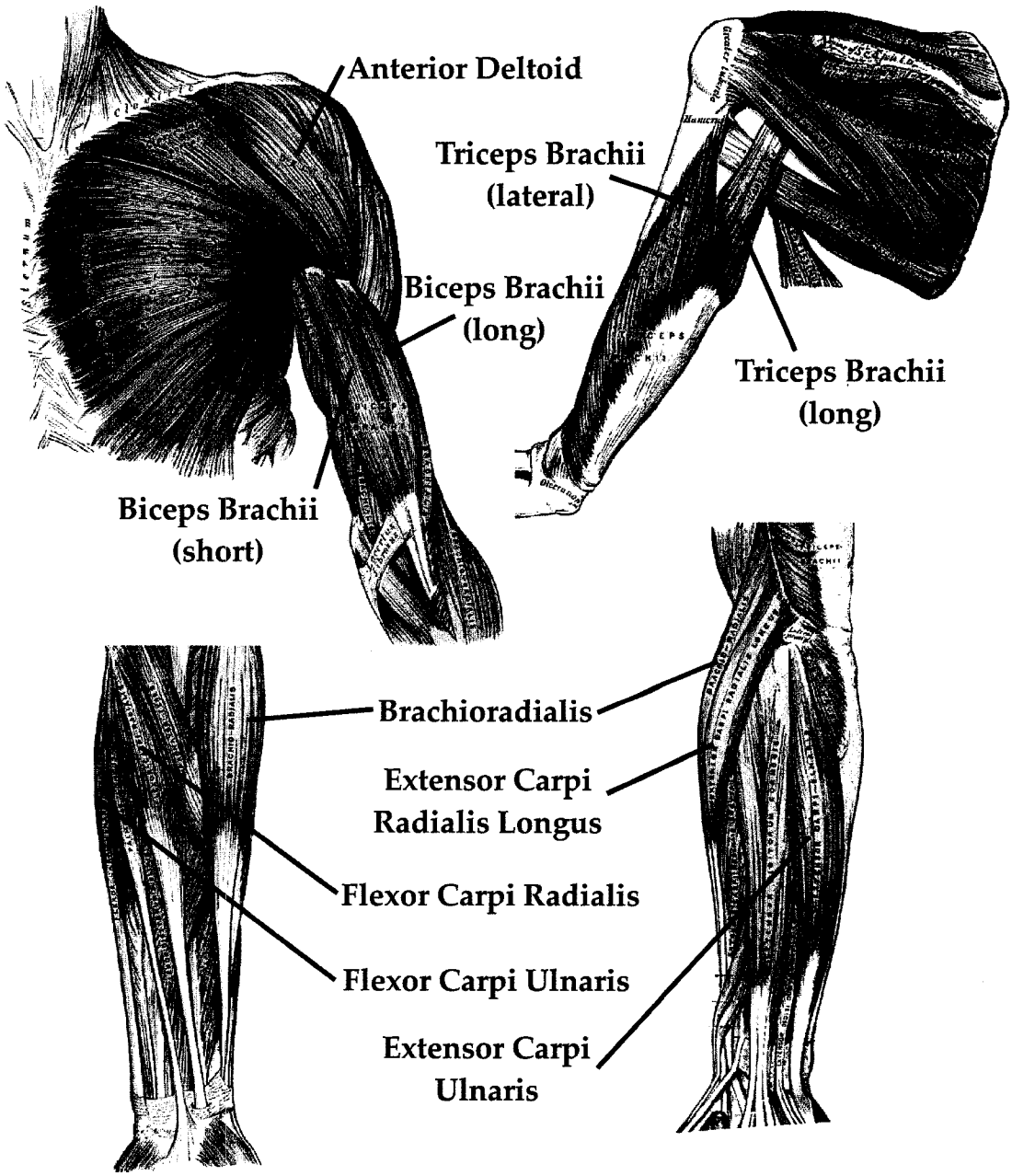

Figure 2: All muscles from which data were collected. Shown are the muscles used for recording EMG activity. AD, anterior deltoid; BB(long), long head of biceps brachii; BB(short), short head of biceps brachii; BRD, brachioradialis; ECRL, extensor carpi radialis longus; ECU, extensor carpi ulnaris; FCR, flexor carpi radialis; FCU, flexor carpi ulnaris; TB(lat), lateral head of triceps brachii; TB(long), long head of triceps brachii.

(Images from Gray's Anatomy, 1918)

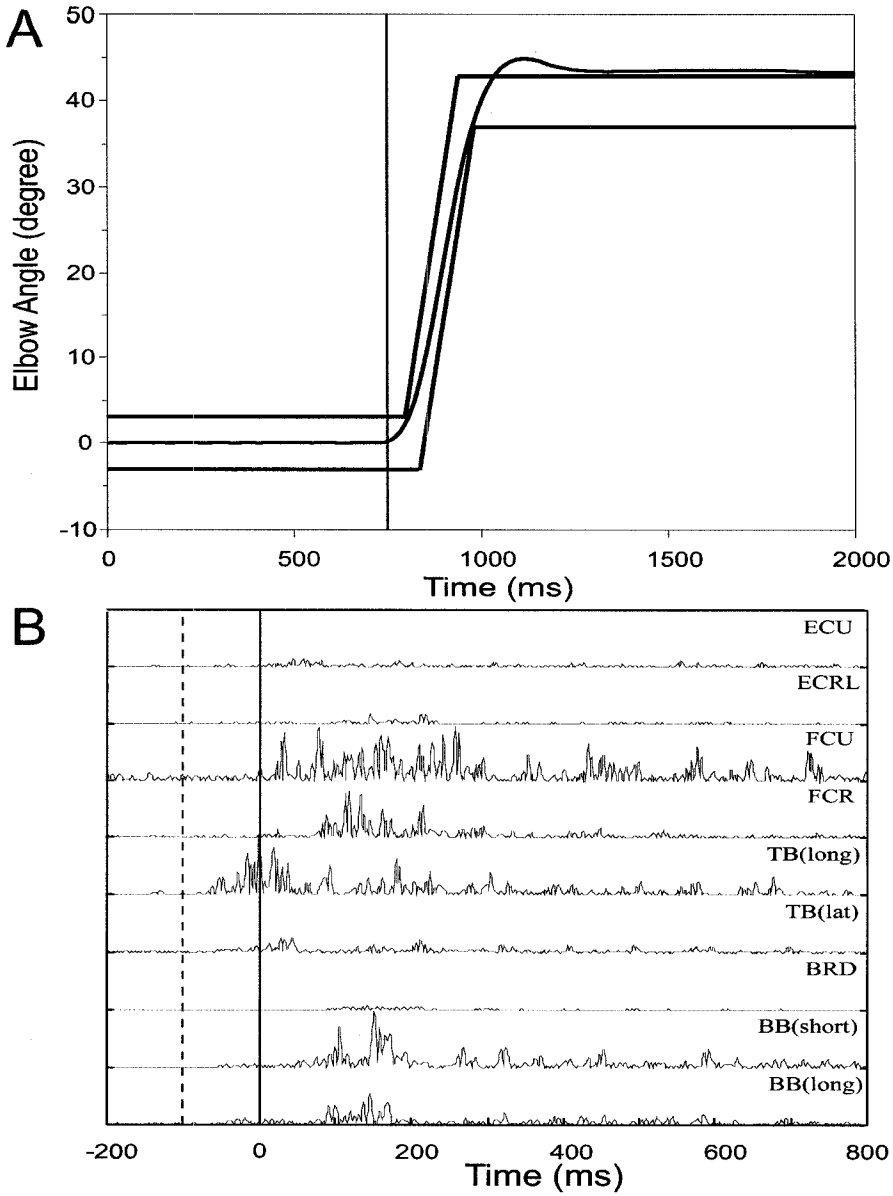

Figure 3: Example of kinematic and EMG data. (A) Shown is an example of a target trace displayed on the monitor in front of the subjects. The trace represents an elbow extension trial, in which the subject was required to move 40 deg at a velocity of 250 deg/s. The blue trace represents the subject's actual elbow movement **(B)** The corresponding EMG activity recorded during the elbow extension trial in **A**. The activity was rectified and normalized to the maximum EMG activity obtained at 50% of maximum voluntary isometric contraction. The solid line at 0ms represents the kinematic onset of elbow movement. Detection of EMG activity began 100ms prior to the onset of movement. Baseline EMG activity was collected over a 100ms duration starting 200ms prior to the onset of movement (i.e. 200 to 100ms). Abbreviations: BB(long), long head of biceps brachii; BB(short), short head of biceps brachii; BRD, brachioradialis; ECRL, extensor carpi radialis longus; ECU, extensor carpi ulnaris; FCR, flexor carpi radialis; FCU, flexor carpi ulnaris; TB(lat), lateral head of triceps brachii; TB(long), long head of triceps brachii.

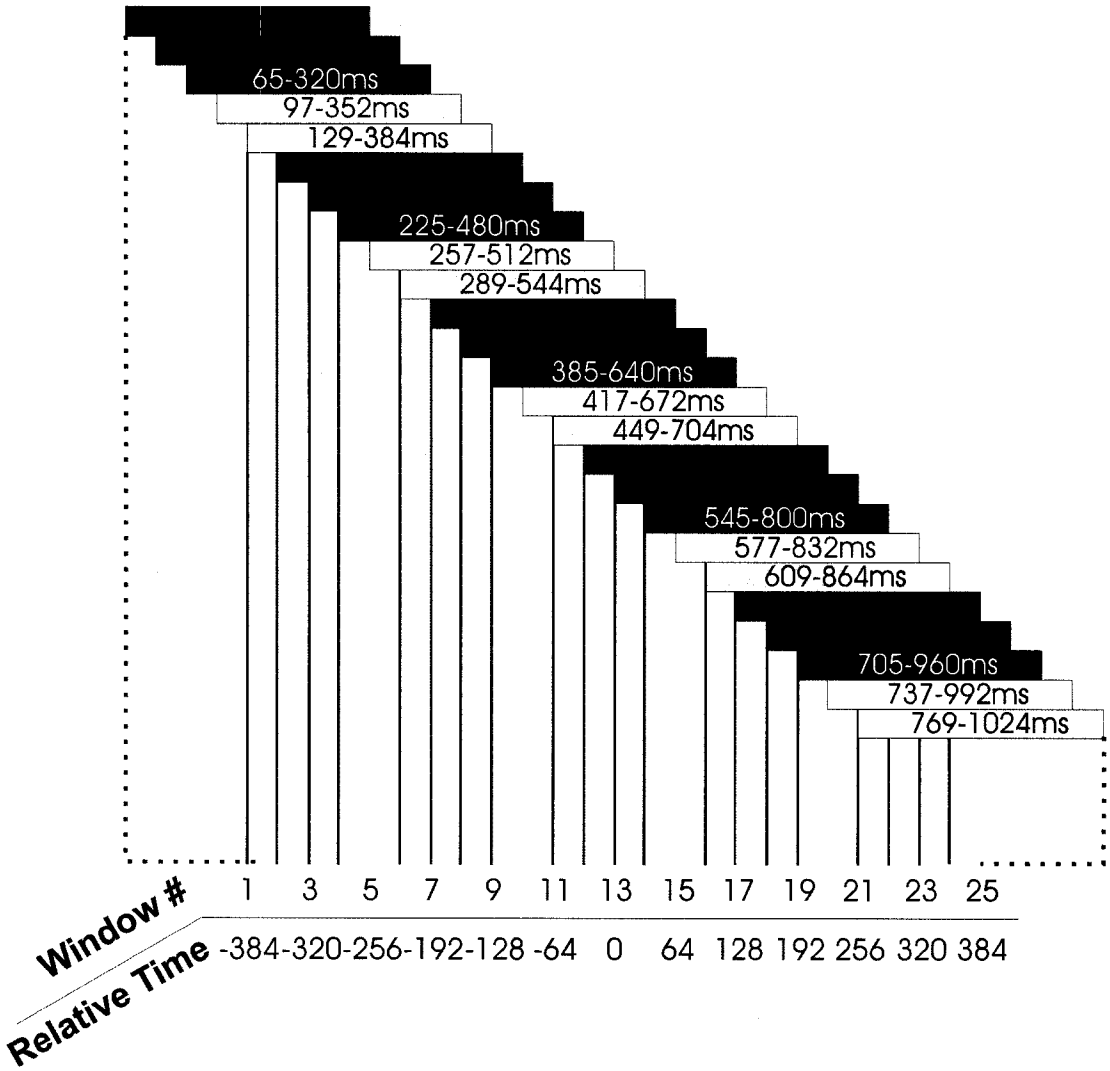

Figure 4: Schematic of construction of coherence spectrograms. Shown is a simple schematic of the sliding window technique used to create time-coherence plots (spectrograms). At this stage, all EMG data has been aligned to the kinematic onset of the movement. 1024 points centred on the kinematic onset of the movement were extracted from the original data. Therefore, each rectangle represents one 256ms window of data. The numbers inside the boxes represent the indices of the data points contained within each box. The lines descending from the rectangles represent the centre of each successive window. The bottom two rows represent the window number (out of 25 total time windows), as well as the centre of each window relative to 0ms being the kinematic onset of the movement.

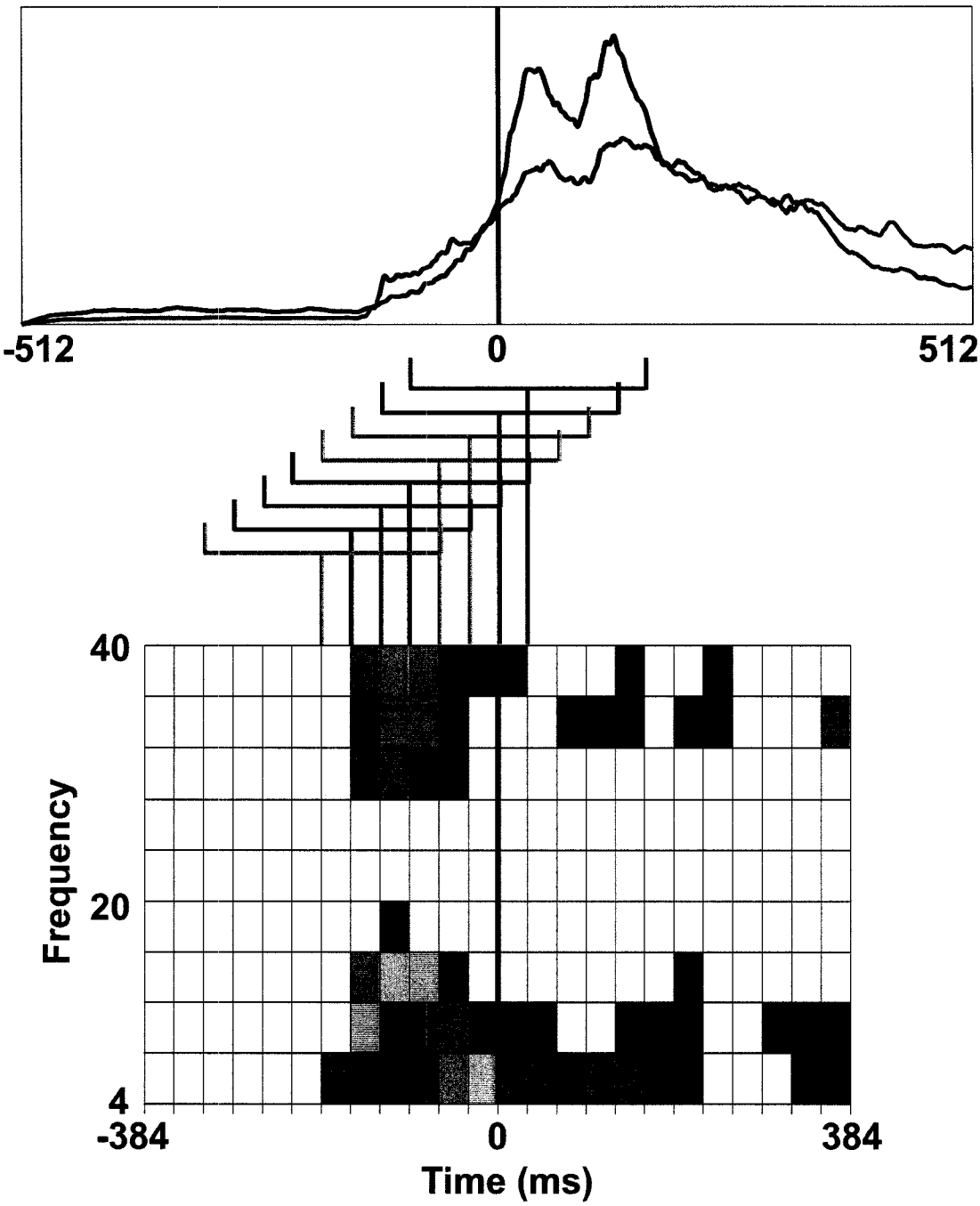

Figure 5: Construction of coherence spectrograms. Shown is an example of how the algorithm computes a time-coherence map. The top shows EMG from two muscles averaged across all trials of one particular movement. The bottom shows the coherence spectrogram computed by windowing successive periods of EMG. The lines in the middle show how the EMG data is aligned with the spectrogram for some example windows.

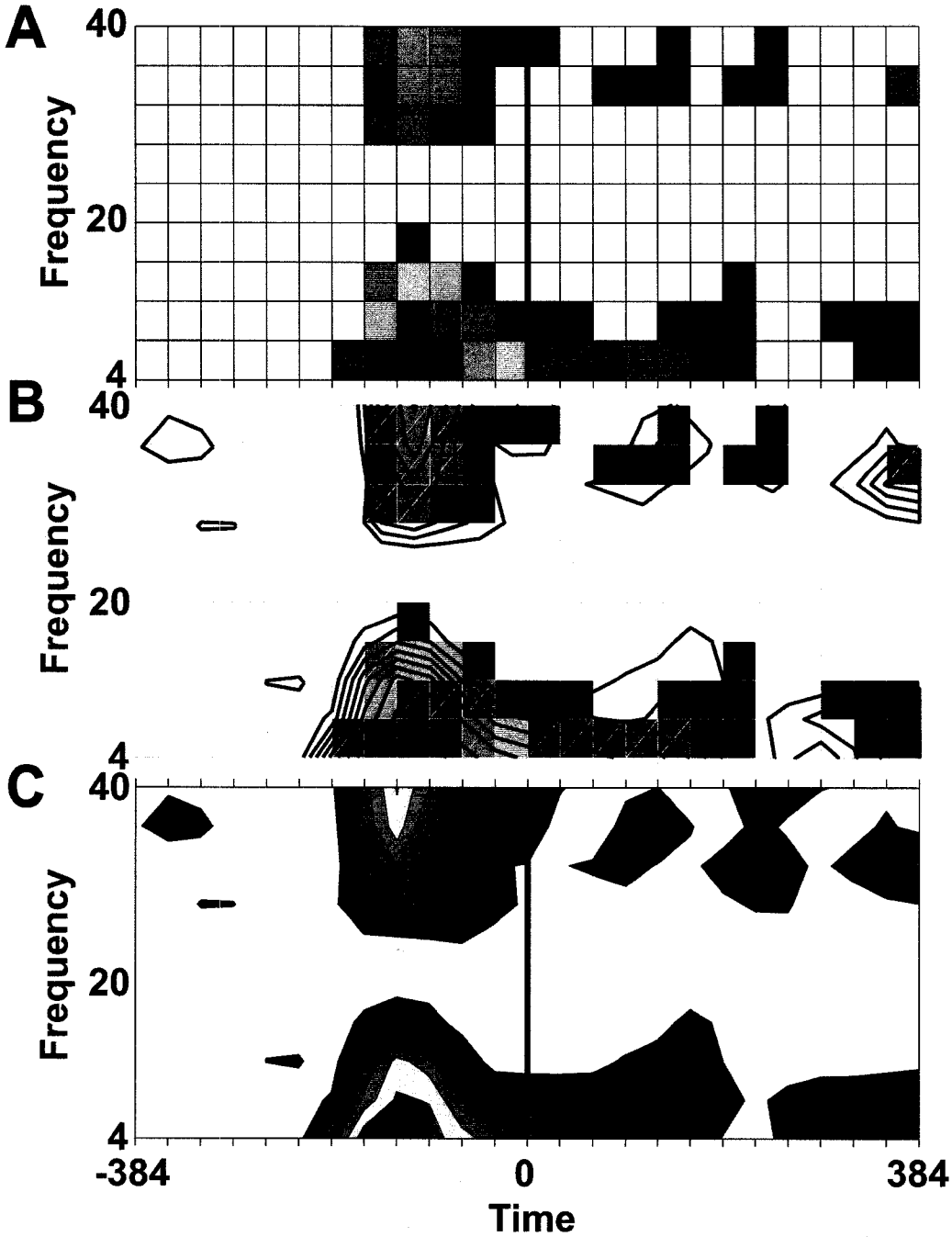

Figure 6: Depiction of contour line generation. Shown is the same coherence spectrogram as in Figures 4. **A**) The original surface plot that is constructed from the successive windowing technique previously discussed. **B**) The same surface plot shown with contour lines overlain on it. The contour lines depict the slope of adjacent windows and give the appearance of non-discrete windows. **C**) The final coherence spectrogram using only filled contours. All subsequent spectrograms are presented in this manner.

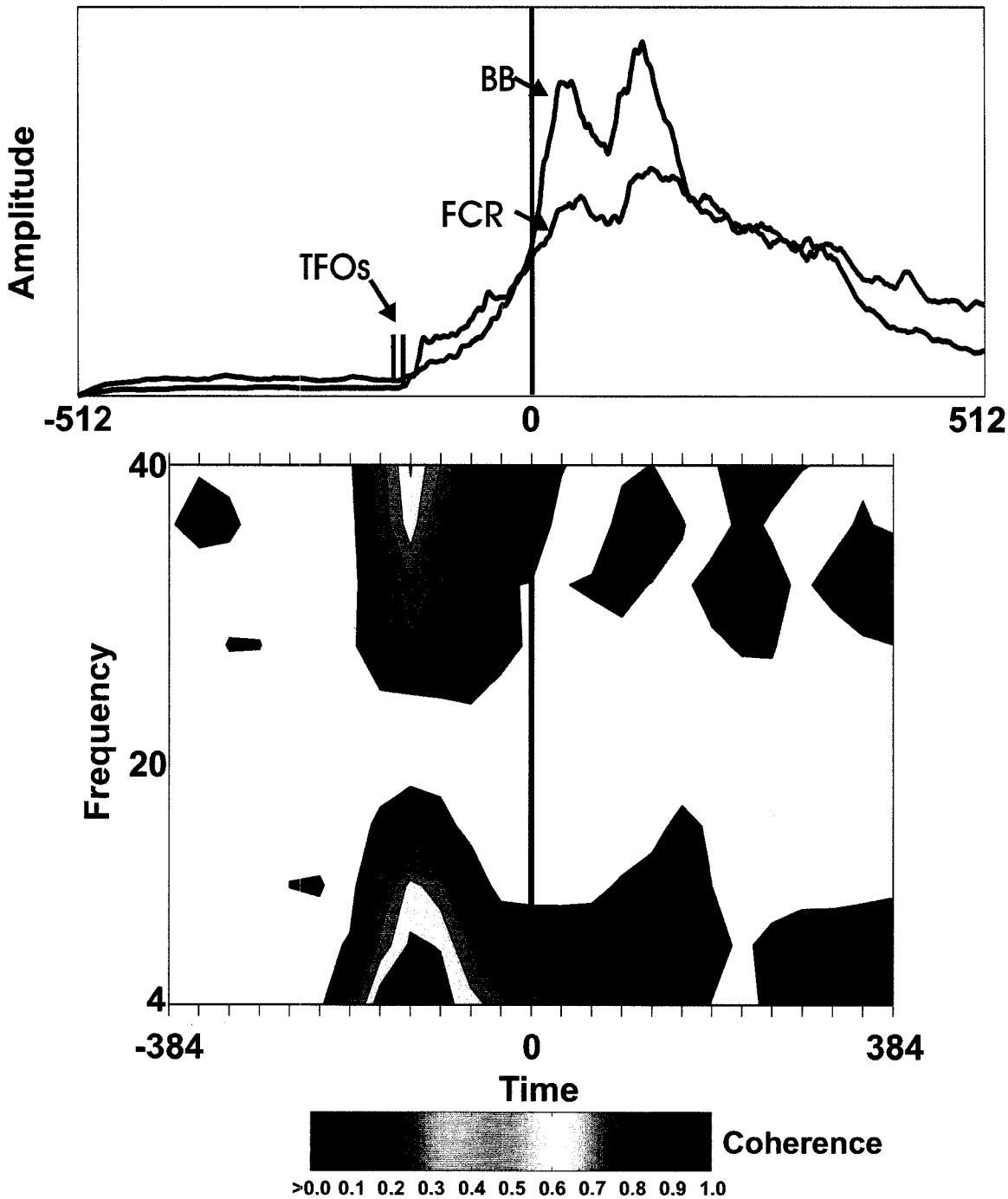

Figure 7: Distinct coherence peaks appear to be related to the onset of EMG activity TFOs. An example of coherence for a muscle pair in one movement condition. The top plot is the average rectified EMG trace versus time generated during all trials of a movement for each of the two muscles. The vertical lines indicate the average time of first onset of EMG activity in the constituent EMG patterns. At the bottom is a frequency spectrogram that plots frequency vertically and time horizontally to show the temporal evolution of coherence throughout the course of the movement. The value of coherence is as per the colour bar.

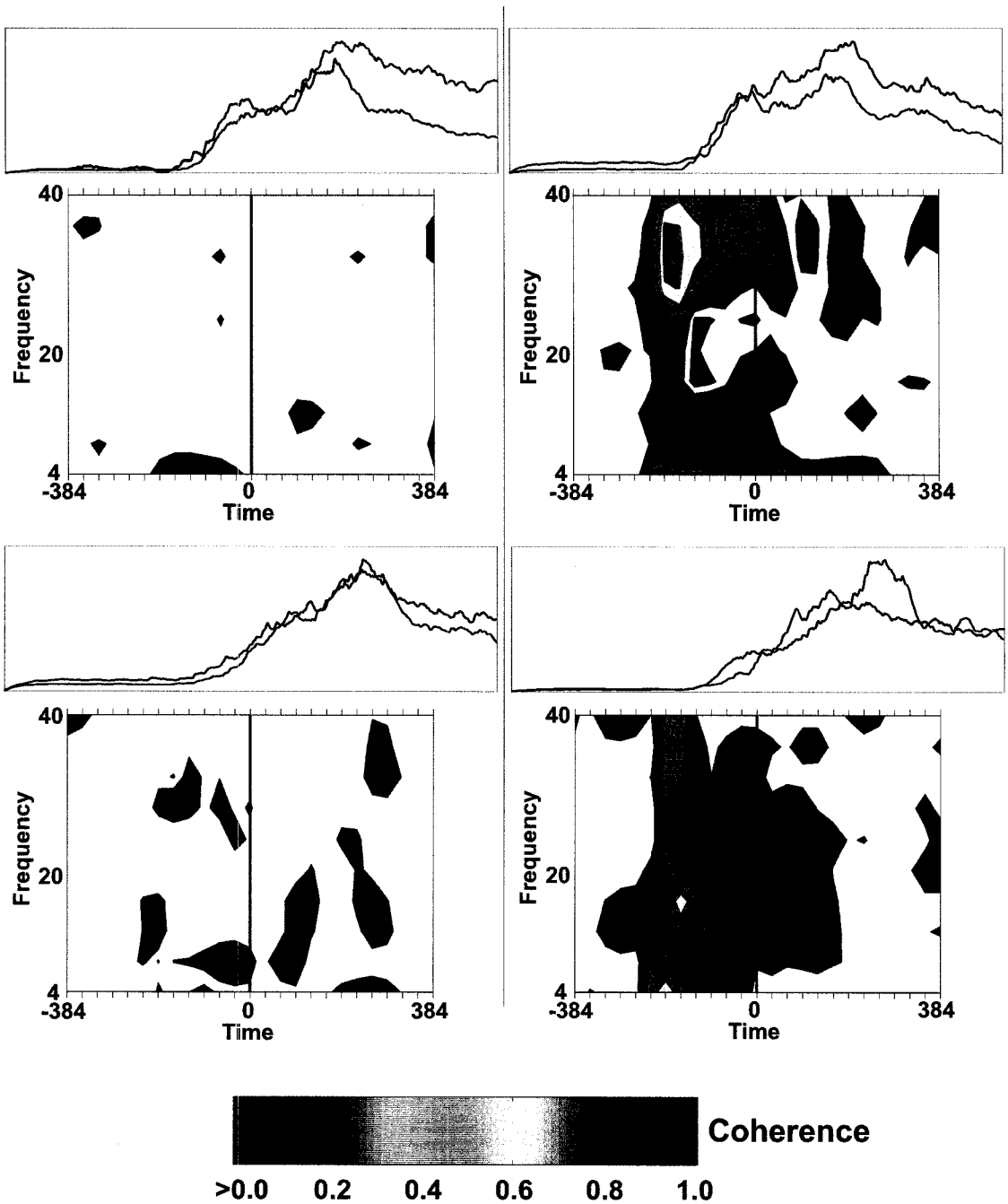

Figure 8: The temporal alignment of EMG activity does not necessarily produce coherence. As a qualitative confirmation of the results, shown are four example spectrograms computed from different muscle pairs. Importantly, allEMG patterns appear to be approximately temporally coincident. However, only the two example spectrograms on the right exhibit appreciable coherence. Thus, coherence is not simply a result of temporally aligning phasic EMG traces.

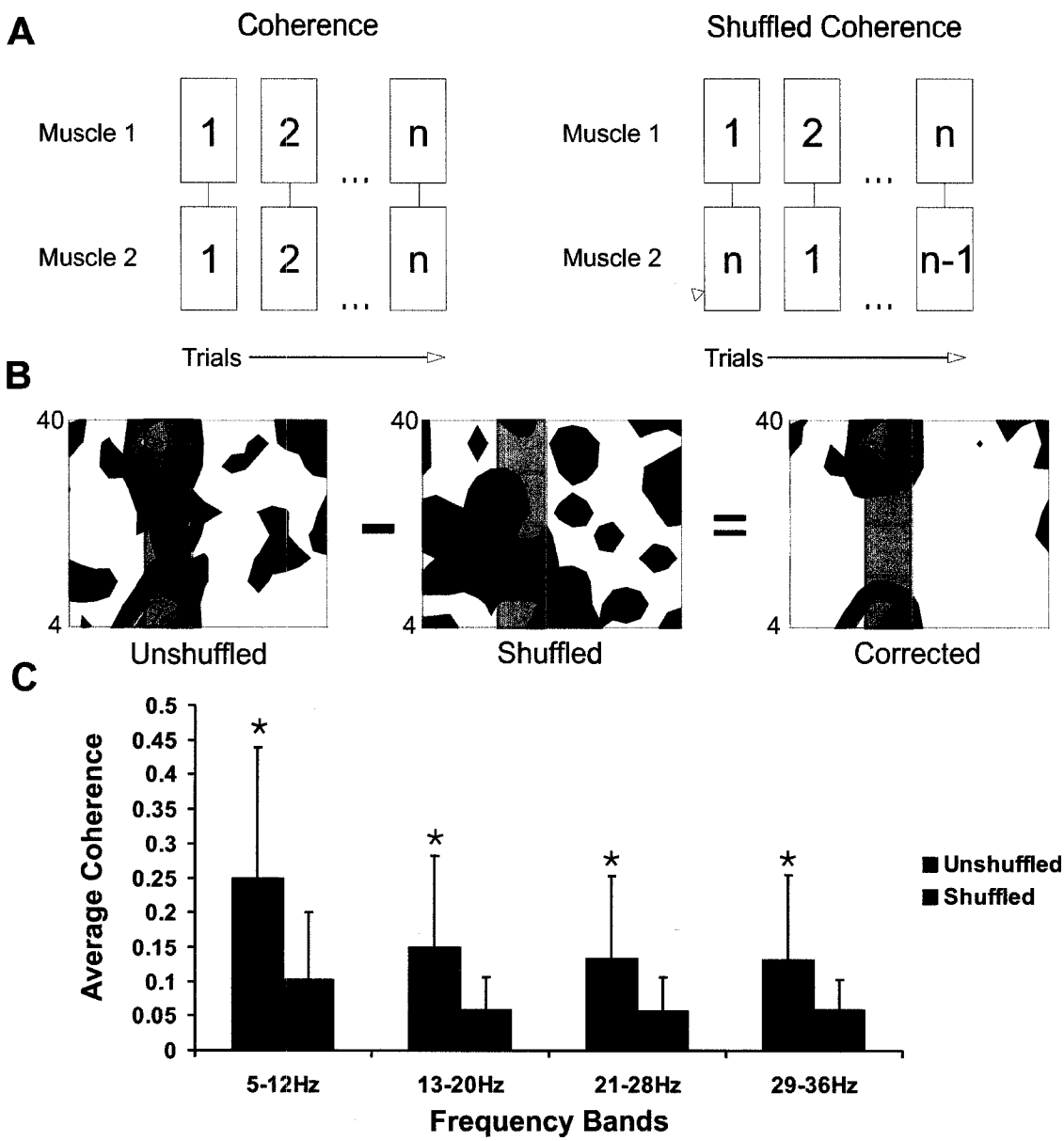

Figure 9: Schematic and Example of Shuffling Procedure. In order to place confidence in the coherence estimates, a second test of the null hypothesis was calculated to determine what level of coherence might be expected coincidentally. **(A)** Schematic representation of the method used to test the null hypothesis. The actual coherence estimate was computed using corresponding sections of the same trial for each muscle (left). To produce the null hypothesis, coherence was computed from one section of a trial versus the corresponding sections of each other trial (right). The average of the misaligned trials - the "shuffled" coherence - was used as a baseline to validate the actual coherence estimates. **(B)** An example of the reduction of an unshuffled coherence estimate using shuffled coherences to produce a final result. New confidence limits are computed for four frequency bands shown with the red overlay **(C)** The results of the shuffling from all subjects and conditions. Properly computed coherence for all muscle pairs/ combinations show significantly increased coherence than shuffled data do in all four of the frequency bands.

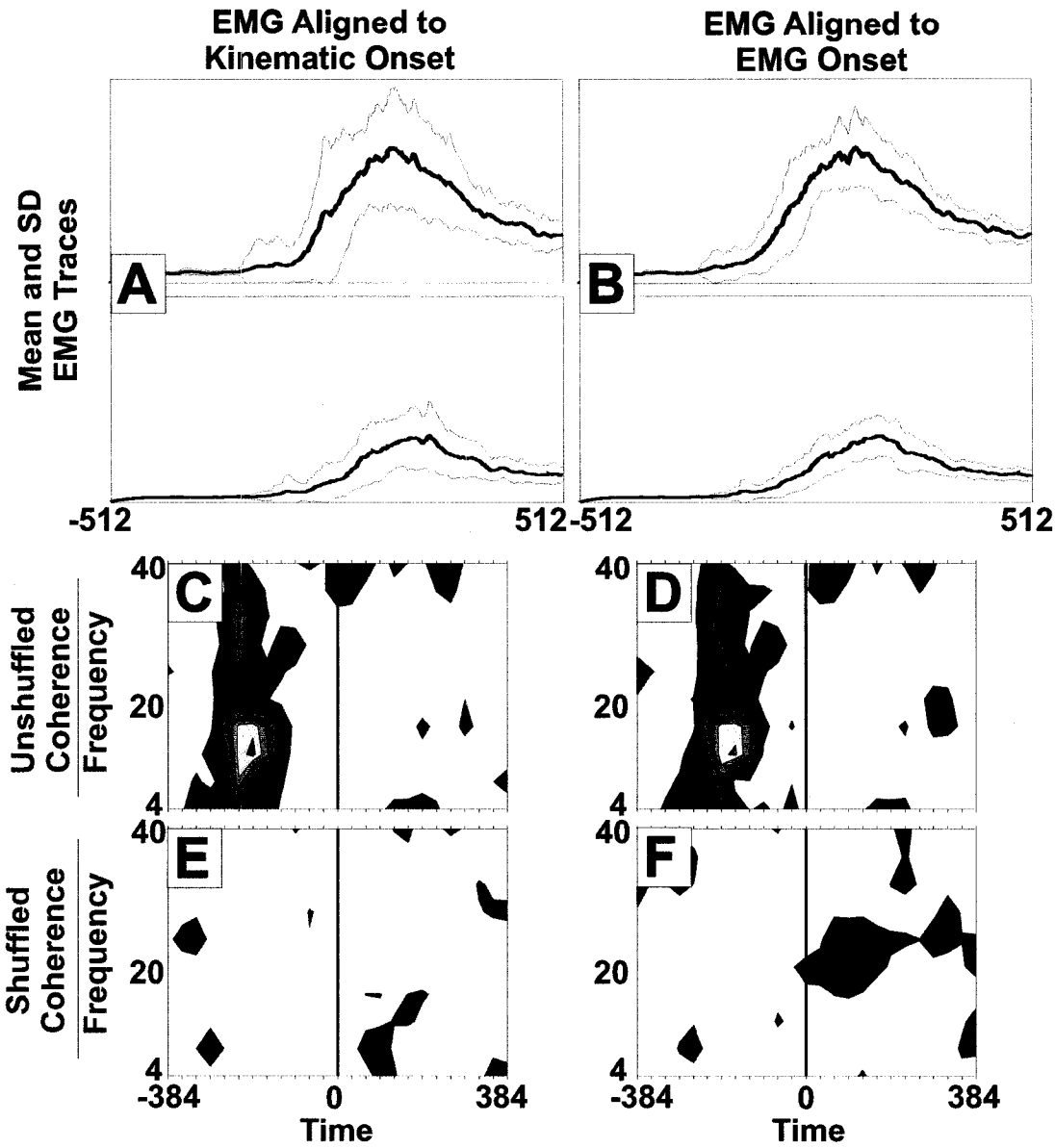

Figure 10: Shuffling trials produces little coherence even if EMG onset times are purposefully aligned. Shown are the results of a stringent confirmation of the shuffling technique. The left column represents a properly computed spectrogram between two muscles with all trials aligned to the kinematic onset and the right column shows the same trials aligned to the same EMG onset. **(A&B)** The mean and SD of all of the EMG traces used to compute the spectrograms. **(C&D)** The spectrograms computed from A & B, respectively. **(E&F)** Little coherence is produced after the shuffling procedure whether the EMG activity is aligned to the kinematic onset (E) or to a common EMG onset (F). This example was chosen because coherence was exhibited when EMG activity was aligned either to the kinematic onset or to a common EMG onset. Thus, the TFOs of all trials were highly consistent, anyway. This explains why coherence was produced when EMG was 'artificially' aligned to a common onset.

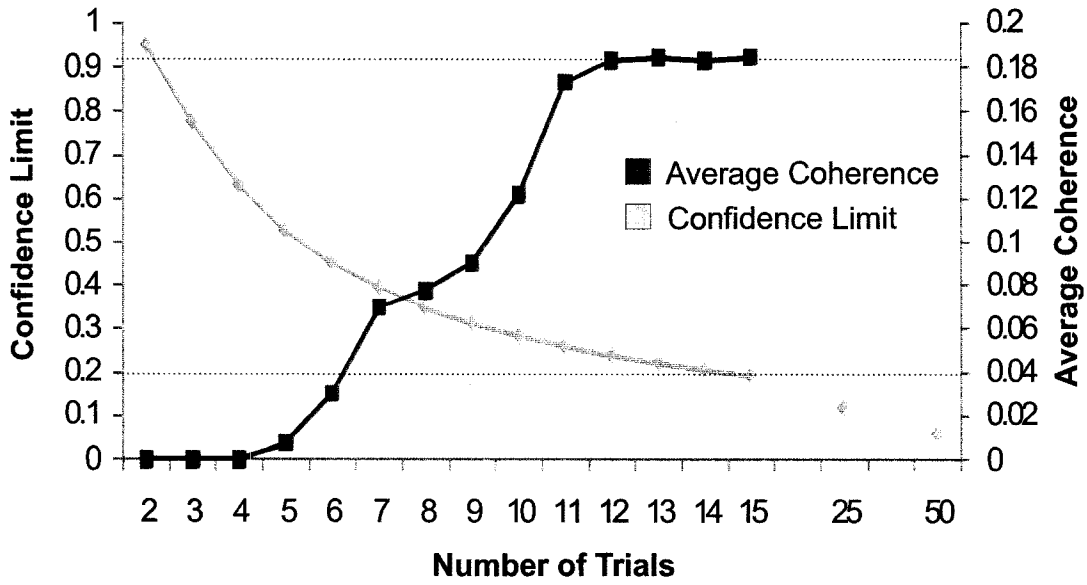

Figure 11: Data Sufficiency Simulation. Comparison of number of trials used to compute spectrograms to confidence limits and detected average coherence. Significant coherence was calculated for various numbers of trials to determine the amount of coherence that could be detected with each set of trials. Importantly, the detected coherence appears to plateau after 11 trials, suggesting that the 15 trials used in these experiments is sufficient. Further, because confidence limits are based on the number of trials, many more trials would need to be used in order to lower the confidence limits appreciably.

4 Results

4.1 Kinematics and EMG

4.1.1 - Kinematics of Performed Movements

The kinematics of all performed elbow movements fell within previously reported results (i.e. Brooks 1986). The mean kinematic performance of all subjects for elbow flexion and extension movements is illustrated in **Figure 12.** The actual or measured elbow velocity is plotted versus the target or control velocity in **Figures 12A and D** for elbow flexion and extension movements, respectively. For all subjects, higher movement velocities were achieved at larger movement amplitudes. On average, the maximally achieved movement velocities were 150, 250 and 350°/s for the 10, 25 and 40° movement amplitudes, respectively. Thus, 450°/s was not often achieved by any of the subjects. Using the lines of identity as a reference, it can be seen that the actual velocity was usually less than the target velocity for target velocities greater than 150°/s (**Figures 12A, D**). The measured primary movement amplitude is plotted versus the control amplitude in **Figures 12B and E** for elbow flexion and extension movements, respectively. Primary movement amplitude refers to the amplitude

of the elbow movement from the initial position to the maximum excursion including target overshoot (Rosenbaum 1991). The secondary movement amplitude for all elbow flexion and extension movements is plotted in Figures **12C and F (insets in B and E)**, respectively. Secondary movement amplitude refers to the magnitude of movement performed by the subjects to correct for missing the target (overshooting or undershooting). Overshoot increased with decreasing movement time.

4.1.2 - Effect of Kinematics on Temporal Patterns of EMG Activity

During low-velocity/high-amplitude movements (i.e., long movement times) agonist elbow and wrist muscles were predominantly activated. With increasing movement velocities and decreasing amplitudes (i.e., decreasing movement times), both agonist and antagonist muscles were recruited. **Figure 13** shows the average EMG activity patterns recorded from the sampled arm (**Figure 13A**) and forearm (**Figure 13B**) muscles in one subject while performing elbow extension movements. The patterns demonstrate that the amplitude of EMG activity in all muscles was dependent on movement velocity. This dependence was particularly evident at the 25° and 40° movement amplitudes. While the activity in all muscles was small and constant at the low velocities (50 and 150°/s), it became crisp and burst-like at higher velocities (250°/s and higher). The 150 - 450°/s EMG traces for the 10° movement amplitude in **Figure 13** are overlapped since the subject was unable to perform the target movements faster than 150°/s (see **Figure 12**). The classical triphasic EMG activity pattern was visible at high velocities between the elbow extensors and flexors. The triphasic EMG pattern was also evident between the wrist ulnar and radial deviators (**Figure 13B**). **Figure 13C** shows all the wrist muscles during elbow flexion between the two conditions of wrist mobility: wrist fixed or wrist free. Note that the patterns of

wrist muscle activity are largely indifferent to the mobility of the wrist.

The TFO of EMG activity in the arm and forearm muscles depended on movement kinematics. To demonstrate this dependence, the TFO of muscle activity from all subjects during elbow flexion movements was plotted as a function of target movement velocity and amplitude in **Figure 14A**. The variability in onset of EMG activity at low velocities was larger than that at higher velocities. At higher velocities, the TFO became regular and all muscles were consistently activated at the same time (e.g., all muscles were activated 0 to 47 ms apart during the 250 to 450°/s target velocities of the 10° amplitude movements). Furthermore, at all velocities, the TFO of wrist muscles was statistically similar ($p>0.05$; ANOVA) to that of elbow muscles, implying that the elbow and wrist acted in concert (i.e. cooperatively) when performing the elbow movements. Between-muscle temporal interactions for all elbow flexion and extension movements provided several general observations. First, the EMG onset latencies of elbow flexor and extensor muscles were significantly different from each other ($p<0.05$; ANOVA). Second, the onset latencies of elbow flexors and wrist flexors/radial deviators (especially FCR) were statistically similar ($p>0.05$; ANOVA), as were the onset latencies of elbow extensors and wrist extensors/ulnar deviators (especially ECU). Third, the onset latencies of all forearm muscles were statistically similar ($p>0.05$; ANOVA) within the majority of elbow flexion and extension movement combinations. Figure 11B shows all of the wrist muscles during elbow flexion movements between the two conditions of wrist mobility. Note that the TFOs of all wrist muscles are largely invariant between the two conditions.

4.2 Coherence

4.2.1 - Consistency of Coherence Between Subjects

The consistency between subjects was calculated for all movement conditions. Qualitatively, it was observed that there was a reasonable degree of consistency between subjects performing the same task. **Figure 15A** shows four example coherence plots of individual subjects performing the same task to highlight their similarity. **Figure 15B** shows mean and standard deviation spectrograms computed across all subjects for the movement task depicted in **Figure 15A.** The mean of these inter-subject trials appears close to each individual trial and, also, the standard deviation map is quite low at all times and frequencies, indicating that all subjects were consistent for this task. The mean, standard deviation and coefficient of variation for each frequency band and for each set of movement conditions was computed across all subjects and the average coefficients of variation for each frequency band are summarized in **Table 1.** The summary indicates that coherence values were somewhat consistent across all subjects for all movement conditions.

Table 1: Summary of Coherence Consistency Between Subjects

Frequency Band	Mean Coefficient of Variation (%)	Range
5-12Hz	21%	4% - 38%
13-20Hz	27%	5%-44%
21-28Hz	18%	4% - 31%
29-36Hz	13%	4%-24%

4.2.2 - Pre-Movement Coherence

Figure 16 shows coherence spectrograms computed for three muscle pairs during extension in a representative subject. Each of the spectrograms was adjusted based on its own shuffled coherence. The first pair **(Figure 16A)**

represents two muscles with primary action about the elbow joint (an 'elbow-elbow' muscle pair). This pair of movement agonists exhibits a high degree of low frequency (<12Hz) pre-movement coherence earlier than 100ms before the kinematic onset of the movement. This coherence disappears at the onset of movement. The second pair (**Figure 16B**) contains a muscle with primary action about the elbow joint compared to a muscle with primary action about the wrist joint (an 'elbow-wrist pair'). Once again, a high degree of pre-movement coherence is exhibited in this pair, despite the separation of these muscles by the elbow joint. It also contains 20Hz coherence that disappears about 100ms before the onset of movement. Finally, the wrist-wrist pair (**Figure 16C**) exhibits a high degree of coherence, despite the fact that the performed movement was an elbow movement. Sixty-two percent (62%) of elbow/elbow pairs exhibited significant pre-movement coherence compared to 48% and 46% of elbow/wrist and wrist/wrist pairs, respectively. Also, elbow/elbow pairs displayed significantly higher values of coherence than elbow/wrist and wrist/wrist pairs ($p<0.01$; ANOVA). **Figure 17** shows the same muscle pairs as in **Figure 16** but the spectrograms represent the mean and standard deviation of coherence across all six subjects in order to further highlight the consistency between subjects. The mean coherence in **Figure 17** closely match the single subject's spectrograms in **Figure 16** and, as in **Figure 15**, the standard deviation spectrograms are quite low (i.e. <0.1) across all frequencies.

4.2.3 - Relationship Between Action of Muscles and Frequency Bands

Because many previous studies have implicated various frequency bands in the performance of different types of movements, analysis was performed to determine if a relationship existed between the primary actions of muscle pairs (i.e. elbow-elbow, elbow-wrist or wrist-wrist) and the frequency bands at which

they were most coherent. **Figure 18** summarizes this analysis. In the figure, coherence was averaged within each of the four frequency bands and separated based on the primary action of the muscle pairs. Elbow-elbow muscle pairs had significantly *more* average coherence ($p<0.05$; ANOVA) in the lowest (5-12Hz) frequency band than did elbow-wrist and wrist-wrist muscle pairs. Wrist-wrist muscle pairs had significantly less average coherence ($p<0.05$; ANOVA) in the 13-20Hz frequency range than the other two combinations and elbow-wrist muscle pairs had significantly less average coherence ($p<0.05$; ANOVA) in the 29-36Hz range than did the other two muscle pair combinations.

4.2.4 - Effect of Wrist Mobility on EMG Activity Patterns and Coherence

To rule out the possibility that the apparent elbow-wrist and wrist-wrist synergies were due to joint dynamics instead of true muscle synergies, trials in which the wrist was free were compared to ones in which the wrist was immobilized. If the wrist muscles were activated in response to the elbow rotation (through feedback mechanisms), an activation lag (significantly different TFO), different muscle activation patterns or a lack of coherence may be expected due to the varying mechanical characteristics of the movement. None of these situations occurred, indicating that the wrist muscles were activated in concert with the elbow muscles. No differences were seen in the TFO data between the two conditions (**i.e. Figure 14B**) or in the triphasic patterns of muscle activation (**i.e. Figure 13C**). Also, there was no statistical difference between the average pre-movement coherent activation of most muscle pairs between the two wrist conditions ($p>0.05$; t-test). Those data are summarized in **Figure 19**. In this figure, each muscle pair in the table is compared by a colour and a value representing how often muscle pair received significant common input before the kinematic onset of movement, as revealed by coherence analysis. Coherence

between constrained and free wrist conditions may be readily compared for both elbow flexion and extension movements. In general, little difference was observed between these two conditions. Taken together, these similarities suggest that the synergistic behaviour observed between elbow-wrist and wrist-wrist muscle pairs is not simply due to the need to stabilize the wrist during the various kinematic conditions of the movement. Rather, they suggest that both elbow and wrist activity were activated cooperatively.

4.2.5 - Effect of Movement Direction on Pre-Movement Coherence

Further statistical analysis of the difference between flexion and extension movements and the difference between wrist mobility conditions was conducted. Pair-wise comparisons of averaged pre-movement coherent activity were made for the conditions of movement: elbow flexion or extension. Again referring to **Figure 19**, data for flexion and extension can be readily compared between the two conditions. Generally, a significant difference existed between flexion and extension ($p<0.01$; t-test) for all movement pairs with flexion movements exhibiting pre-movement coherence 59% of the time compared to 46% for extension movements. Specifically, however, only certain muscle pairings displayed a significant difference between flexion and extension. These pairs are summarized in **Table 2**. It is interesting to note that elbow flexors and radial deviators often exhibited a significant difference between conditions of elbow flexion and extension. No muscle pairs with ulnar deviators displayed a direction effect.

Table 2: Muscle Pairs Exhibiting a Significant Direction Effect

Muscle 1	Muscle 1 Function	Muscle 2	Muscle 2 Function
BB	Elbow Flexor	BRD	Elbow Flexor
BB	Elbow Flexor	TB(lat)	Elbow Extensor
BRD	Elbow Flexor	TB(lat)	Elbow Extensor

BB	Elbow Flexor	ECRL	Radial Deviator
BB	Elbow Flexor	FCR	Radial Deviator
TB(lat)	Elbow Extensor	FCR	Radial Deviator
FCR	Radial Deviator	ECRL	Radial Deviator

Figure 20 compares flexion and extension by removing the influence of wrist mobility. Thus, conditions of wrist free or immobile were averaged together for each movement direction. While some muscle pairs did show a significant difference between wrist free and wrist immobile (0/35 muscle pairs in extension and 6/35 muscle pairs for flexion) (i.e. the black squares in **Figure 19**), it is generally the case that the wrist is not a significant factor in the measurement of common input to muscle pairs.

In order to assess the influences of common input on biomechanically relevant synergistic muscle activation, a final distillation of data was performed based on the primarily mechanical role of each muscle. In this comparison, muscles were grouped as 'Elbow Flexors', 'Elbow Extensors', 'Radial Deviators' or 'Ulnar Deviators'. The results are summarized in **Figure 21**. In this figure, it can be generally seen that flexors received more common input than did extensors. Furthermore, radial deviators received more common input than did ulnar deviators. Generally, muscle pairs involving flexors were coherently activated 57% of the time, compared to 46% for extensors ($p<0.05$; t-test). Muscle pairs involving radial deviators were activated 56% of the time, compared to 42% for ulnar deviators ($p<0.05$; t-test).

4.2.6 - Effect of Movement Kinematics on Pre-Movement Coherence

The effect of movement time on the amount of coherent activation of two muscles before a movement begins is exemplified by the series of 2D plots in

Figure 22 for one of the subjects. As the movement velocity increases, so does coherence. To assess whether a relationship exists between pre-movement coherence and movement time, correlation was performed between the average coherence for all significantly coherent muscle pairs and the actual movement time at which the movements were performed. **Figure 23** displays the general significant ($p<0.01$; Pearson r) linear and power relationships between pre-movement coherence and movement time. R-squared for the linear correlation is 0.78 and for the power correlation is 0.91. However, similar to the effects for movement direction, not all individual muscle pairs exhibited a velocity effect. Rather, only those muscle pairs that included a primary mover of the elbow joint showed such an effect. **Table 3** shows the muscle pairs that exhibited a significant velocity effect.

Table 3: Muscle Pairs Exhibiting a Significant Velocity Effect

Muscle 1	Muscle 1 Function	Muscle 2	Muscle 2 Function
BB	Elbow Flexor	BRD	Elbow Flexor
BB	Elbow Flexor	TB(lat)	Elbow Extensor
BB	Elbow Flexor	FCR	Radial Deviator
BRD	Elbow Flexor	FCR	Radial Deviator
BRD	Elbow Flexor	ECRL	Radial Deviator
TB(lat)	Elbow Extensor	FCR	Radial Deviator
ECRL	Radial Deviator	FCR	Radial Deviator

The effect of the movement amplitude was minimal. There was no global effect of the movement amplitude, although 2 of the 36 muscle pairs did exhibit a significant relationship ($p<0.05$). These two muscle pairs, both involving wrist muscles, appear in **Table 4**.

Table 4: Muscle Pairs Exhibiting a Significant Excursion Effect

Muscle 1	Muscle 1 Function	Muscle 2	Muscle 2 Function
ECRL	Radial Deviator	FCU	Ulnar Deviator
ECRL	Radial Deviator	TB(lat)	Elbow Extensor

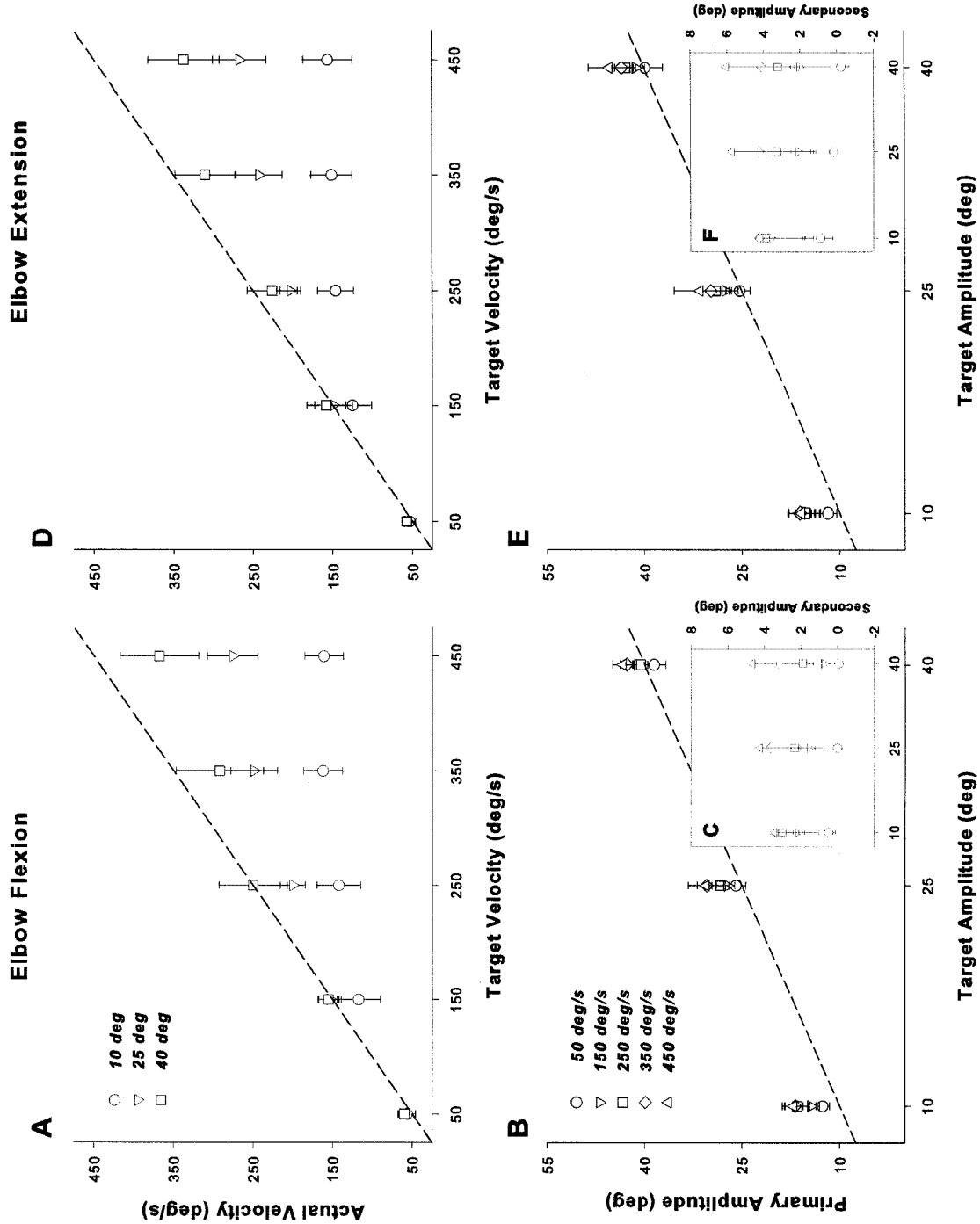

Figure 12: Summary of the performance of movements. The mean +/- SD values of actual movement velocity and amplitude for all subjects are plotted against the target values. (A,D): Actual movement velocity for elbow flexion and extension movements, respectively. (B,E): Actual primary movement amplitude for elbow flexion and extension movements, respectively. (C,F - insets): Actual secondary movement amplitude for flexion and extension movements, respectively. Lines of identity appear as a reference.

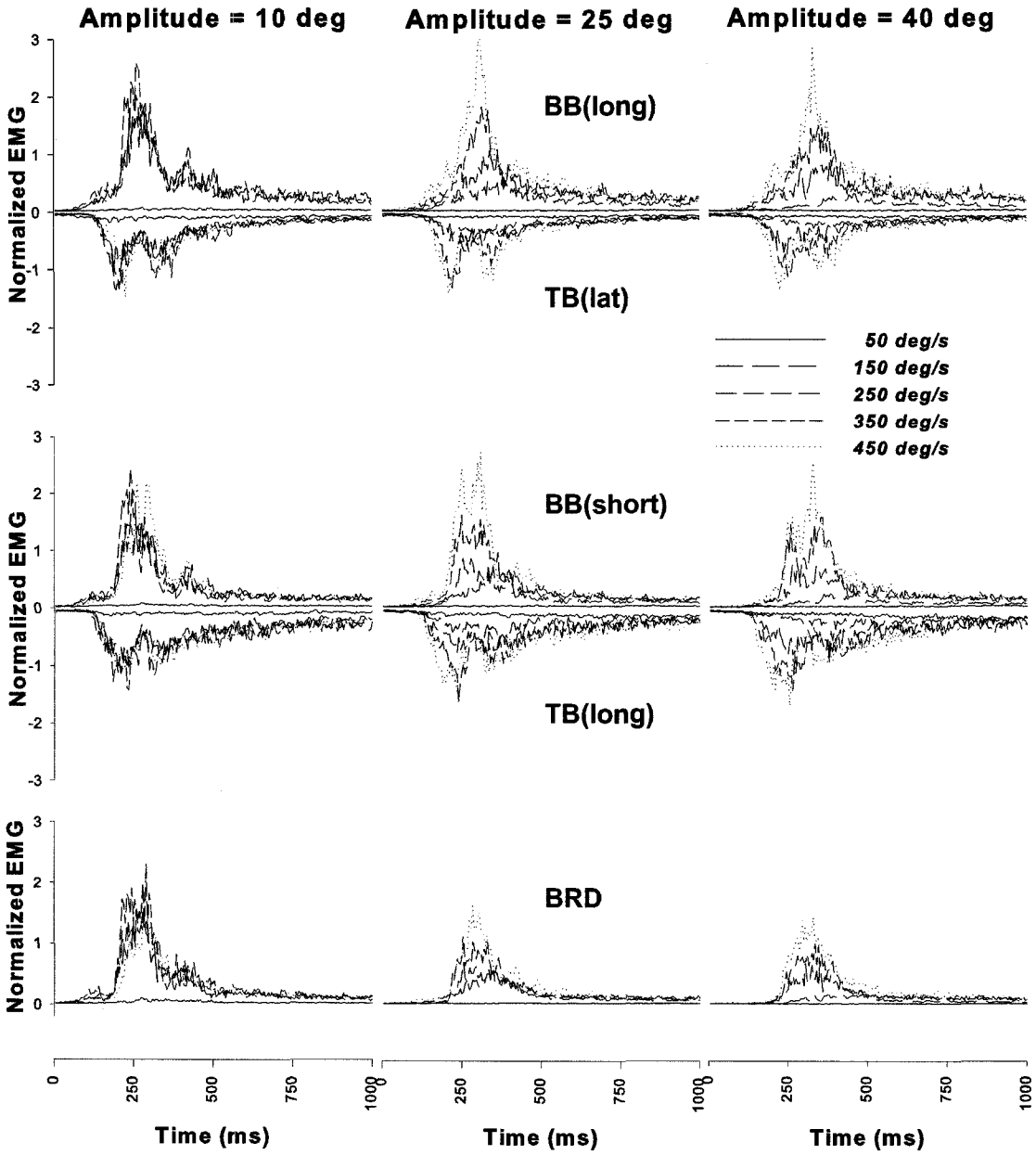

Figure 13A: EMG activity for elbow muscles. Shown are the average normalized EMG patterns corresponding to all elbow extension movements performed by one subject with the wrist free to move. All muscles are of the arm. Each trace is the average of all trials obtained per movement combination. The EMG traces are rectified and normalized to the maximum 5ms activity obtained during 50% maximum voluntary isometric contractions. Traces are grouped by target movement amplitude. Abbreviations as in Figure 2.

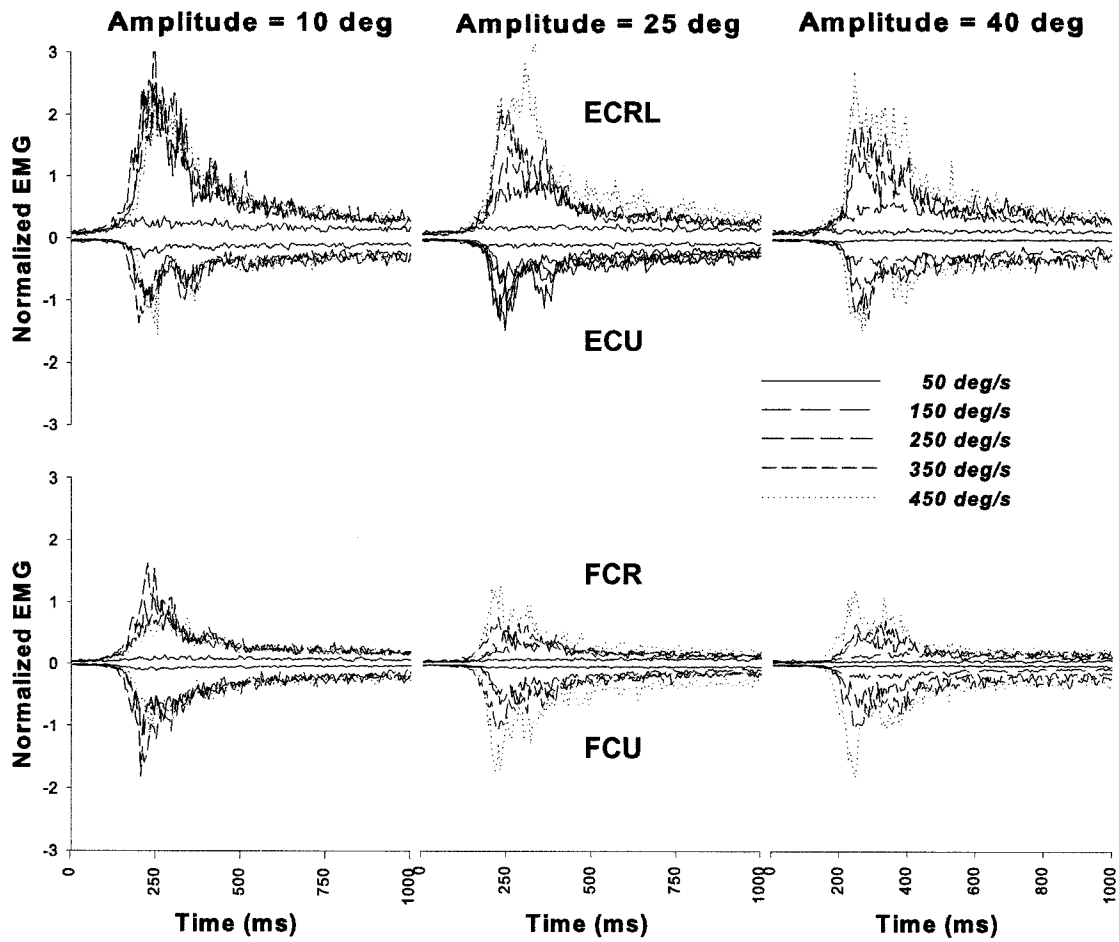

Figure 13B: EMG activity for wrist muscles. Shown are the average normalized EMG patterns corresponding to all elbow extension movements performed by one subject with the wrist free to move. All muscles are of the forearm. Each trace is the average of all trials obtained per movement combination. The EMG traces are rectified and normalized to the maximum 5ms activity obtained during 50% maximum voluntary isometric contractions. Traces are grouped by target movement amplitude. Abbreviations as in Figure 2.

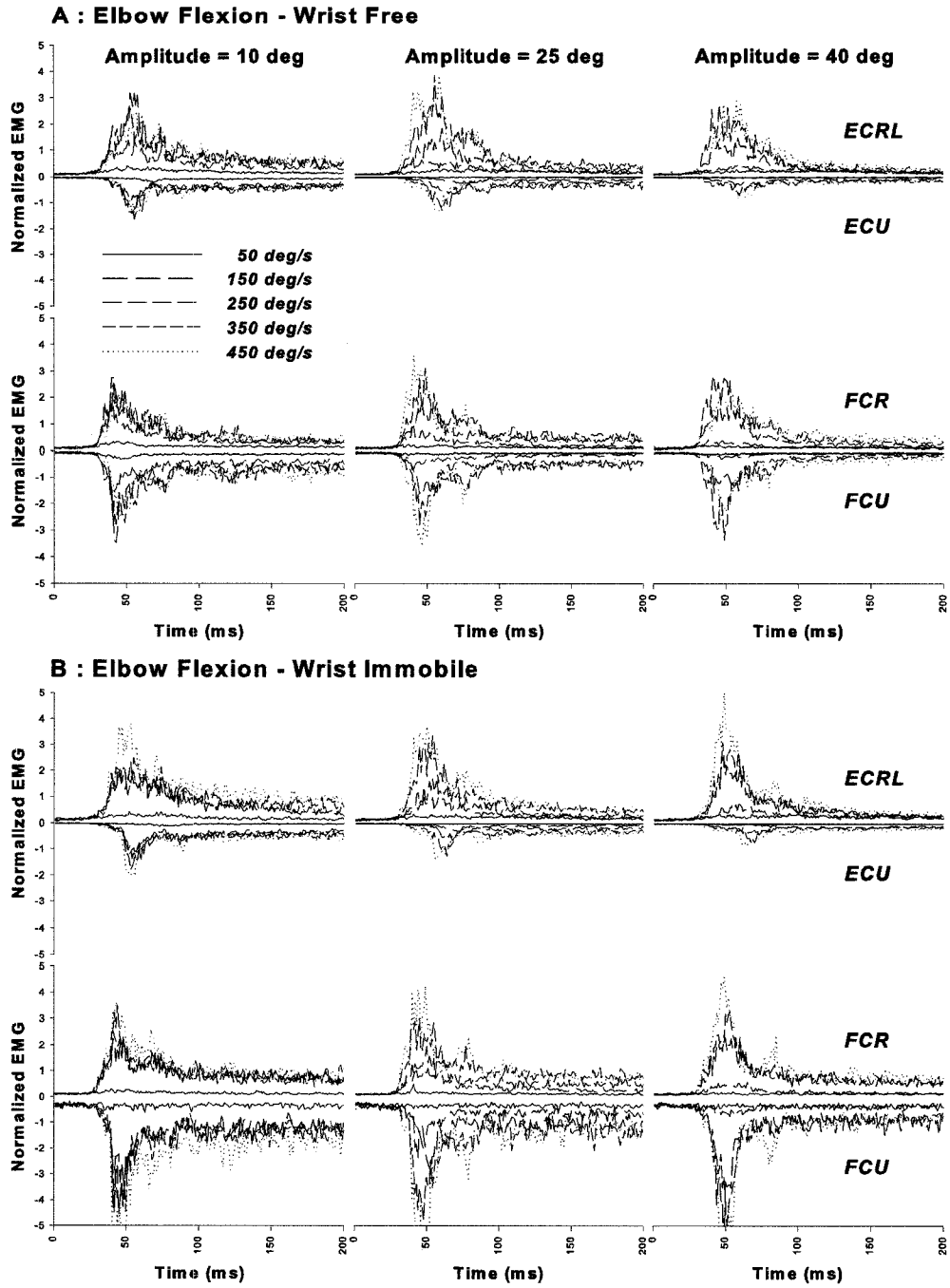

Figure 13C: Wrist muscle EMG activity for wrist fixed and free. Shown are the average normalized EMG patterns corresponding to elbow flexion movements performed by one subject with the wrist free to move (A) and the wrist fixed in place (B). All muscles are of the forearm. Each trace is the average of all trials obtained per movement combination. The EMG traces are rectified and normalized to the maximum 5ms activity obtained during 50% maximum voluntary isometric contractions. Traces are grouped by target movement amplitude. Abbreviations as in Figure 2.

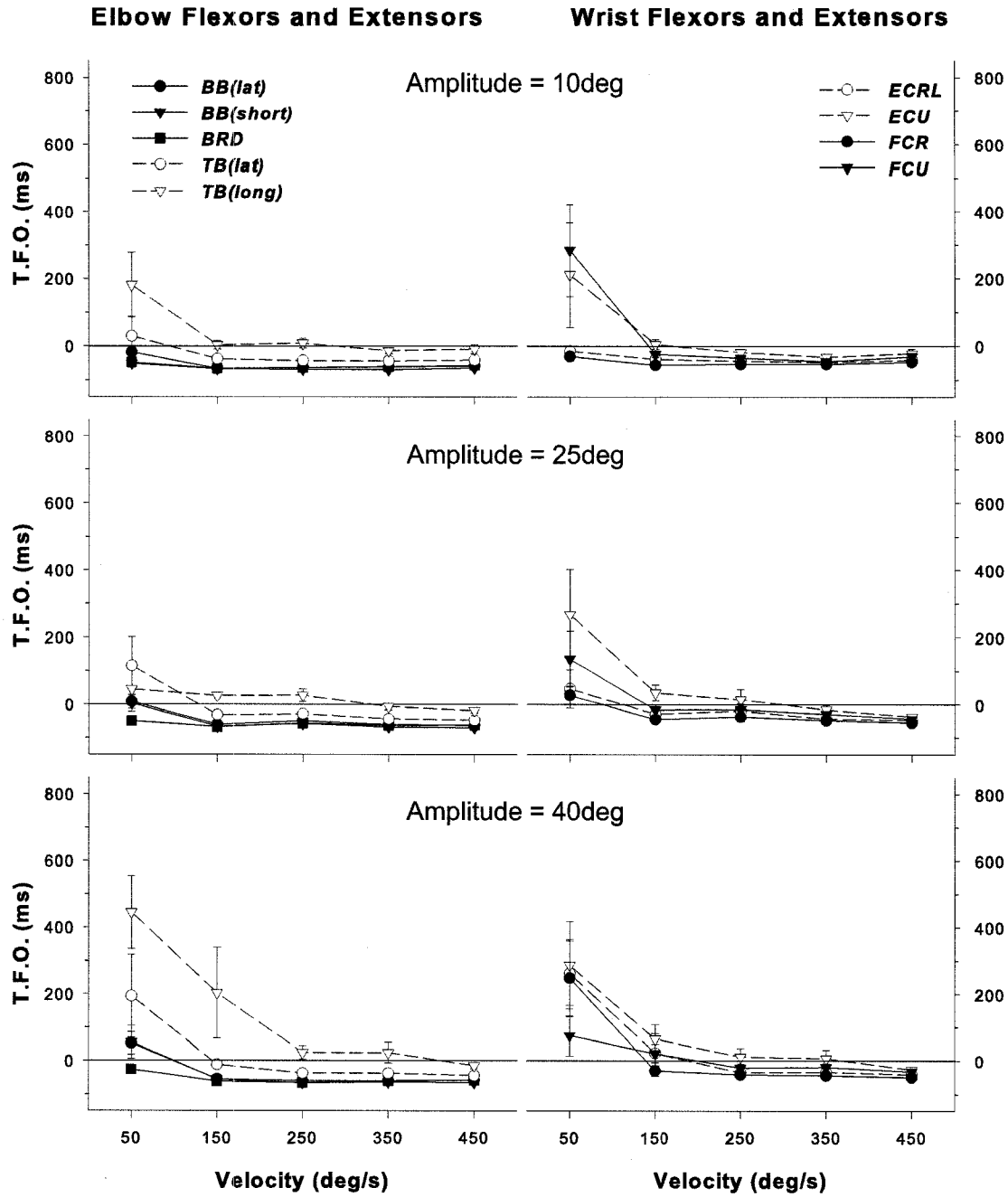

Figure 14A: Consistency of EMG onset time as a function of movement velocity and amplitude. Shown is the mean +/- SEM of time of first onset (TFO) of muscle activity for all subjects grouped by movement amplitude during flexion movements. Left column graphs represent the TFO of elbow flexors and extensors while right column graphs represent the TFO of wrist flexors and extensors. In all graphs, TFOs of flexor muscles are depicted by filled symbols and solid lines and TFOs of extensors are depicted by open symbols and dashed lines. The solid, horizontal line at 0 ms represents the kinematic onset of elbow movement. Abbreviations as in Figure 2.

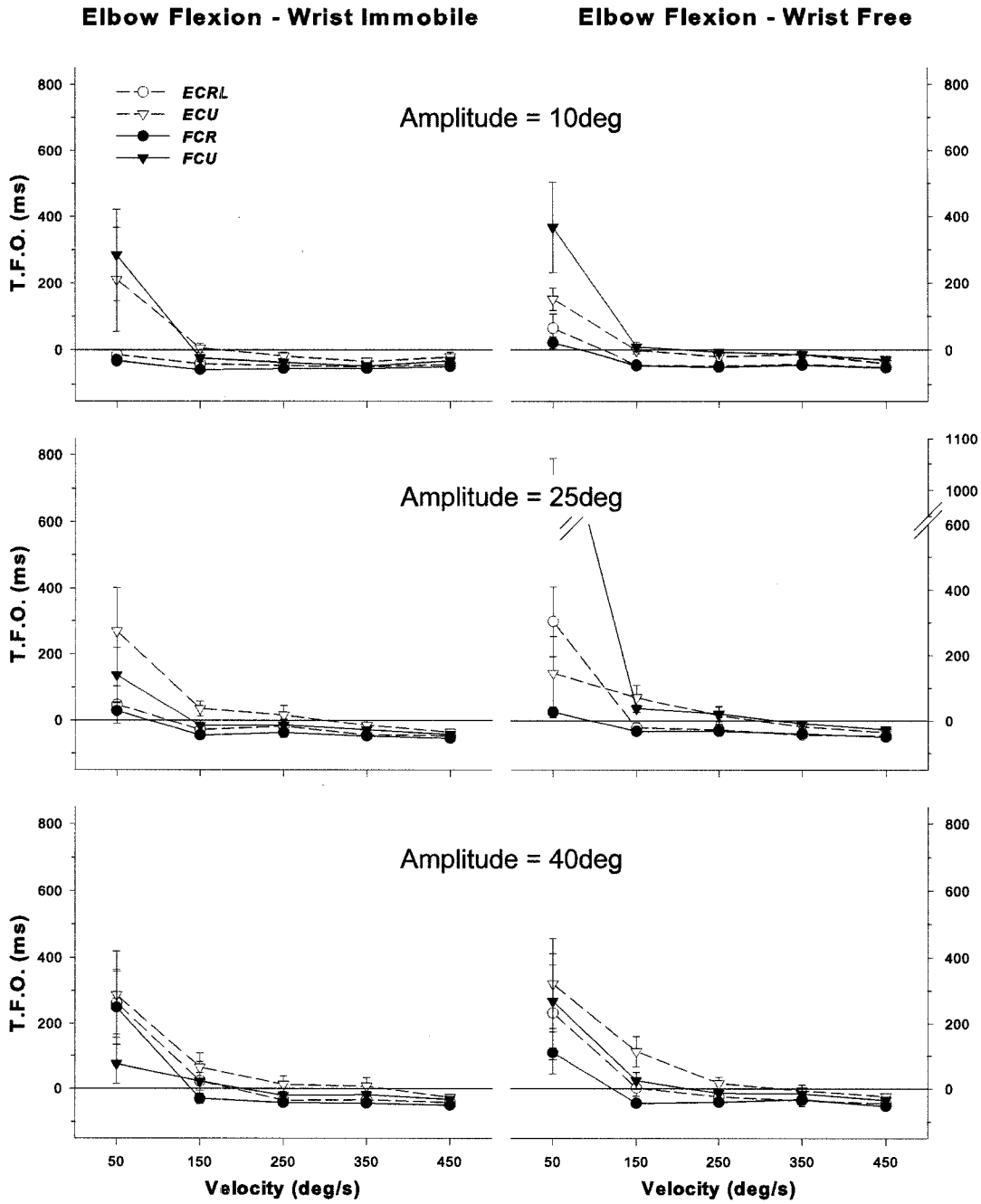

Figure 14B: Wrist muscle EMG activity is consistent between wrist fixed and wrist free conditions. Shown is the mean +/- SEM of time of first onset (TFO) of muscle activity for all subjects grouped by movement amplitude during flexion movements. Left column graphs represent the TFO of wrist flexors and extensors with the wrist joint fixed in place while right column graphs represent the TFO of wrist flexors and extensors with the wrist joint free to move. Little difference exists between these conditions. In all graphs, TFOs of flexor muscles are depicted by filled symbols and solid lines and TFOs of extensors are depicted by open symbols and dashed lines. The solid, horizontal line at 0 ms represents the kinematic onset of elbow movement. Abbreviations as in Figure 2.

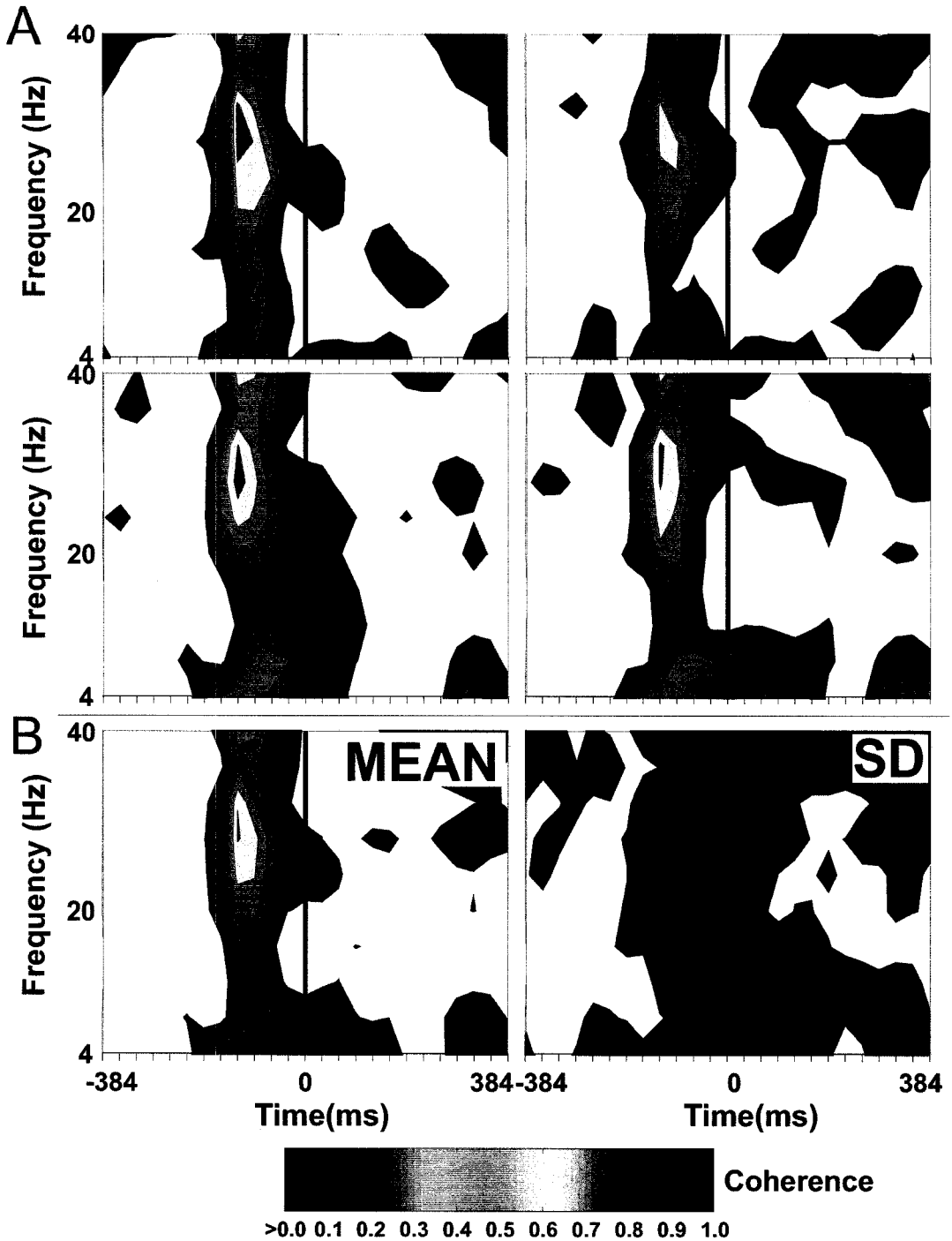

Figure 15: Spectrograms are consistent between subjects. (A) Shown are example coherence spectrograms for four of the six subjects performing the same task with the same two muscles. The plots provide a qualitative indication that there is relative consistency of the spectrograms obtained between subjects. **(B)** The mean spectrogram from all six subjects (left) and the standard deviation of the spectrograms (right). The mean generally represents each individual spectrogram and the standard deviation spectrogram is all quite low (i.e. <0.1), indicating that there is a high level of consistency between subjects for this task.

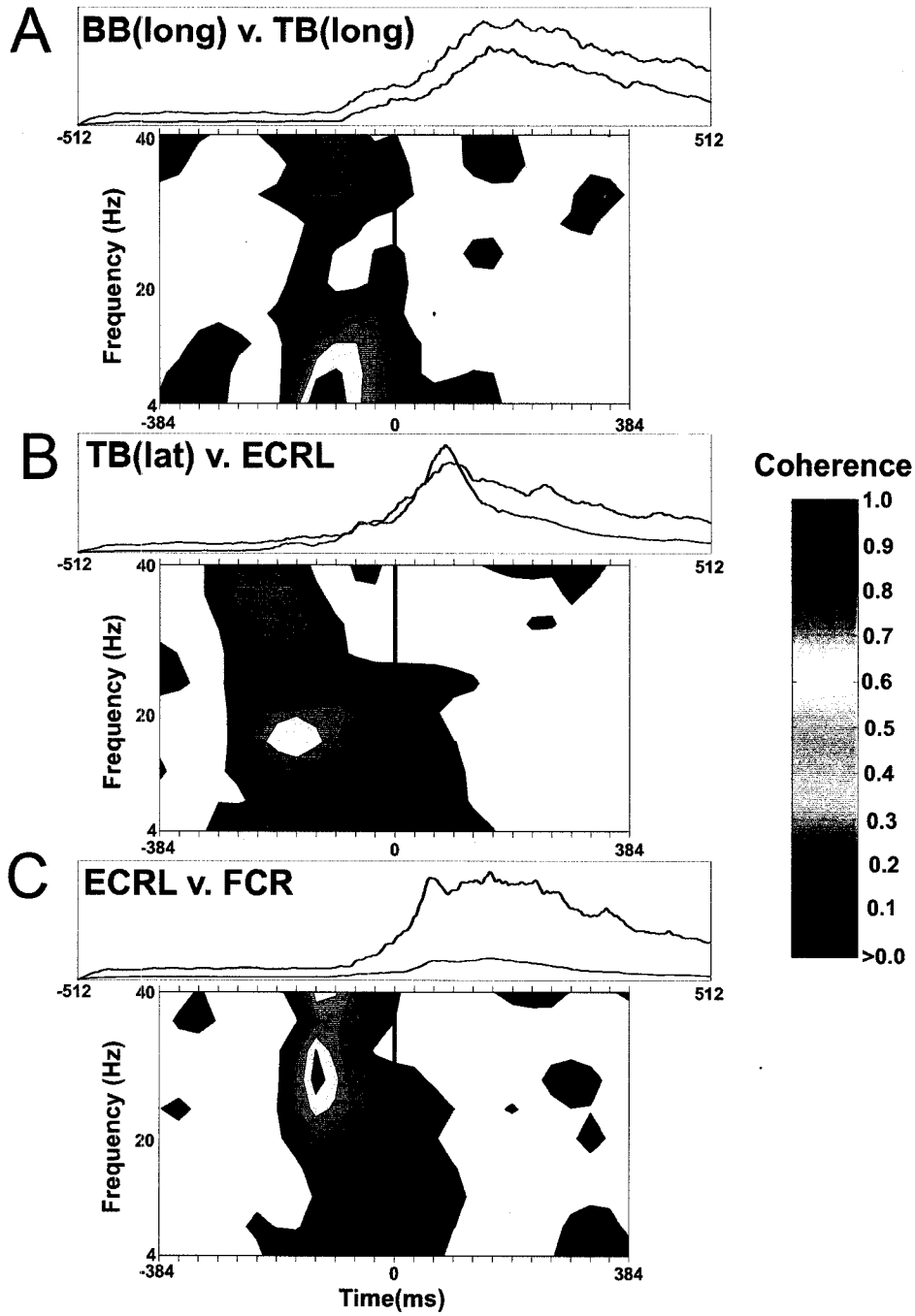

Figure 16: Example coherence spectrograms for different joint combinations. Shown are spectrograms obtained from an elbow-elbow **(A)**, elbow-wrist **(B)** and wrist-wrist **(C)** muscle pair with the wrist joint free to move. The first pair (elbow-elbow) exhibits a high degree of low frequency pre-movement coherence earlier than 100ms before the kinematic onset of the movement (the solid black line at 0ms) that disappears at the onset. The second pair (elbow-wrist) exhibits a high degree of relatively low frequency coherence despite the separation of the these muscles by the elbow joint. The third pair (wrist-wrist) exhibits relatively high frequency coherence despite the elbow-targeted task.

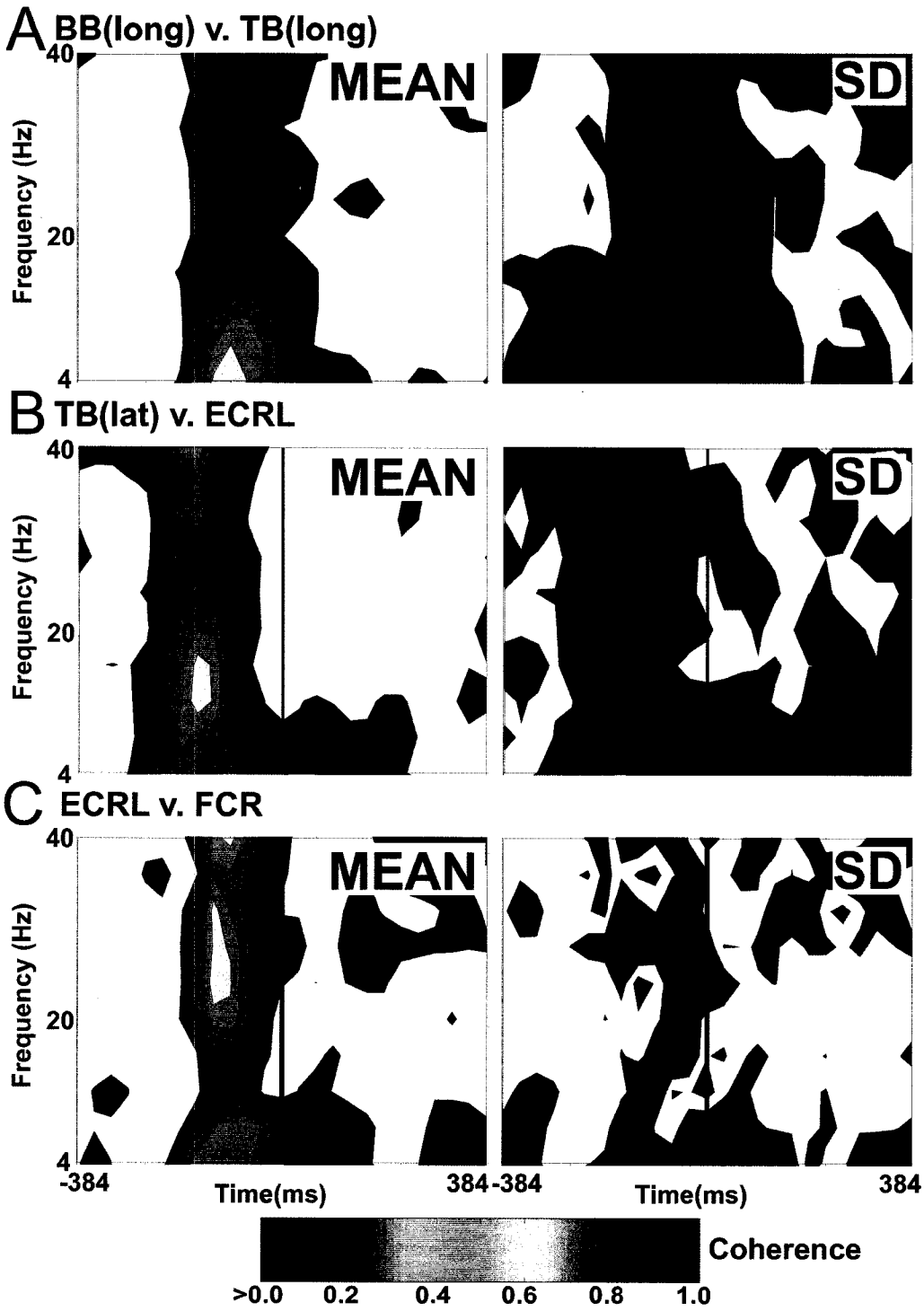

Figure 17: Mean and standard deviation spectrograms for all subjects. Shown are spectrograms from the same muscle pairs as in Figure 13. In order to ensure that similar trends held across all six subjects, mean and standard deviation spectrograms were computed for the three muscle pairs. Comparison with Figure 13 shows that the mean closely resembles the individual spectrograms and the standard deviation, while widespread, is quite low.

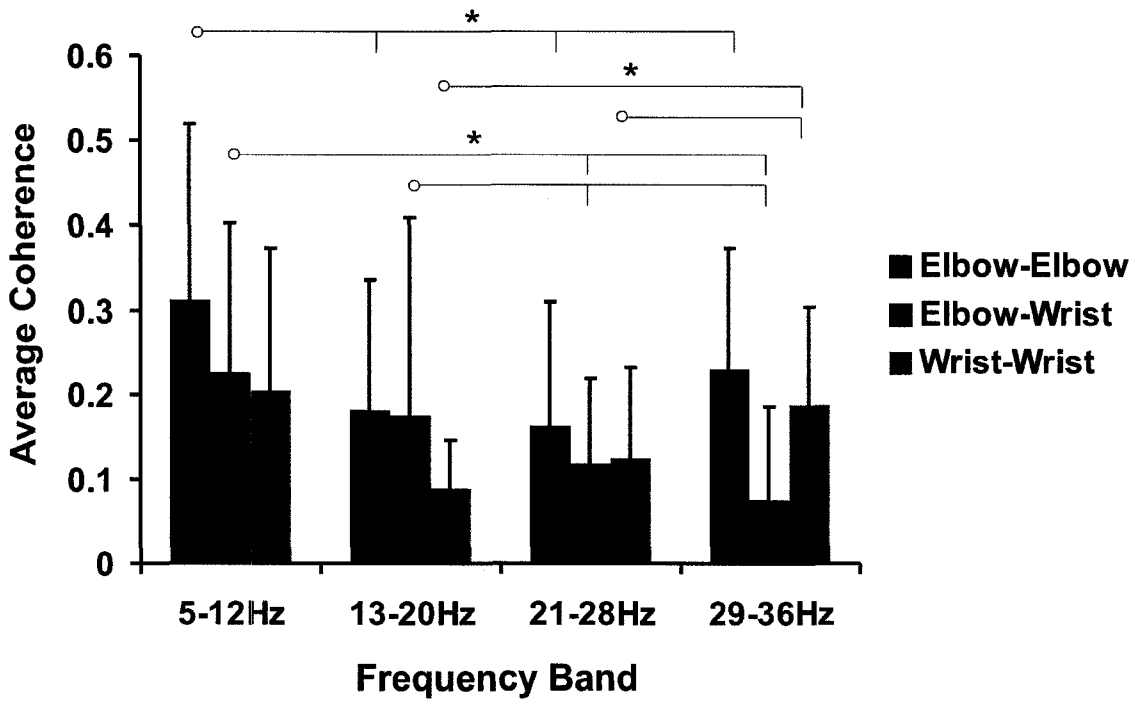

Figure 18: Relationship between mechanical action of muscle pairs and coherence frequency bands. For each of the three possible joint combinations (elbow-elbow, elbow-wrist and wrist-wrist muscle pairs), the average coherence for all conditions is shown for each of the four frequency bands. This figure shows that, for example, higher frequency coherence (29-36Hz) is highly associated with elbow-elbow and wrist-wrist pairs but not elbow-wrist pairs. Elbow-wrist pairs showed their highest average coherence in the 13-20Hz range and elbow-elbow are highest at low (5-12Hz) frequencies. This is very similar to the exemplar spectrograms in Figure 13. Asterisks denote significance ($p>0.05$)

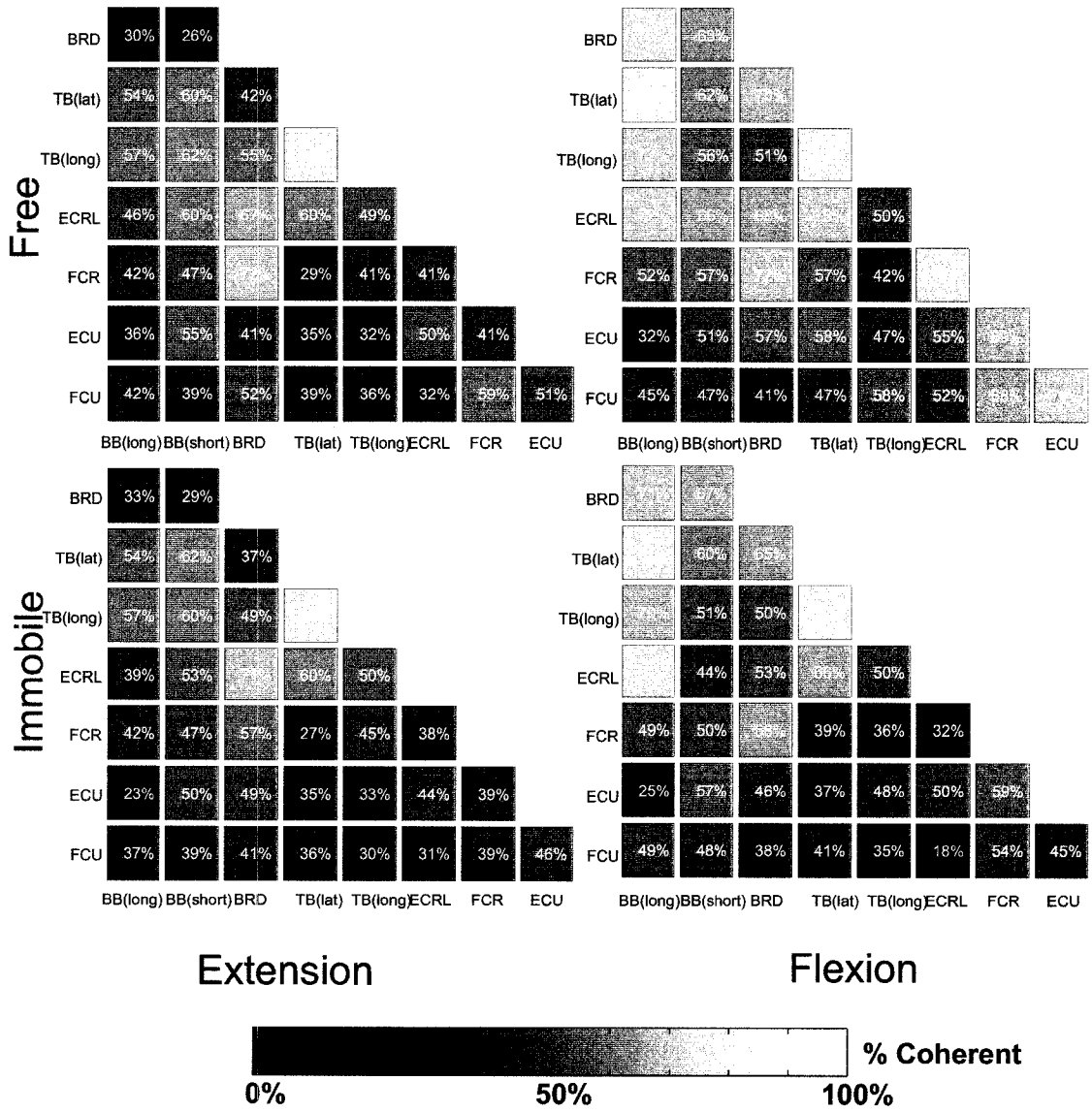

Figure 19: Comparison of the coherent activation of all muscle groups and each movement condition. Shown are plots that compare the prevalence of pre-movement coherence for each muscle pair between movement direction and wrist mobility conditions. The colour of each box represents the percentage that is included within the box. This plot allows convenient qualitative and quantitative comparison between various conditions and all muscles pairings. Black squares in the top corner of a box indicate that a significant difference existed for that muscle pair between wrist conditions.

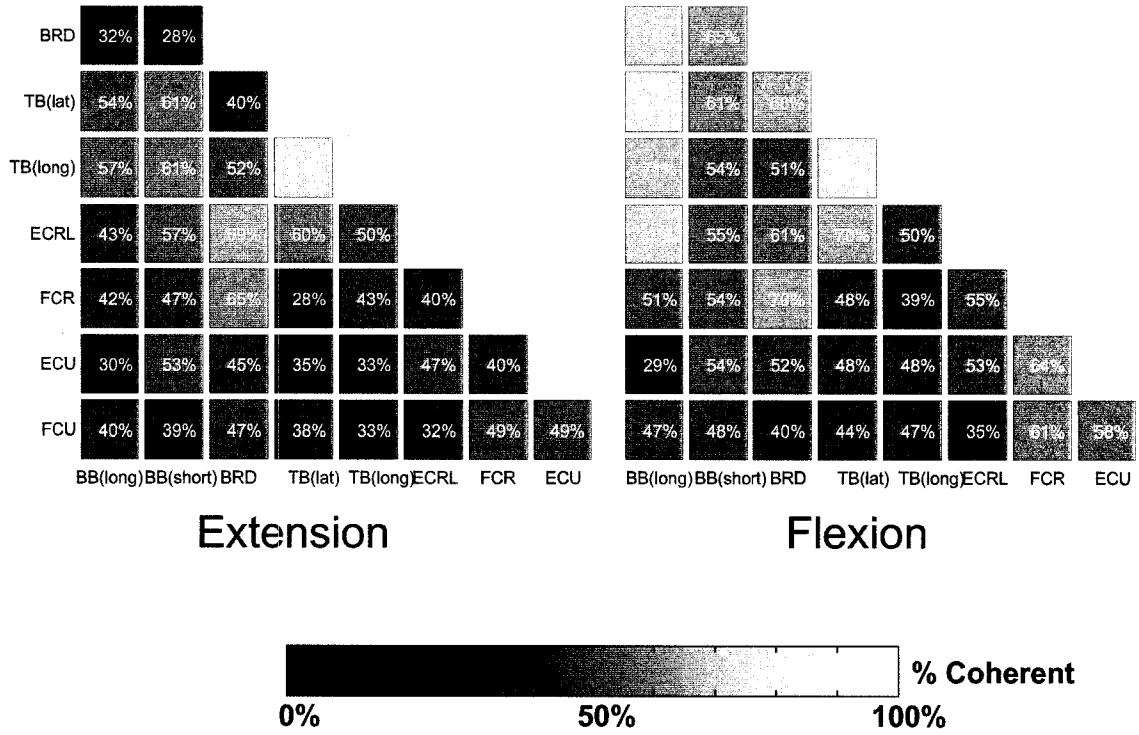

Figure 20: Comparison of the coherent activation of all muscle groups and each movement direction. Shown are plots that compare the prevalence of pre-movement coherence for each muscle pair and movement direction. This plot represents the same data as in Figure 16, except that the two wrist conditions have been averaged together for this plot because they were commonly not significantly different from each other. The colour of each box represents the percentage that is included within the box.

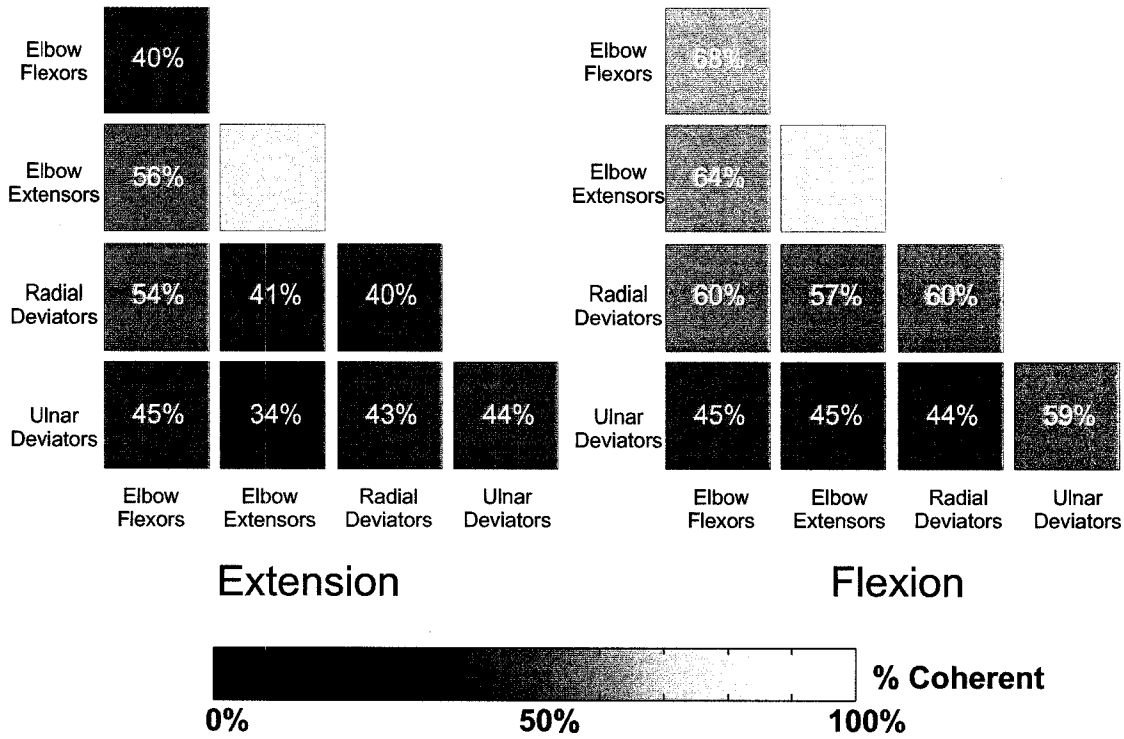

Figure 21: Comparison of the coherent activation of muscle groups with similar mechanical function. Shown are plots that compare the coherent activation for four groups of muscles between the two movement directions. The plots represent the same data as in Figure 16 & 17 except that each of the muscles pairs was put into a group based on its primary mechanical action. The colour of each box represents the percentage that is included within the box.

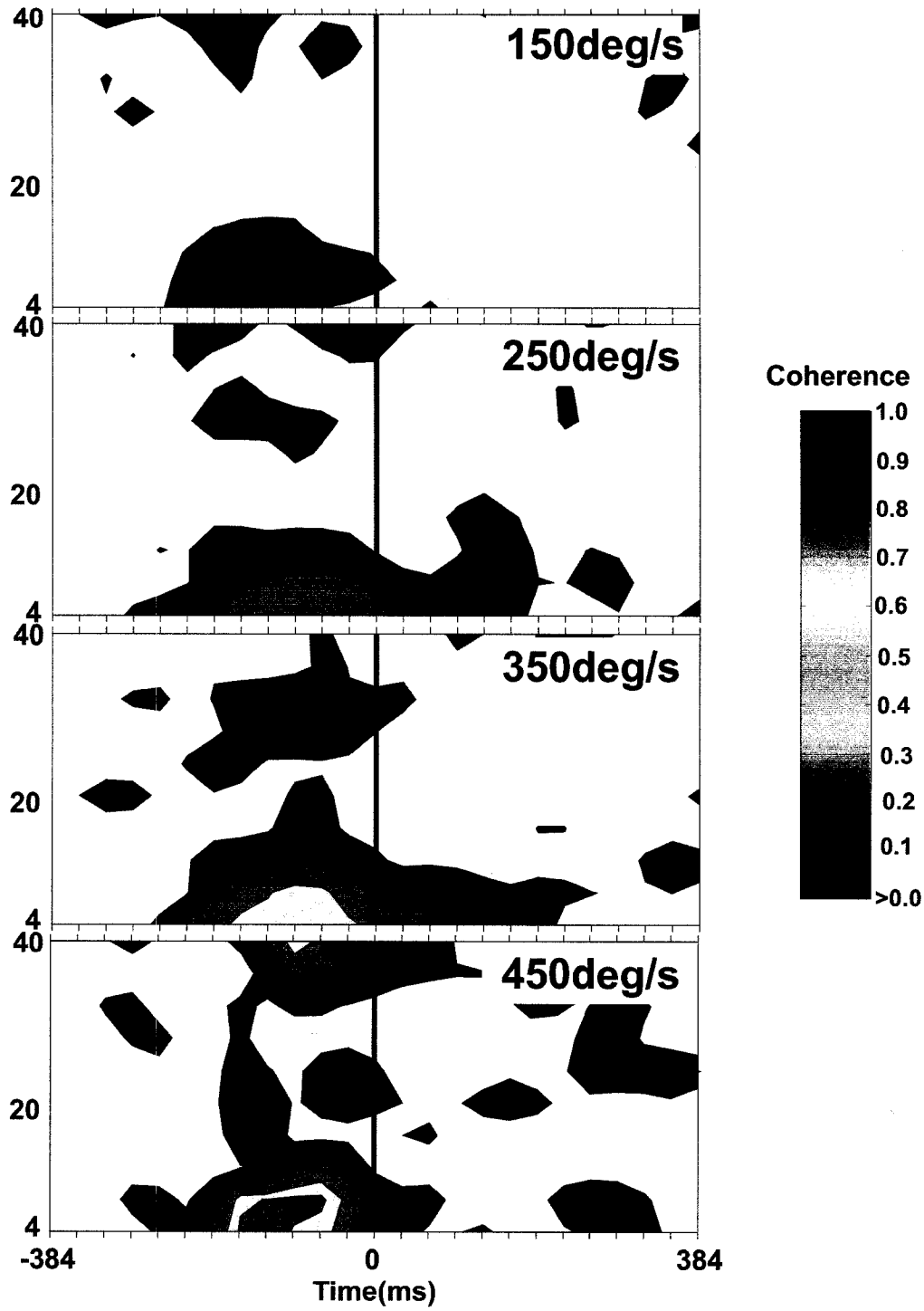

Figure 22: Area of coherence may be related to movement time. Shown are four spectrograms from two elbow muscles in one subject during an extension movement. The speed of the movement appears in the bottom right corner of each plot and the colour scale indicates the level of coherence. The solid vertical line at 0ms represents the kinematic onset of the movement. As movements become faster, there appears to be a modulation of pre-movement coherent area.

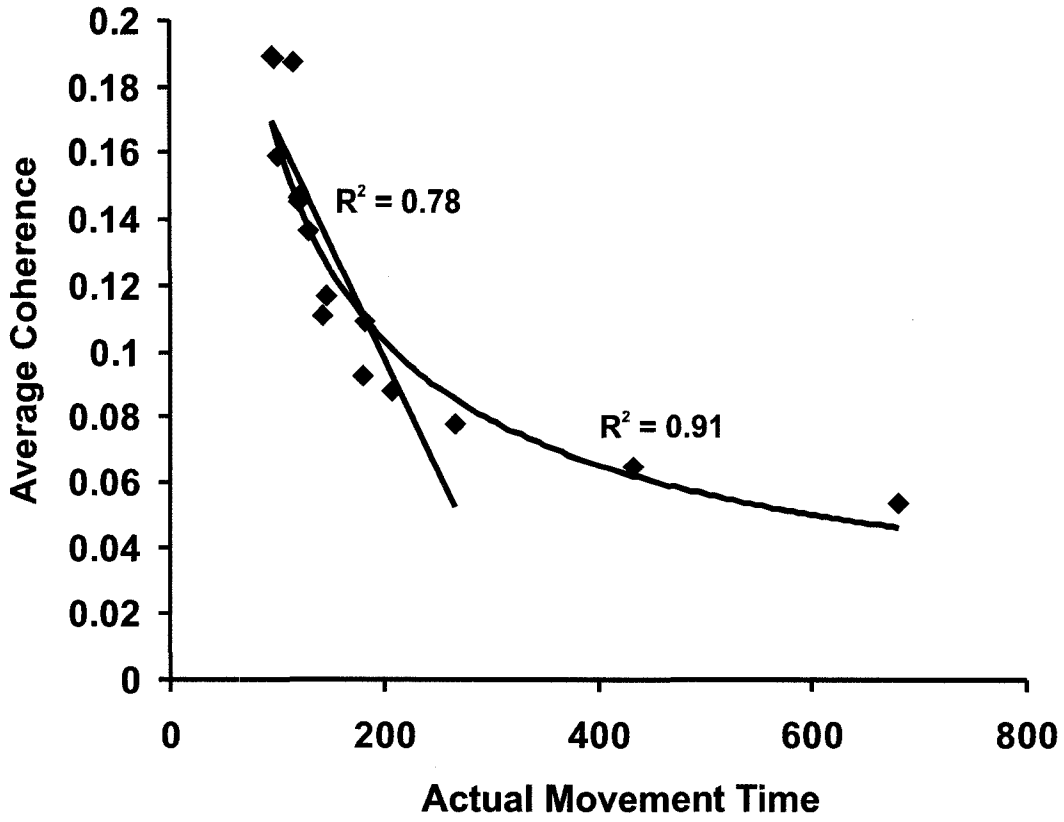

Figure 23: A significant relationship exists between pre-movement coherence and movement time. Each point represents the average coherence of all muscle pairs deemed significant by the aforementioned tests. R-squared for the linear correlation is 0.78 ($p<0.01$, Pearson r) and for the power fit is 0.91. The points at 500 and 800ms were not included in the correlation because the movement times are very different from the others.

5 Discussion

5.1 General Observations

The overall goal of this study was to examine the prevalence of coupling between muscles actuating the elbow and muscles actuating the wrist during reaching movements. Muscle activation patterns and their consistency were quantified for a range of movement velocities and amplitudes. These temporal techniques were used to investigate feed-forward muscle activation. Further, the prevalence of common input to pairs of muscles was measured as an indication of the degree of synergism between muscles in preparation for reaching tasks. It was determined that coherence is capable of measuring common input to pairs of muscles in preparation for voluntary reaching tasks. The kinematic demands of the elbow flexion and extension movements affected the TFO of EMG activity in all muscles and the degree of their coupling as measured by coherence analysis. During low velocity movements, muscles exhibited a highly variable TFO of EMG activity and their coherent activation was decreased. During higher velocity movements, the variability in the muscle's TFO decreased and evidence of coherence was exhibited. For all elbow movements, arm and forearm muscles tended to act in a coordinated manner.

5.2 EMG Patterns and Onset Consistency Indicate Coupling

In the current study, seemingly built-in elbow-wrist coupling was present within motor programs targeting the elbow joint. Such a finding facilitates the expansion of the concept of muscle synergies from focusing on pairs of agonist-antagonist muscles acting about a single joint to including distal-acting muscles mechanically linking the primary movement joint and more distal joints. The built-in elbow-wrist coupling was manifested in several features of the forearm EMG activity patterns and of the pre-movement coherence patterns. Ulnar and radial deviators of the wrist exhibited the classical triphasic EMG activity pattern that is traditionally noted between the primary movement agonists and antagonists (elbows muscles, in this case) and the onset latencies of the wrist radial and ulnar deviators were generally similar to the onset latencies of the elbow flexors and extensors, respectively. Therefore, the timing and patterns of the wrist muscles suggests that they were activated in concert with the muscles of the elbow.

Because of the position of the forearm, the wrist was not forced into flexion and extension by the elbow movement, but was rather affected by the inertia of radial or ulnar deviation. Thus, for example, when elbow flexion occurred there was a tendency for the wrist to be inertially forced into ulnar deviation. This effect of inertia was at least partially overcome by activation of radial deviators. The activation of radial deviators could either be part of a central command signal for elbow flexion or part of a secondary command signal created via afferent input in order to compensate for erroneous wrist movements induced by inertia (c.f. Latash et al. 1995). However, when the wrist was immobilized, the activation of the wrist muscles counteracting inertia occurred before the perceptible onset of elbow movement. Hence, activation of the radial deviators

did not occur in response to afferent signals and was incorporated into the central command for the arm movement.

5.3 Pre-Movement Coherence Indicates Coupling

5.3.1 – Measuring Coherence During Phasic Voluntary Movements

This work reports, for the first time, methodology for measuring the strength of coupling between various muscle pairs. The coupling that is reported in this research has been verified to be a result of neural mechanisms and not a processing artifact. The novel method of 'shuffling' trials to produce a null-hypothesis ensures a conservative estimate of coherence. This is because shuffling of trials constituting one set of conditions eliminates any true physiological relationship between the two trials. The fact that shuffled coherence is significantly less than that obtained from properly computed coherence suggests that care should be taken when computing coherence between multiple trials, as is commonly done in this field.

The ability of coherence techniques to determine coupling driven by neural connectivity suggests that it may be possible to quantify the plastic changes that take place in the inter-connectivity of motor pools (e.g. modifications in Ia and Renshaw interneuron synaptic strength) following injury and subsequent rehabilitation. This may be highly beneficial in the assessment and treatment of neuromotor disabilities using techniques such as operant conditioning.

5.3.2 – Coherence Between Antagonistic and Agonistic Muscle Pairs

It is thought that EMG-EMG coherence reflects common input to motoneurons (Kilner et al. 1999). Hence, inter-muscular coherence may result from common cortical oscillations (Baker et al. 1997) or interneuronal

connections between two muscles. It has been reported previously that oscillations in cortical local field potentials are not related to actual movement execution but, rather, are likely related to aspects of movement preparation (Sanes and Donoghue 1993; Murthy and Fetz 1996; Murthy and Fetz 1996). These observations are similar to the synchronous activity reported by Evans and Baker who observed that coherence was especially strong before the onset and after the offset of movements when, they postulated, the coupling needs to be established and then desynchronized during active movements (Evans and Baker 2003). Similarly, in the present study, the strongest coupling was observed in the preparatory stages of the performed movements.

Not surprisingly, the strongest coupling is shown between muscles operating the same joint in either an agonist or antagonist role. More interestingly, a varying degree of coherence existed between many important muscles of the wrist and elbow during this simple single joint movement. A few general trends of the differences in coherence warrant further discussion. First, elbow flexor muscles received significantly more common input than did elbow extensor muscles. This may be due to physiological differences in the activation of different muscles based on their importance. Flexors of the arm, for example, are considered 'anti-gravity' muscles in primates and may be preferentially activated in all tasks. In studies involving direct recording from primate interneurons, neurons driving flexor muscles were found to be nearly twice as prevalent as those driving extensor muscles (Perlmutter et al. 1998). Similarly, intraspinal stimulation of the cervical primate cord preferentially activated flexor muscles in a similar ratio (Moritz et al. 2007). Results of the former study also noted a distinct preference to activate radial deviators during wrist tasks, irrespective of movement direction or wrist orientation (Perlmutter et al. 1998). This is similar

to the increased activation of radial rather than ulnar components described in **Table 1** and **Figure 16**. The results of these direct recording and stimulation experiments of spinal interneurons lend significant credence to the results reported in this thesis.

5.3.3 – Coherence Between Inter-joint Muscle Pairs

A significant finding in this study is the presence of coupling between muscles of the arm and forearm in the preparatory stages of volitional movements targeting the elbow. This corresponds to the same period of time in which many of the muscle pairs exhibit their TFO of EMG activity. Inter-muscular coherence in these stages has been previously reported in muscles under strong, direct cortical control, such as those muscles of the fingers (i.e. Baker et al. 1997); however, presently, those results are extended to propose a role for coherent activation in the preparation of multi-joint movements.

There was a high degree of coherence between muscles operating at different joints (i.e. the elbow and wrist). This is in stark contrast to the results of earlier studies suggesting that no such coupling was present between muscles operating at different joints (Bremner et al. 1991; Bremner et al. 1991; Gibbs et al. 1995; Halliday et al. 2003). Major differences in methodology must be noted between these studies and the present study, however. Firstly, Bremner et al. (1991a), Bremner et al. (1991b) and Gibbs et al. (1995) utilized standard time-based cross-correlation to assess common input. While this technique can be effective in demonstrating coupling, it has been shown to also be prone to false negativity (Kirkwood and Sears 1978). Perhaps more importantly, Bremner et al. (1991a), Bremner et al. (1991b), Gibbs et al. (1995) and Halliday et al. (2003) each analyzed very different muscle groups than are analyzed here. Bremner et al. (1991a) and

Bremner et al. (1991b) examined finger movements, whereas Gibbs et al. (1995) and Halliday et al. (2003) examined lower limb movements. Finger movements may exhibit very different coupling than the arm movements performed herein because of the high degree of direct cortical input to finger muscles that is required for the precision and specificity of the fingers in higher mammals.

Similar to the results obtained for activation patterns and TFO consistency, there were no differences in the coherence obtained when the wrist joint was either free or immobilized. If there were a difference in coherence patterns when the wrist condition changed, it might be expected that the apparently synergistic patterns were, in fact, simply a reflection of a response initiated in order to produce mechanical stabilization of the wrist joint. No difference between conditions where the wrist was free or immobile further suggests that the elbow-wrist muscle synergies were pre-programmed and that wrist activity was built-in as part of the motor program(s).

5.3.4 – Frequency Bands Related to Muscle Pair Function

Coherence at different frequency bands was related to the joint that the muscle pair operates (i.e. elbow-elbow, elbow-wrist, wrist-wrist). Some frequency bands were more strongly related to different muscle pair functions. For example, like in the exemplar spectrograms in **Figure 16**, elbow-elbow pairs exhibited strong low frequency coherence, as well as significant peaks at higher frequencies (>20Hz). Further, elbow-wrist pairs were best represented by the two mid-range frequency bands (13-28Hz), just like in **Figure 16B**. Finally, the wrist-wrist pairs exhibited little low frequency coherence, but showed more activity at higher frequencies, similar to the pair shown in **Figure 16C**. Lower frequency coherence in various motor areas has been noted during voluntary

movements (Vallbo and Wessberg 1993; Feige et al. 2000) and has been suggested to be highly related to fast, voluntary movements, as well (Conway et al. 2004). Higher frequency components, on the other hand are more commonly noted in hold and precision grip tasks (Farmer et al. 1993; Conway et al. 1995). Therefore, the activity of different frequency bands in relation to the function of the muscle pairs in the present study fits well with previously reported data. Muscle pairs whose primary role was to rotate the elbow (i.e. elbow-elbow muscle pairs) exhibited low frequency coherence before the kinematic onset of movements. Muscle pairs whose role was little more than stabilization of the wrist joint (i.e. wrist-wrist muscle pairs) exhibited higher frequency coherence. The role of pairs of muscles in these reaching tasks dictated the frequency range at which they were coherent. Therefore, multiple frequency ranges of coherent activation are important for generating various aspects of motor commands.

5.4 Effect of Movement Parameters on Coupling

5.4.1 – Effect of Movement Velocity and Amplitude

The variability in the kinematic features of volitionally performed movements has been considered to be an indicator of the variability in motor programs of the neuromuscular system (Darling and Cooke 1987; Gordon and Ghez 1987; Gottlieb et al. 1988; Jaric et al. 1992). The corresponding variability in EMG activity patterns has been studied to a lesser extent.

In contrast to low velocities, at high velocities the onset latencies of muscles were highly consistent (**Figure 14A**). These results support the existence of differential control schemes based on movement time. In addition to the high consistency in the TFO of EMG activity patterns during fast movements, elbow

agonist and antagonist muscles were activated almost simultaneously (Freund and Budingen 1978; Latash et al. 1995). This could explain the physiological limitations the subjects encountered when performing movements requiring less than 80 ms to complete (**Figure 12**). For targeted movements requiring 22 to 40 ms, agonist and antagonist muscles were, on average, activated 0 to 33 ms apart (**Figure 14A**), suggesting that the initial deceleration phase of the movement was initiated simultaneously with, or shortly after the initiation of the acceleration phase, thereby significantly limiting the peak velocity of the movement. The temporal coincidence of muscle activation in these movements suggests that they were initiated in a pre-programmed fashion. During low-velocity movements (slower than 150°/s) the time of onset of muscle activity was relatively variable. Such variability could imply a larger number of potential motor schemes for executing slow movements or that a combination of multiple motor strategies may be employed to accomplish the same goal. Moreover, since slow movements require relatively long movement times, a change in motor strategy based, for example on available sensory feedback could be invoked while subjects try to correct for errors in their movement trajectory (Angel et al. 1971; Schmidt and Russell 1972; Angel 1977; Schmidt et al. 1979; Berardelli et al. 1996). The large variability in TFO during slow movements is likely due to the adjustment of these movements based on feedback (Rosenbaum 1991). Both descending commands and the state of the periphery could contribute to this variability in the nervous system. The level of neuronal excitability in supraspinal and spinal centres plays an important role in choosing motor strategies as well as in inducing ongoing modifications of the chosen strategies at the spinal cord level (Bernshtein 1967; Schmidt et al. 1979; McCrea 1992). The modulation of the pre-movement coherent signal with movement time may be indicative of this neuronal excitability and, hence, of the selection and

combination of appropriate motor programs necessary to accomplish a desired movement.

A statistically significant correlation existed between movement time and the pre-movement coherence (**Figure 23**). The "grading" effect is most prevalent in the shortest movement times and decreases as movement time increases. Such a trend indicates that the longer, more feedback-controlled movements are not as coherently activated, likely because the need for a pre-programmed motor plan is no longer present. Moreover, consistent with the reduced variability in muscle TFO at high velocities, an increased value of coherence could represent fewer possible motor strategies employed in order to accomplish the faster movements. Hence, the increase in coherence, representing an increase in activity from common inputs (cortical oscillations or spinal interneurons) may represent a specificity of modular motor programs. Pairs of wrist muscles did not exhibit a significant grading effect (they did, however, still exhibit pre-movement coherence). This may be a result of the fact that these muscles were activated due to the requirement of mechanical stability about the wrist joint.

5.4.2 – Effect of Movement Direction

A significant direction effect was exhibited in many muscle pairs that include a muscle with primary action about the elbow joint (such as BB or TB; **Table 2**). However, several muscle pairs showed no difference in the computed coherence patterns between elbow flexion and extension movements. This is consistent with the expectation that the biceps and triceps brachii muscles are of prime importance in controlling the actuation of the forearm about the elbow joint, with the other muscles facilitating the movement to a lesser degree and providing stability. Hence, some prime movers appeared to exhibit task-dependent

(direction-dependent) coupling whereas no combinations of inter-joint and distal joint muscles do. The indifference to movement direction of non-primary mover muscles supports the suggestion that these inter-joint and distal joint muscles are pre-programmed to maintain limb stability during the movements.

5.5 Muscles Cross Multiple Joints

The muscles analyzed in this study have been treated as acting on a single-joint. Anatomically, however, all of the muscles cross two joints. It could therefore be proposed that the results presented here are simply a consequence of the inherent activation of the wrist when the elbow is deviated. However, the distance of the wrist muscle origins from the elbow joint produces a small enough moment arm so as to minimize its influence. Also, mechanical fixation of the wrist does not produce any appreciable change in muscle activation patterns nor in the prevalence of coherent activation of elbow/wrist synergists, further discounting the influence of mechanical coupling producing the reported results.

5.6 Concluding Comments

This study was designed to investigate the characteristics of inter-joint coupling in humans. Evidence was found for robust inter-joint coupling between those muscles operating the elbow and wrist, even though the movements performed were focused on the elbow. Muscle activation patterns associated with the movements in this study are consistent with the use of a feed-forward controller, suggesting that inter-joint coupling may be pre-programmed in the spinal cord or cortex. To this end, evidence was found for muscle synergism via common neuronal input to muscle pairs. Coherence analysis was capable of detecting and quantifying this common input. Both muscle activation

patterns and strengths of common inputs were heavily modulated with the parameters of the reaching task. These results are important because they provide an understanding of how the nervous system coordinates the action of multiple muscles in preparation for reaching tasks in healthy individuals. Similar analysis on individuals who have suffered damage or disease to the nervous system will yield further insights into normal and altered control of reaching movements.

6 Conclusions and Future Directions

The goal of this project was to characterize inter-joint coupling between muscles of the arm and forearm. Coupling has been demonstrated using both temporal and spectral analysis techniques. Further, this thesis has demonstrated that, with advanced signal processing methodology, it is possible to quantify the degree to which synergist and antagonist muscles receive common neural input. The ability for the nervous system to activate multiple synergistic muscles synchronously is seen as an important computational simplification that can reduce the complexity of controlling multi-joint movements. Therefore, the ability to measure the inter-connectivity between different motor pools from the electrical activity associated with motor output (i.e. EMG activity) offers important insights into the neural control of movement. Further, it may serve to facilitate a greater understanding of the plastic changes that take place within the brain and spinal cord following damage or disease, as well as the efficacy of rehabilitative interventions (such as those based on operant conditioning or functional electrical stimulation) to restore functional degrees of motor control.

As movements become faster, the nervous system is no longer able to act in a 'closed-loop' fashion by incorporating peripheral feedback and recalculations

into an on-going movement. Rather, it must rely on a 'feed-forward' controller: one that must activate a multitude of goal-appropriate muscles at a time delay that is incompatible with the latency of afferent input to the spinal cord. Classically, this feed-forward controller has been characterized by triphasic muscle activations between agonist and antagonist muscles of the same joint. Interestingly, the results reported here, as well as other research (i.e. Debicki and Gribble 2004; Debicki and Gribble 2005), have noted that muscle activity at 'non-focal' joints is intrinsically 'coupled' to the activity of the primary joint. These results provide evidence that synergistic muscle activation, even across multiple joints, can occur in a feed-forward fashion. The results herein also show that, as movements are required to be performed faster, synergist and antagonist muscle onset times all occur before the perceptible (kinematic) onset of movement. Also, the variation of these latencies varies systematically with the speed of the ensuing movement. This consistency may suggest that more stereotypical motor programs are activated in fast volitional movements.

In a novel application of the methodology, coherence techniques were used to assess the degree to which inter-joint muscles receive common input from neural structures. Coherence provides even stronger evidence for pre-programmed muscle synergies because muscles that would be expected to be highly synergistic or antagonistic in certain arm movements receive the highest level of common input as measured by coherence analysis. For the first time, this work reports the prevalence of coherence between vastly separated muscles of the arm and forearm and relates these results to the biomechanical action of the muscles during volitional arm movements. A novel shuffling technique was employed in order to confidently perform coherence analysis on phasic EMG activity, such as that in this study. These results are also promising because they

provide an interesting and reasonably straight-forward way to measure the inter-connectivity of motor pools following damage to the nervous system and subsequent rehabilitation. It is expected that differences in coherence between synergistic muscle pairs will have a strong relationship to various pathological conditions.

An understanding of the modulation of common input to muscle pairs is important from a physiological perspective because it offers insight into how the nervous system solves the 'degrees of freedom' problem through computational simplifications, such as those provided by the inherent inter-connectivity of motor units at the segmental spinal level. Also, work should be done to determine the prevalence of coupling during feedback-evoked movements. An interesting possibility may be that the same connectivity that gives rise to the synergistic activation of muscles in the volitional movements performed in this research may be activated in stretch-evoked movements, as well. Such a result would support theories suggesting the flexible combination of elemental motor programs – "motor primitives" - to produce a myriad of motor output.

The measurement of connectivity is interesting from a clinical perspective because modifications in the inter-connectivity of muscles would be expected following intensive rehabilitative training such as robotic training, functional electrical stimulation or operant conditioning. Therefore, future studies should determine the effectiveness of using coupling analysis to measure rehabilitative success.

7 References

Almeida, G. L., et al. (1995). "Organizing principles for voluntary movement: extending single-joint rules." J Neurophysiol **74**(4): 1374-81.

Angel, R. W. (1977). "Antagonist muscle activity during rapid arm movements: central versus proprioceptive influences." J Neurol Neurosurg Psychiatry **40**(7): 683-6.

Angel, R. W., et al. (1971). "Tracking errors amended without visual feedback." J Exp Psychol **89**(2): 422-4.

Aoyagi, Y., et al. (2004). "The role of neuromuscular properties in determining the end-point of a movement." IEEE Trans Neural Syst Rehabil Eng **12**(1): 12-23.

Ashworth, B. (1964). "Preliminary Trial of Carisoprodol in Multiple Sclerosis." Practitioner **192**: 540-2.

Baker, S. N., et al. (1997). "Coherent oscillations in monkey motor cortex and hand muscle EMG show task-dependent modulation." J Physiol **501 (Pt 1)**: 225-41.

Bennett, D. J., et al. (2001). "Evidence for plateau potentials in tail motoneurons of awake chronic spinal rats with spasticity." J Neurophysiol **86**(4): 1972-82.

Berardelli, A., et al. (1996). "Single-joint rapid arm movements in normal subjects and in patients with motor disorders." Brain **119 (Pt 2)**: 661-74.

Bernshtein, N. A. (1967). The co-ordination and regulation movements. Oxford, New York,, Pergamon Press.

Bizzi, E., et al. (2000). "New perspectives on spinal motor systems." Nat Rev Neurosci **1**(2): 101-8.

Bohannon, R. W. and M. B. Smith (1987). "Interrater reliability of a modified Ashworth scale of muscle spasticity." Phys Ther **67**(2): 206-7.

Boorman, G., et al. (1991). "Reciprocal Ia inhibition in patients with spinal spasticity." Neurosci Lett **127**(1): 57-60.

Bremner, F. D., et al. (1991). "Correlation between the discharges of motor units recorded from the same and from different finger muscles in man." J Physiol **432**: 355-80.

Bremner, F. D., et al. (1991). "Variation in the degree of synchronization exhibited by motor units lying in different finger muscles in man." J Physiol **432**: 381-99.

Brooks, V. B. (1986). The neural basis of motor control. New York, Oxford University Press.

Burke, D. (1992). "Movement Programs in the Spinal-Cord." Behavioral and Brain Sciences **15**(4): 722-722.

Conway, B. A., et al. (1995). "Synchronization between motor cortex and spinal motoneuronal pool during the performance of a maintained motor task in man." J Physiol **489 (Pt 3)**: 917-24.

Conway, B. A., et al. (2004). "Low frequency cortico-muscular coherence during voluntary rapid movements of the wrist joint." Brain Topogr **16**(4): 221-4.

d'Avella, A. and E. Bizzi (2005). "Shared and specific muscle synergies in natural motor behaviors." Proc Natl Acad Sci U S A **102**(8): 3076-81.

d'Avella, A., et al. (2006). "Control of fast-reaching movements by muscle synergy combinations." J Neurosci **26**(30): 7791-810.

Darling, W. G. and J. D. Cooke (1987). "Changes in the variability of movement trajectories with practice." J Mot Behav **19**(3): 291-309.

Debicki, D. B. and P. L. Gribble (2004). "Inter-joint coupling strategy during adaptation to novel viscous loads in human arm movement." J Neurophysiol **92**(2): 754-65.

Debicki, D. B. and P. L. Gribble (2005). "Persistence of inter-joint coupling during single-joint elbow flexions after shoulder fixation." Exp Brain Res **163**(2): 252-7.

Dietz, V. (1992). "Human neuronal control of automatic functional movements: interaction between central programs and afferent input." Physiol Rev **72**(1): 33-69.

Dum, R. P. and P. L. Strick (1996). "Spinal cord terminations of the medial wall motor areas in macaque monkeys." J Neurosci **16**(20): 6513-25.

Dumont, R. J., et al. (2001). "Acute spinal cord injury, part I: pathophysiologic mechanisms." Clin Neuropharmacol **24**(5): 254-64.

Edgley, S., et al. (1986). "The heteronymous monosynaptic actions of triceps surae group Ia afferents on hip and knee extensor motoneurones in the cat." Exp Brain Res **61**(2): 443-6.

Evans, C. M. and S. N. Baker (2003). "Task-dependent intermanual coupling of 8-Hz discontinuities during slow finger movements." Eur J Neurosci **18**(2): 453-6.

Farmer, S. F., et al. (1993). "The frequency content of common synaptic inputs to motoneurones studied during voluntary isometric contraction in man." J Physiol **470**: 127-55.

Feige, B., et al. (2000). "Dynamic synchronization between multiple cortical motor areas and muscle activity in phasic voluntary movements." J Neurophysiol **84**(5): 2622-9.

Fetz, E. E. and P. D. Cheney (1980). "Postspike facilitation of forelimb muscle activity by primate corticomotoneuronal cells." J Neurophysiol **44**(4): 751-72.

Fetz, E. E., et al. (2000). "Functions of mammalian spinal interneurons during movement." Curr Opin Neurobiol **10**(6): 699-707.

Fetz, E. E., et al. (2002). "Roles of primate spinal interneurons in preparation and execution of voluntary hand movement." Brain Res Brain Res Rev **40**(1-3): 53-65.

Flash, T. and B. Hochner (2005). "Motor primitives in vertebrates and invertebrates." Curr Opin Neurobiol **15**(6): 660-6.

Freund, H. J. and H. J. Budingen (1978). "The relationship between speed and amplitude of the fastest voluntary contractions of human arm muscles." Exp Brain Res **31**(1): 1-12.

Gaunt, R. A., et al. (2006). "Intraspinal microstimulation excites multisegmental sensory afferents at lower stimulus levels than local alpha-motoneuron responses." J Neurophysiol **96**(6): 2995-3005.

Georgopoulos, A. P., et al. (1982). "On the relations between the direction of two-dimensional arm movements and cell discharge in primate motor cortex." J Neurosci **2**(11): 1527-37.

Gibbs, J., et al. (1995). "Organization of inputs to motoneurone pools in man." J Physiol **485 (Pt 1)**: 245-56.

Giszter, S. F., et al. (1993). "Convergent force fields organized in the frog's spinal cord." J Neurosci **13**(2): 467-91.

Gordon, J. and C. Ghez (1987). "Trajectory control in targeted force impulses. III. Compensatory adjustments for initial errors." Exp Brain Res **67**(2): 253-69.

Gottlieb, G. L., et al. (1988). "Practice improves even the simplest movements." Exp Brain Res **73**(2): 436-40.

Gross, J., et al. (2002). "The neural basis of intermittent motor control in humans." Proc Natl Acad Sci U S A **99**(4): 2299-302.

Grosse, P., et al. (2002). "EEG-EMG, MEG-EMG and EMG-EMG frequency analysis: physiological principles and clinical applications." Clin Neurophysiol **113**(10): 1523-31.

Halliday, D. M., et al. (2003). "Functional coupling of motor units is modulated during walking in human subjects." J Neurophysiol **89**(2): 960-8.

Halliday, D. M., et al. (1995). "A framework for the analysis of mixed time series/point process data--theory and application to the study of physiological tremor, single motor unit discharges and electromyograms." Prog Biophys Mol Biol **64**(2-3): 237-78.

Hebb, D. O. (1949). The Organization of Behaviour. New York, Wiley.

Henneman, E., et al. (1965). "Functional Significance of Cell Size in Spinal Motoneurons." J Neurophysiol **28**: 560-80.

Hoffman, D. S. and P. L. Strick (1995). "Effects of a primary motor cortex lesion on step-tracking movements of the wrist." J Neurophysiol **73**(2): 891-5.

Hultborn, H., et al. (1986). "Changes in polysynaptic Ia excitation to quadriceps motoneurones during voluntary contraction in man." Exp Brain Res **63**(2): 436-8.

Ivanenko, Y. P., et al. (2004). "Five basic muscle activation patterns account for muscle activity during human locomotion." J Physiol **556**(Pt 1): 267-82.

Jankowska, E. (1992). "Interneuronal relay in spinal pathways from proprioceptors." Prog Neurobiol **38**(4): 335-78.

Jaric, S., et al. (1992). "Effects of practice on final position reproduction." Exp Brain Res **91**(1): 129-34.

Jasper, H. H. and W. Penfield (1949). "Electrocorticograms in man: Effect of voluntary movement upon the electrical activity of the precentral gyrus." Arch. Psych Z. Neurol.(183): 163-174.

Johnson, G. R. (2002). "Outcome measures of spasticity." Eur J Neurol **9 Suppl 1**: 10-6; dicussion 53-61.

Kakei, S., et al. (1999). "Muscle and movement representations in the primary motor cortex." Science **285**(5436): 2136-9.

Kilner, J. M., et al. (2000). "Human cortical muscle coherence is directly related to specific motor parameters." J Neurosci **20**(23): 8838-45.

Kilner, J. M., et al. (1999). "Task-dependent modulation of 15-30 Hz coherence between rectified EMGs from human hand and forearm muscles." J Physiol **516 (Pt 2)**: 559-70.

Kirkwood, P. A. and T. A. Sears (1978). "The synaptic connexions to intercostal motoneurones as revealed by the average common excitation potential." J Physiol **275**: 103-34.

Krakauer, J. and C. Ghez (2000). Principles of neural science. E. R. Kandel, J. H. Schwartz and T. M. Jessell. New York, McGraw-Hill, Health Professions Division: xii, 1414 p.

Lance, J. W. (1980). "The control of muscle tone, reflexes, and movement: Robert Wartenberg Lecture." Neurology **30**(12): 1303-13.

Latash, M. L., et al. (1995). "Feedforward postural adjustments in a simple two-joint synergy in patients with Parkinson's disease." Electroencephalogr Clin Neurophysiol **97**(2): 77-89.

Latash, M. L., et al. (1995). "The relation between posture and movement: A study of a simple synergy in a two-joint task." Human Movement Science **14**: 79-107.

Lau, B., et al. (2007). "Strategies for generating prolonged functional standing using intramuscular stimulation or intraspinal microstimulation." IEEE Trans Neural Syst Rehabil Eng **15**(2): 273-85.

Lemay, M. A. and W. M. Grill (2004). "Modularity of motor output evoked by intraspinal microstimulation in cats." J Neurophysiol **91**(1): 502-14.

Loeb, G. E. and C. Ghez (2000). Principles of neural science. E. R. Kandel, J. H. Schwartz and T. M. Jessell. New York, McGraw-Hill, Health Professions Division: xii, 1414 p.

McCrea, D. A. (1992). "Can sense be made of spinal interneuron circuits? ." Behavior and Brain Sciences **15**: 633-643.

Mendell, L. M. (1984). "Modifiability of spinal synapses." Physiol Rev **64**(1): 260-324.

Moritz, C. T., et al. (2007). "Forelimb movements and muscle responses evoked by microstimulation of cervical spinal cord in sedated monkeys." J Neurophysiol **97**(1): 110-20.

Murthy, V. N. and E. E. Fetz (1996). "Oscillatory activity in sensorimotor cortex of awake monkeys: synchronization of local field potentials and relation to behavior." J Neurophysiol **76**(6): 3949-67.

Murthy, V. N. and E. E. Fetz (1996). "Synchronization of neurons during local field potential oscillations in sensorimotor cortex of awake monkeys." J Neurophysiol **76**(6): 3968-82.

Mushahwar, V. K., et al. (2004). "Movements generated by intraspinal microstimulation in the intermediate gray matter of the anesthetized, decerebrate, and spinal cat." Can J Physiol Pharmacol **82**(8-9): 702-14.

Mushahwar, V. K., et al. (2000). "Spinal cord microstimulation generates functional limb movements in chronically implanted cats." Exp Neurol **163**(2): 422-9.

Mushahwar, V. K., et al. (2002). "Intraspinal micro stimulation generates locomotor-like and feedback-controlled movements." IEEE Trans Neural Syst Rehabil Eng **10**(1): 68-81.

Mussa-Ivaldi, F. A., et al. (1994). "Linear combinations of primitives in vertebrate motor control." Proc Natl Acad Sci U S A **91**(16): 7534-8.

Nakajima, K., et al. (2000). "Striking differences in transmission of corticospinal excitation to upper limb motoneurons in two primate species." J Neurophysiol **84**(2): 698-709.

Pearson, K. G. and J. Gordon (2000). Principles of neural science. E. R. Kandel, J. H. Schwartz and T. M. Jessell. New York, McGraw-Hill, Health Professions Division: xii, 1414 p.

Perlmutter, S. I., et al. (1998). "Activity of spinal interneurons and their effects on forearm muscles during voluntary wrist movements in the monkey." J Neurophysiol **80**(5): 2475-94.

Pierrot-Deseilligny, E., et al. (1982). "Reversal in cutaneous of Ib pathways during human voluntary contraction." Brain Res **233**(2): 400-3.

Pierrot-Deseilligny, E. and D. J. Burke. (2005). "The circuitry of the human spinal cord: its role in motor control and movement disorders."

Prut, Y. and E. E. Fetz (1999). "Primate spinal interneurons show pre-movement instructed delay activity." Nature **401**(6753): 590-4.

Reinkensmeyer, D. J., et al. (2004). "Robotics, motor learning, and neurologic recovery." Annu Rev Biomed Eng **6**: 497-525.

Rosenbaum, D. A. (1991). Human motor control. San Diego, Academic Press.

Rosenberg, J. R., et al. (1989). "The Fourier approach to the identification of functional coupling between neuronal spike trains." Prog Biophys Mol Biol **53**(1): 1-31.

Saigal, R., et al. (2004). "Intraspinal microstimulation generates functional movements after spinal-cord injury." IEEE Trans Neural Syst Rehabil Eng **12**(4): 430-40.

Sanes, J. N. and J. P. Donoghue (1993). "Oscillations in local field potentials of the primate motor cortex during voluntary movement." Proc Natl Acad Sci U S A **90**(10): 4470-4.

Satkunam, L. E. (2003). "Rehabilitation medicine: 3. Management of adult spasticity." Cmaj **169**(11): 1173-9.

Schmidt, R. A. and D. G. Russell (1972). "Movement velocity and movement time as determiners of degree of preprogramming in simple movements." J Exp Psychol **96**(2): 315-20.

Schmidt, R. A., et al. (1979). "Motor-output variability: a theory for the accuracy of rapid motor acts." Psychol Rev **47**(5): 415-51.

Segal, R. L. and S. L. Wolf (1994). "Operant conditioning of spinal stretch reflexes in patients with spinal cord injuries." Exp Neurol **130**(2): 202-13.

Shadmehr, R. and S. P. Wise (2005). The computational neurobiology of reaching and pointing : a foundation for motor learning. Cambridge, Mass., MIT Press.

Sheffler, L. R. and J. Chae (2007). "Neuromuscular electrical stimulation in neurorehabilitation." Muscle Nerve **35**(5): 562-90.

Sherrington, C. S. (1906). The integrative action of the nervous system. New York, C. Scribner's Sons.

Simoyama, M. and R. Tanaka (1974). "Reciprocal La inhibition at the onset of voluntary movements in man." Brain Res **82**(2): 334-7.

Spooren, A. I., et al. (2006). "Measuring change in arm hand skilled performance in persons with a cervical spinal cord injury: responsiveness of the Van Lieshout Test." Spinal Cord **44**(12): 772-9.

Todorov, E. (2000). "Direct cortical control of muscle activation in voluntary arm movements: a model." Nat Neurosci **3**(4): 391-8.

Toma, K., et al. (2002). "Movement rate effect on activation and functional coupling of motor cortical areas." J Neurophysiol **88**(6): 3377-85.

Tresch, M. C. and E. Bizzi (1999). "Responses to spinal microstimulation in the chronically spinalized rat and their relationship to spinal systems activated by low threshold cutaneous stimulation." Exp Brain Res **129**(3): 401-16.

Vallbo, A. B. and J. Wessberg (1993). "Organization of motor output in slow finger movements in man." J Physiol **469**: 673-91.

Wessberg, J. and N. Kakuda (1999). "Single motor unit activity in relation to pulsatile motor output in human finger movements." J Physiol **517 (Pt 1)**: 273-85.

Wolf, S. L. and R. L. Segal (1996). "Reducing human biceps brachii spinal stretch reflex magnitude." J Neurophysiol **75**(4): 1637-46.

Wolpaw, J. R. (1997). "The complex structure of a simple memory." Trends Neurosci **20**(12): 588-94.

Wolpaw, J. R., et al. (1983). "Adaptive plasticity in the spinal stretch reflex." Brain Res **267**(1): 196-200.

Wolpaw, J. R. and A. M. Tennissen (2001). "Activity-dependent spinal cord plasticity in health and disease." Annu Rev Neurosci **24**: 807-43.

Appendix A Spectral Analysis Code

```
%%%%%%%%%%%%%%%%%%%%%%%%%%%%%%%%%%%%%%%%%%%%%%%%%%%%%%%%%%%%%%%%%%%%%%%%%%%%
%% COH_DIRECTORY function...highest level
%%%%%%%%%%%%%%%%%%%%%%%%%%%%%%%%%%%%%%%%%%%%%%%%%%%%%%%%%%%%%%%%%%%%%%%%%%%%

function coh_directory(folder_path, summary_path, file_ext, subject, movement, preCoh,
prePh, preCl, cohNames)

sessions = zeros(1,2);
flt_files = dir(fullfile(folder_path,file_ext));
session_count = 0;
sessions = [];
moveData = [];
moveName = [];

for file = 3:length(flt_files)

    file_name = flt_files(file).name;

    %parse the file name for the session #
    %with the file name convention, this is chars 3 and 4
    if length(file_name) == 11
        session_number = file_name(3:4);
    else
        session_number = file_name(3);
    end

    %call a function to check if this session_number is a repeat
    if checkRepeat(session_number,sessions) == 1, continue, end;

    if (str2num(session_number) == 65) || (str2num(session_number) == 66) ||
(str2num(session_number) == 67), continue, end;

    session_count = session_count + 1;
    sessions(session_count,1) = str2num(session_number);

    %count the number of files that belong to this session
    file_count = 0;
    for i = 1:length(flt_files)
        if findstr(lower([subject,session_number]),flt_files(i).name) > 0
            % Right file length?
            if (length(flt_files(i).name) - 9 ) == length(session_number)
                file_count = file_count + 1;
            end
        end
    end

    %store the number of sessions in the matrix, too
```

```
    sessions(session_count,2) = file_count;

end

%Get the Breakpoints by loading the associated XLS file
movement = lower(fixMovement(movement));
XLpath = [summary_path,'\',lower(subject),'\',movement,'\brk',movement(1:4),'.xls'];

XLMatrix = xlsread(XLpath);

for session = 1:length(sessions(:,1))

    if session == 1
        startPoint = 1;
        endPoint = sessions(1, 2);
    else
        startPoint = sum(sessions(1:(session-1),2)) + 1;
        endPoint = startPoint + sessions(session, 2) - 1;
    end

    %Get the appropriate data from the XL Matrix
    velocity = XLMatrix(startPoint,3);
    excursion = XLMatrix(startPoint,4);
    kinOffsets = XLMatrix(startPoint:endPoint,11);
    kinOnsets = XLMatrix(startPoint:endPoint,13);
    EMGOnsets = XLMatrix(startPoint:endPoint,20:29);

    disp(EMGOnsets);
    [x,y] = size(EMGOnsets)
    for i = 1:x
        for j = 1:y
            if EMGOnsets(i,j) < -1, EMGOnsets(i,j) = 0, end
        end
    end
    disp(mean(EMGOnsets));

    % Run coherence analysis on the group of files comprising a session
    file_prefix = lower([subject,num2str(sessions(session,1))]);
    %disp(['    - Analysing session #:',num2str(sessions(session,1))]);
    coh_session(folder_path, subject, movement(1:4), file_prefix, sessions(session,2),
kinOnsets, kinOffsets, EMGOnsets, velocity, excursion, preCoh, prePh, preCl, cohNames);

end

function isRepeat = checkRepeat(session_number, sessions)

if isempty(sessions), isRepeat = 0;, return;, end;

isRepeat = 0;

for i = 1:length(sessions(:,1))
    if str2num(session_number) == sessions(i,1)
        isRepeat = 1;
        break;
    end
end;

%A function to reformat the directory name to a four letter string that
%characterizes the type of movement that we are analysing
function fixedMovement = fixMovement(movement_string)

fixedMovement = '';
charsWanted = 4;

if findstr(' ', movement_string) == charsWanted + 1
    %we'll assume this means that it's already formatted properly
    fixedMovement = movement_string(1:charsWanted);
end

for i = 1:charsWanted
    [firstWord, Remainder] = strtok(movement_string,' ');
```

```
    fixedMovement = [fixedMovement firstWord(1)];
    movement_string = Remainder;
end

%%%%%%%%%%%%%%%%%%%%%%%%%%%%%%%%%%%%%%%%%%%%%%%%%%%%%%%%%%%%%%%%%%%%%%%%%%%%
%% COH_SESSION function...highest level
%%%%%%%%%%%%%%%%%%%%%%%%%%%%%%%%%%%%%%%%%%%%%%%%%%%%%%%%%%%%%%%%%%%%%%%%%%%%

function coh_session(folder_path, subject, movement, session_set, trial_files, kinOnsets,
kinOffsets, EMGOnsets, velocity, excursion, preCoh, prePh, preCl, cohNames)

% A couple of the changeable variables for this m-file
write_path = 'C:\temp';
smoothBin = 20; %At 1000Hz, smoothing reduces density (i.e 20 produces effective samp rate
50Hz)
chunkSize = 512; %The background window of 100ms - 512?
threadLength = 2000;
choppedLength = 1024;

% The definitions of all the muscles
muscles = char('BB(lat)', 'BB(short)', 'BRD', 'ECRL', 'ECU', 'FCR', 'FCU', 'TB(lat)',
'TB(long)');

%Get Matlab to generate all possible combinations of the muscles depending
%on the k value (the number of channels to compare at a time)
muscle_combos = nchoosek(1:length(muscles),2);
%muscle_combos = [1 8 ; 2 8 ; 1 3 ; 2 3 ; 1 4 ; 2 4 ; 4 5 ; 6 7 ; 8 4 ; 9 4 ; 8 5 ; 9 5 ;
5 7 ; 4 6; 8 9];

% This is gonna' have to be assumed about the *.flt files but,
% realistically shouldn't ever change.
channels = 10;
channel_offset = 5; % Because the EMG channels start at col#5

%Define a temporary folder path to toss the ascii files into that's not on
%the freakin' DVD drive (you're an idiot for trying...)
velexc = [num2str(velocity),'-',num2str(excursion)];
write_path = makeSubDir(write_path,'coherence'); %Make the main directory
write_path = makeSubDir(write_path,subject); %Make this subject's directory
write_path = makeSubDir(write_path,movement); %Make the movement dir
write_path = makeSubDir(write_path,velexc); %Make the session dir

%Figure out the proper mean
count = 0;
tally = 0;
for a = 1:length(kinOnsets)
    if kinOnsets(a) < threadLength
        count = count + 1;
        tally = tally + kinOnsets(a);
    end
end
avKinOnset = ceil(tally/count);

%Shift the record so that all the array positions are valid, if appropriate
bias = avKinOnset - 512;
if bias > 0, bias = 0;, end;
bias = abs(bias); %The bias ensures that, if an avKinOnset happens to be less than 500,
that the record is shifted right

Calculate the theoretical movement time and shift, if appropriate
moveTime = excursion/velocity*1000;
if moveTime >= 500
   bias = bias + (moveTime - 450)  %To see the whole of the shorter records, shift further
end

stitchedData = [];
kinProfiles = [];
for trial_file = 0:(trial_files-1)

    kOnset = kinOnsets(trial_file+1);
```

```
    if kOnset >= threadLength; continue, end;

    %Ensure that the proper file name is being created
    if trial_file < 10
        file_suff = ['0',num2str(trial_file)];
    else
        file_suff = num2str(trial_file);
    end

    file = [folder_path,'\',session_set,'0',file_suff,'.flt'];

    %Try to open the reference file
    try
        EMGdata = readf2h(file);
    catch
        %disp(['    - Referenced file: ',file, ' skipped due to error.']);
        continue;
    end

    %Now that the file is open, grab each channel in that session and the
    %kinematic profile
    thread = EMGdata(1:threadLength,channel_offset:channels+channel_offset-1);
    kinProfile = EMGdata(1:threadLength,1);

    %Line up all the kinematic onsets to the average kinOnset
    shiftCount = (avKinOnset - kOnset);
    if shiftCount > 0
        %shift this record right (i.e insert rows of zeros before)
        thread = [zeros(shiftCount,10) ; thread(1:(threadLength-shiftCount),:)];
        kinProfile = [zeros(shiftCount,1) ; kinProfile(1:(threadLength-shiftCount))];
    elseif shiftCount < 0
        %shift this record left (i.e. append zeros after)
        thread = [thread(abs(shiftCount)+1:threadLength,:) ; zeros(abs(shiftCount),10)];
        kinProfile = [kinProfile(abs(shiftCount)+1:threadLength) ;
zeros(abs(shiftCount),1)];
    end

    %Now, chop off either end of the EMG and kinematic profile
    thread = thread(avKinOnset-511+bias:avKinOnset+512+bias,:); %slice to 1024 points
    kinProfile = kinProfile(avKinOnset-511+bias:avKinOnset+512+bias);

    stitchedData = cat(3,stitchedData, thread);

    kinProfiles = [kinProfiles kinProfile];

end

nTrials = length(stitchedData(1,1,:));

for trial = 1:nTrials
    allMean = mean(stitchedData(1:50,:,trial));
    stitchedData(:,:,trial) = stitchedData(:,:,trial) - ones(1024,1)*allMean;
end

%Prepare average EMG to plot
[b,a] = butter(1,10/1024,'low');
[d,c] = butter(1,50/1024, 'low');

stitchedDataS = abs(stitchedData);
stitchedDataS = filter(d,c,stitchedDataS)
stitchedDataS = filter(b,a,stitchedDataS);

meanData = mean(stitchedDataS,3);
SDData = std(stitchedDataS,0,3);


nTrials = length(stitchedData(1,1,:));

%Notch out 60Hz noise
w0 = 60/500; bw = w0/200;
[b,a] = iirnotch(w0,bw);
```

```
stitchedData = filter(b, a, stitchedData);

%Make sure that all data is around the baseline
for trial = 1:nTrials
    allMean = mean(stitchedData(1:50,:,trial));
    stitchedData(:,:,trial) = stitchedData(:,:,trial) - ones(choppedLength,1)*allMean;
end

meanKin = mean(kinProfiles,2);
avKinOnset = 511 + bias; %Readjust avKinOnset for chopped length

% Now loop to compare each of the relevant muscles to each other
for combo = 1:length(muscle_combos(:,1))

    m1_index = muscle_combos(combo,1); %upper_muscles(um);
    m2_index = muscle_combos(combo,2); %lower_muscles(lm); %

    m1_muscle = deblank(muscles(m1_index,:));
    m2_muscle = deblank(muscles(m2_index,:));

    %Rearrange data in [samples x muscles x time] matrix
    sliceLength = 256; %125;
    sliceOverlap = 224; %100;  %0 means no overlap, 63 means 50%

    slices = [];
    for slice = 1:25
        trialSlices = [];
        for trial = 1:nTrials          %length(kinOnsets)
            start = (slice-1)*(sliceLength-sliceOverlap) + 1;
            finish = (slice-1)*(sliceLength-sliceOverlap) + sliceLength;
            if trial == 1
                disp([num2str(start), ' ' , num2str(finish), ' ' , num2str(start-
finish)]);
            end
            trialSlices = [trialSlices ; stitchedData(start:finish,m1_index,trial)
stitchedData(start:finish,m2_index,trial)];
        end
        slices = cat(3,slices,trialSlices);
    end


    %Rearrange data in columnar fashion as [rows,cols] = [data,muscles]
    vertData = [];
    for trial = 1:nTrials
        vertData = [vertData ; [stitchedData(:,m1_index,trial)
stitchedData(:,m2_index,trial)]];
    end

    mMeanData = [meanData(:,m1_index) meanData(:,m2_index)];
    mSDData = [SDData(:,m1_index) SDData(:,m2_index)];

    coh_analysis(slices, vertData, mMeanData, mSDData, m1_muscle, m2_muscle, velocity,
excursion, movement,avKinOnset, bias, meanKin, write_path);

end

% ************************************

%A function to reformat the directory name to a four letter string that
%characterizes the type of movement that we are analysing
function fixedMovement = fixMovement(movement_string)

fixedMovement = '';
charsWanted = 4;

if findstr(' ', movement_string) == charsWanted + 1
    %we'll assume this means that it's already formatted properly
    fixedMovement = movement_string(1:charsWanted);
end

for i = 1:charsWanted
```

```
    [FirstWord, Remainder] = strtok(movement_string,' ');
    fixedMovement = [fixedMovement FirstWord(1)];
    movement_string = Remainder;
end

% A function to create a given subdirectory in a given directory
function new_path = makeSubDir(base_path, newDir)

if exist ([base_path,'\',newDir]) == 0
    mkdir(base_path,newDir);
end

new_path = [base_path,'\',newDir];

function coded = encodeNum(velocity, excursion, movement, combo)

%Each type of record must have a matching coding scheme because all the
%records will be out of alignment otherwise
%Each record will be encoded thusly: 'vvveemcc' or 'vveemcc'
%The first 'c' might be zero, but that will not be lost in the conversion back to decimal.

velocity = num2str(velocity);
excursion = num2str(excursion);
movement = num2str(moveID(movement));
combo = num2str(combo);
if length(combo) == 1, combo = ['0', combo];, end;

coded = str2num([velocity, excursion, movement, combo]);

function numID = moveID(string)

if strcmp(string, 'eewf')
    numID = 1;
elseif strcmp(string, 'eewi')
    numID = 2;
elseif strcmp(string, 'efwf')
    numID = 3;
elseif strcmp(string, 'efwi')
    numID = 4;
end

%%%%%%%%%%%%%%%%%%%%%%%%%%%%%%%%%%%%%%%%%%%%%%%%%%%%%%%%%%%%%%%%%%%%%%%%%%%%%%%
%% COH_ANALYSIS function...highest level
%%%%%%%%%%%%%%%%%%%%%%%%%%%%%%%%%%%%%%%%%%%%%%%%%%%%%%%%%%%%%%%%%%%%%%%%%%%%%%%

function coh_analysis(slices, vertData, mMeanData, mSDData, muscle1, muscle2, velocity,
excursion, movement,avKinOnset, bias, meanKin, write_path)

image_type = 'eps';
samp_rate = 1024;
f_max = 100;

plotCoh = [];

EMG1 = abs(vertData(1:1024,1));
EMG2 = abs(vertData(1:1024,2));

vertData = abs(vertData);
slices = abs(slices);

file_path = [write_path,'\',muscle1,'-',muscle2];
image_patht = [write_path,'\',muscle1,'-',muscle2,'.eps'];
image_pathj = [write_path,'\',muscle1,'-',muscle2,'.jpg'];
mat_path = [write_path,'\',muscle1,'-',muscle2,'.mat'];

suptitle([muscle1,' versus ',muscle2,' @ ',num2str(velocity),' deg/s to ',
num2str(excursion), ' degrees'])

[num_points num_muscles num_slices] = size(slices);
num_trials = num_points/256;
```

```
% In order to shift the data
allCoh = [];
allShifted = [];
plotCoh = [];
Coh = [];

%Properly compute coherence
for slice = 1:num_slices
   [f,t,cl] = coh_spectral(slices(:,1,slice),slices(:,2,slice),samp_rate,8);
   freq_pts = round(100/cl.df);
   plotCoh = [plotCoh f(1:freq_pts,4)];
end

all = sum([plotCoh(2,:) ; plotCoh(3,:) ; plotCoh(4,:) ; plotCoh(5,:) ; plotCoh(6,:) ;
plotCoh(7,:) ; plotCoh(8,:) ; plotCoh(9,:) ; plotCoh(10,:)])/9; %4-40Hz
NonShiftAv = [mean(reshape(plotCoh(2:3,8:9),4,1)) ; mean(reshape(plotCoh(4:5,8:9),4,1)) ;
mean(reshape(plotCoh(6:7,8:9),4,1)) ; mean(reshape(plotCoh(8:10,8:9),6,1))];
NonShiftSD = [std(reshape(plotCoh(2:3,8:10),6,1)) ; std(reshape(plotCoh(4:5,8:10),6,1)) ;
std(reshape(plotCoh(6:7,8:10),6,1)) ; std(reshape(plotCoh(8:10,8:10),9,1))]

%Shift slices for shuffled coherence
slices(:,2,:) = circshift(slices(:,2,:),256);

%Recompute coherence

for slice = 1:num_slices
    [f,t,cl] = coh_spectral(slices(:,1,slice),slices(:,2,slice),samp_rate,8);
    freq_pts = round(100/cl.df);
    Coh = [Coh f(1:freq_pts,4)];
end

ShiftAv = [mean(reshape(Coh(2:3,8:9),4,1)) ; mean(reshape(Coh(4:5,8:9),4,1)) ;
mean(reshape(Coh(6:7,8:9),4,1)) ; mean(reshape(Coh(8:10,8:9),6,1))];
ShiftSD = [std(reshape(Coh(2:3,8:9),4,1)) ; std(reshape(Coh(4:5,8:9),4,1)) ;
std(reshape(Coh(6:7,8:9),4,1)) ; std(reshape(Coh(8:10,8:9),6,1))];

%Determine if this record is considered significantly coherent at any
%frequency band
SigCoherent = 0;
for p = 1:4
    if NonShiftAv(p) > (ShiftAv(p) + 2*ShiftSD(p))
        SigCoherent = 1;
    end
end

%SUBSTRACT VALUES
%Push real confidence limits down to shifted conf lims
%If values are below confidence limits: push to zero
for x = 1:10
    if x == 1 || x == 2 || x == 3, q = 1;
    elseif x == 4 || x == 5 , q = 2;
    elseif x == 6 || x == 7 , q = 3;
    elseif x == 8 || x == 9 || x == 10 , q = 4;
    end
    for y = 1:length(plotCoh(1,:))
        if plotCoh(x,y) < ShiftAv(q) + (2*ShiftSD(q))
            plotCoh(x,y) = 0;
        else
            plotCoh(x,y) = plotCoh(x,y) - ShiftAv(q);
            if plotCoh(x,y) < 0, plotCoh(x,y) = 0;, end
        end
    end
end

%Now determine the average amount of coherence across all f bands
totalCoh = mean(reshape(plotCoh(2:10,8:9),18,1));

CorrectedAv = [mean(reshape(plotCoh(2:3,8:9),4,1)) ; mean(reshape(plotCoh(4:5,8:9),4,1)) ;
mean(reshape(plotCoh(6:7,8:9),4,1)) ; mean(reshape(plotCoh(8:10,8:9),6,1))];

%Determine the location of the 'onset' label based on kinematic onset
```

```
%centreTick = (avKinOnset/1000)*num_slices;
freqSteps = [1];
for a = 1:5
    freqSteps = [freqSteps ; ((freq_pts-1)/5)*a + 1];
end

% Plot the mean EMG and the resulting spectrogram

fig = figure('visible','on');

plot(mMeanData(:,1),'b','linewidth',2);

disp([muscle1,',',muscle2,' ',movement,' ',num2str(excursion*1000/velocity),'
',num2str(totalCoh),' ',num2str(SigCoherent),' ',num2str(CorrectedAv(1)),'
',num2str(CorrectedAv(2)),' ',num2str(CorrectedAv(3)),' ',num2str(CorrectedAv(4)),'
',num2str(NonShiftAv(1)),' ',num2str(NonShiftAv(2)),' ',num2str(NonShiftAv(3)),'
',num2str(NonShiftAv(4)),' ',num2str(ShiftAv(1)),' ',num2str(ShiftAv(2)),'
',num2str(ShiftAv(3)),' ',num2str(ShiftAv(4))]);

save(mat_path,'plotCoh')
eval(['print -depsc2 ', image_patht]);
eval(['print -djpeg ', image_pathj]);
delete(fig) %close the figure

%%%%%%%%%%%%%%%%%%%%%%%%%%%%%%%%%%%%%%%%%%%%%%%%%%%%%%%%%%%%%%%%%%%%%%%%%%%%
%% COH_SPECTRAL function...highest level
%%%%%%%%%%%%%%%%%%%%%%%%%%%%%%%%%%%%%%%%%%%%%%%%%%%%%%%%%%%%%%%%%%%%%%%%%%%%

function [f,t,cl] = coh_spectral(dat1,dat2,samp_rate,seg_pwr);

pts_tot=length(dat1);           % Determine size of data vector.
seg_size=2^seg_pwr;             % DFT segment length (T).
seg_tot=fix(pts_tot/seg_size);  % Number of complete segments (L).
samp_tot=seg_tot*seg_size;      % Number of samples to analyse: R=LT.

% Arrange data into L columns each with T rows.
rd1=reshape(dat1(1:samp_tot),seg_size,seg_tot);
rd2=reshape(dat2(1:samp_tot),seg_size,seg_tot);

trend_x=(1:seg_size)';

%Create a Hanning window to reduce spectral leakage
window  = hanning(seg_size);

for i=1:seg_tot
    % Linear trend removal.
    p=polyfit(trend_x,rd1(:,i),1);          % Fit 1st order polynomial.
    rd1(:,i)=rd1(:,i)-p(1)*trend_x(:)-p(2); % Subtract from ch 1.
    p=polyfit(trend_x,rd2(:,i),1);          % Fit 1st order polynomial.
    rd2(:,i)=rd2(:,i)-p(1)*trend_x(:)-p(2); % Subtract from ch 2.

    %Apply the Hanning window to each disjoint section
    rd1(:,i) = window.*rd1(:,i);
    rd2(:,i) = window.*rd2(:,i);
end

% Take DFT across columns/segments
fd1=fft(rd1);
fd2=fft(rd2);

norm=2*pi*seg_size;             % Normalization for spectral estimates.
f11=mean(abs(fd1.*fd1)/norm,2); % Spectrum 1
f22=mean(abs(fd2.*fd2)/norm,2); % Spectrum 2
f21=mean(fd2.*conj(fd1)/norm,2); % Cross spectrum

deltaf=samp_rate/seg_size;      % Resolution - spacing of Fourier frequencies in Hz.

%Build f output
seg_size_2=(2:seg_size/2+1)';
f(:,1)=(seg_size_2-1)*deltaf;
% Log spectra
```

```
f(:,2)=log10(f11(seg_size_2));
f(:,3)=log10(f22(seg_size_2));
% Coherence and phase
f(:,4)=abs(f21(seg_size_2)).*abs(f21(seg_size_2))./(f11(seg_size_2).*f22(seg_size_2));
f(:,5)=angle(f21(seg_size_2));

% Estimate cross-corr using inverse DFT
deltat=1000.0/samp_rate;            % dt in msec.
cov=ifft(f21);                      % Inverse DFT.

%Build t output
t(:,1)=((1:seg_size)'-seg_size/2-1)*deltat;
t([seg_size/2+1:seg_size,1:seg_size/2],2)=real(cov(1:seg_size))*2*pi;

% Construct cl structure, confidence limits for parameter estimates.
cl.seg_size=seg_size;               % T.
cl.seg_tot=seg_tot;                 % L.
cl.seg_tot_var=seg_tot;             % Effective no of segments
cl.samp_tot=samp_tot;               % R.
cl.samp_rate=samp_rate;             % Sampling rate.
cl.dt=deltat;                       % Delta t.
cl.df=deltaf;                       % Delta f.
cl.f_c95=0.8512*sqrt(1/seg_tot);    % 95% for spectral estimates
cl.ch_c95=1-0.05^(1/(seg_tot-1));   % 95
```